

United States Naval Postgraduate School



A NUMERICAL INVESTIGATION OF THE NON-LINEAR
MECHANICS OF WAVE DISTURBANCES IN PLANE
POISEUILLE FLOWS

by

hcc love
T. H. Gawain and W. H. Clark
entry

2 September 1971

This document has been approved for public release
and sale; its distribution is unlimited.

QA911
.G16

20091105006

NAVAL POSTGRADUATE SCHOOL
Monterey, California

Rear Admiral A. S. Goodfellow, Jr.
Superintendent

M. U. Clauser
Academic Dean

ABSTRACT:

The response of a plane Poiseuille flow to disturbances of various initial wavenumbers and amplitudes is investigated by numerically integrating the equation of motion. It is shown that for very low amplitude disturbances the numerical integration scheme yields results that are consistent with those predictable from linear theory. It is also shown that because of non-linear interactions a growing unstable disturbance excites higher wavenumber modes which have the same frequency, or phase velocity, as the primary mode. For very low amplitude disturbances these spontaneously generated higher wavenumber modes have a strong resemblance to certain modes computed from the linear Orr-Sommerfeld equation.

In general it is found that the disturbance is dominated for a long time by the primary mode and that there is little alteration of the original parabolic mean velocity profile. There is evidence of the existence of an energy equilibrium state which is common to all finite-amplitude disturbances despite their initial wavenumbers. This equilibrium energy level is roughly 3-5% of the energy in the mean flow which is an order of magnitude higher than the equilibrium value predicted by existing non-linear theories.

T. H. Gawain
T. H. Gawain
Professor of Aeronautics

W. H. Clark
W. H. Clark
Visiting Assistant Professor

Approved by:

Released by:

R. W. Bell
R. W. Bell
Chairman
Department of Aeronautics

C. E. Menneken
C. E. Menneken
Dean of Research Administration

NPS-57Gn71091A

2 September 1971

TABLE OF CONTENTS

	Page
1. Introduction	1
2. Background	2
3. Basic Equations	6
4. Numerical Model	11
5. Linear Calculations	16
6. Numerical Integration of the Vorticity Equation	21
a) Small Amplitude Disturbances	21
b) Finite Amplitude Disturbances	25
7. Conclusions.	36
References	39
Figures	41
Appendix (Program Listing)	78
Distribution List	118
Form DD 1473	120

1. Introduction

In this paper we present some results from a numerical investigation of the phenomena of stability, transition and turbulence in incompressible channel flows. Ideally, the goal of such an investigation would be to numerically integrate the Navier-Stokes equations and thereby be able to follow the growth of some unstable disturbance which perturbs an initial laminar Poiseuille flow. It would then be possible to observe in detail how this growing disturbance eventually produces a fully developed, stationary turbulent flow. Presumably, if one were to repeat such a calculation for a large number of initial disturbances then the final turbulent flow could be described by an ensemble average over all the initial conditions.

The results of such a computation would represent an exact (to within the limits of the numerical model) solution to the turbulence problem. Since turbulence is an inherently three-dimensional phenomenon, these computations would have to be carried out on a three-dimensional grid; unfortunately, the computational grid would have to be large enough to contain the large "eddies" representing the initial disturbance and still be able to resolve the smallest energy dissipation length scales of the final turbulence. Even at low Reynolds numbers the ratio of the larger length scale to the smallest scale is several orders of magnitude. The number of grid points is proportional to the cube of this ratio; hence, a complete three-dimensional solution is impractical, if not impossible, despite the large storage capacity of modern computers. (Emmons 1970) To overcome this impractically large storage requirement we have drastically simplified the problem by treating the flow on a

two-dimensional basis. It is recognized that a two-dimensional treatment can not adequately represent true physical turbulence. Never-the-less the two-dimensional problem can be handled without further approximation and, as will be pointed out in the next section, two-dimensional solutions are of interest in their own right.

2. Background

During the past decade considerable effort was devoted to developing theories for the response of plane Poiseuille flows to finite-amplitude disturbances. The most significant contribution of these theories (in particular, those of Stuart and Watson (1960) and Reynolds and Potter (1967)) was in showing that the square of the amplitude ($|A_1|^2$) of an initially infinitesimal unstable disturbance is governed by an equation of the form

$$\frac{d |A_1|^2}{dt} = k_1 |A_1|^2 + k_2 |A_1|^4 \quad (1)$$

Equation 1, which can be derived from the Navier-Stokes equations, is an approximation valid in a region in the $(\alpha-R_e)$ -plane which is close to the "neutral curve". Here R_e denotes the Reynolds number and α the wave number of the disturbance. For disturbances with very small amplitudes the second term on the right of equation 1 must be negligible; hence, the square of the disturbance amplitude has an exponential growth and the constant, k_1 , is related to the exponential amplification factor of the linear theory (i.e., $k_1 = -2 \beta_{11}$). Of particular interest is the case of $k_1 > 0$ for which the flow is unstable to small disturbances.

If $k_2 < 0$ then it is possible that the higher order terms will eventually balance the leading term and the amplitude growth is limited such that

$$\begin{aligned} \frac{d |A_1|^2}{dt} &\rightarrow 0 \\ |A_1|^2 &\rightarrow -k_1/k_2 \end{aligned} \tag{1b}$$

as

$$t \rightarrow +\infty$$

Under such conditions a "supercritical equilibrium state" is said to exist. On the other hand, if $k_1 > 0$ and $k_2 > 0$ then no positive limiting value for $|A_1|^2$ is possible according to equation 1. It is possible to evaluate k_2 based on Stuart's (1960) theory and the necessary calculations have been carried out by Pekeris and Shkoller (1967) and Reynolds and Potter (1967). These authors have found that under certain conditions $k_2 < 0$ for some unstable disturbances. Both Pekeris and Shkoller and Reynolds and Potter have found that for regions near the lower branch of the "neutral curve" $k_2 < 0$ while $k_2 > 0$ near the upper branch. Hence, one can conclude that disturbances whose wavelength corresponds to a point near the lower branch can grow according to the non-linear theory and reach a supercritical equilibrium state. On the other hand, for unstable disturbances whose wavelength corresponds to a point in the (α, R_e) plane near the upper branch the non-linear theory does not seem to be applicable. At least the existing theories give us no information about the growth of such a disturbance beyond the linear range of amplitudes.

Such "supercritical equilibrium states" are not observed experimentally in channel flows; instead the initial instabilities lead immediately to three dimensional turbulent flows. It seems, that no experimental verification of this aspect of finite-amplitude theory is possible. A computer simulation of a two dimensional channel flow is, perhaps, the best way of investigating the two dimensional response of a plane Poiseuille flow to an initial unstable disturbance. A computer simulation offers, in addition to its two dimensionality, the advantage of providing an "exact" solution to the equations of motion ("exact" to within the limits of a finite difference representation) without introducing any approximations concerning the relative magnitudes of the various modes of which the disturbance is composed.

The present paper presents the results of a numerical investigation of the response of a plane Poiseuille flow to various initial disturbances. An attempt has been made to present the results in a manner that will facilitate comparison with the existing non-linear theory. The difficulty in making such comparisons is due to the fact that the theories mentioned concern the growth of an unstable disturbance with zero initial amplitude (at time $t = -\infty$) which grows at first according to linear theory and finally reaches an amplitude of such magnitude that the non-linear equations are appropriate. In a numerical simulation, with limited computation time available, the initial disturbance must have some finite amplitude. The growth rates predicted by the finite-amplitude theories are very small and the time required to follow the growth of a very small disturbance to the non-linear range consumes enormous amounts of computer time. For this reason the numerical

investigator is tempted to start his calculations by using a disturbance whose amplitude is of such magnitude that the entire linear range can be bypassed. It will be pointed out in Section 6 that there seem to be significant qualitative differences in the flow when large initial amplitudes are used as compared with those for which very small initial amplitudes are used in the calculations.

Another aspect of the present investigation was to determine under what circumstances, if any, a two dimensional representation of the flow could be made to resemble in some respects three dimensional turbulent flows.

It is clear that the "supercritical equilibrium states" in which the unstable disturbance mode remains dominant do not resemble turbulence in which the disturbance energy is distributed over a wide spectral range. Also in a "supercritical equilibrium state" the resultant mean velocity profile differs only slightly from the parabolic laminar profile while for turbulent flows the mean velocity profiles bear little resemblance to the original laminar one. It is recognized that there are significant differences between two dimensional and true three dimensional turbulence. This is particularly evident in the energy spectrum and mechanism for the transfer of energy and vorticity between the various spectral components (Lilly (1968) and Kraichnan (1967)).

However, could it be possible that for some choice of initial disturbance mode shapes and amplitudes the structure of the resultant two dimensional flow could lie somewhere between the (relative)

simplicity of a supercritical equilibrium state and the "complete chaos" characterizing a true turbulent flow? This aspect of the present paper will be discussed in Section 6.

3. Basic Equations

Consider the two dimensional flow of an incompressible fluid between two parallel planes. The governing equations of motion are

$$\frac{\partial \zeta}{\partial t} - \frac{\partial \Psi}{\partial y} \frac{\partial \zeta}{\partial x} + \frac{\partial \Psi}{\partial x} \frac{\partial \zeta}{\partial y} = \frac{1}{Re} \nabla^2 \zeta \quad (2a)$$

and

$$\zeta = \nabla^2 \Psi \quad (2b)$$

where ζ and Ψ are the vorticity and stream function respectively with ζ and Ψ defined by

$$u = - \frac{\partial \Psi}{\partial y} ; \quad v = \frac{\partial \Psi}{\partial x} \quad (3a)$$

$$\zeta = \frac{\partial v}{\partial x} - \frac{\partial u}{\partial y} . \quad (3b)$$

The variables are assumed to be normalized on suitable characteristic lengths and velocities which are shown in Figure 1 along with other parameters of interest. The velocity components can be expressed as

$$u = U(y) + u' ; \quad v = v' ; \quad \zeta = - \frac{dU}{dy} + \zeta' \quad (4)$$

$$\Psi = 3/2 \left(\frac{1}{3} y^3 - y \right) + \Psi'$$

where the primed quantities which depend on x, y, t represent the instantaneous departure of the flow from the original laminar flow. Substituting equations 4 into equations 2 results in

$$\frac{\partial \zeta'}{\partial t} + U \frac{\partial \zeta'}{\partial x} - 3 \frac{\partial \Psi'}{\partial x} - \frac{\partial \Psi'}{\partial y} \frac{\partial \zeta'}{\partial x} + \frac{\partial \Psi'}{\partial x} \frac{\partial \zeta'}{\partial y} = \frac{1}{R_e} \nabla^2 \zeta' \quad (5a)$$

$$\zeta' = \nabla^2 \Psi' \quad (5b)$$

The conditions of zero slip at the wall and constant mass flow rate imply that the stream function, Ψ' , satisfy the boundary conditions

$$\Psi' = \partial \Psi' / \partial y = 0 \quad \text{at} \quad y = \pm 1. \quad (6)$$

By considering periodic solutions to equation 2 the boundary conditions in the streamwise direction are fixed by

$$\Psi' (x, y, t) = \Psi' (x \pm 2nL, y, t) \quad (7a)$$

$$\zeta' (x, y, t) = \zeta' (x \pm 2nL, y, t) \quad (7b)$$

where the basic period is $2L$. Equations 5a and 5b with the boundary conditions (6) and (7) are to be solved for $\Psi'(x, y, t)$ for a given initial value of $\Psi'(x, y, 0)$.

At this point it is convenient to define some parameters that are useful in describing the flow structure. The assumed periodicity implies homogeneity in the streamwise direction; hence, all averaging is done with respect to the streamwise coordinate, x . The average value of any quantity, $q(x, y, t)$, is denoted by an overbar and obtained by integrating over one period of the basic wavelength.

$$\bar{q} (y, t) = \frac{1}{2L} \int_{-L}^L q(x, y, t) dx \quad (8)$$

It should again be emphasized that in our representation the flow is arbitrarily divided into a laminar and a disturbance part. Hence, the total streamwise velocity component is given by

$$u(x,y,t) = U(y) + u'(x,y,t) \quad (9)$$

and the mean velocity is

$$\bar{u}(y,t) = U(y) + \bar{u}'(y,t) \quad (10)$$

The difference between the mean and local values of any quantity is referred to as the turbulent part of that quantity and is denoted by a circumflex. Thus we have

$$\hat{u}(x,y,t) = u(x,y,t) - \bar{u}(y,t) = u' - \bar{u}' \quad (11a)$$

$$\hat{v}(x,y,t) = v'(x,y,t) \quad (11b)$$

$$\hat{\Psi}(x,y,t) = \Psi'(x,y,t) - \bar{\Psi}'(y,t) \quad (11c)$$

$$\hat{\zeta}(x,y,t) = \zeta'(x,y,t) - \bar{\zeta}'(y,t) \quad (11d)$$

and

$$\hat{u} = - \frac{\partial \hat{\Psi}}{\partial y} \quad (11e)$$

$$\bar{u}' = - \frac{\partial \bar{\Psi}'}{\partial y} \quad (11f)$$

$$\hat{v} = \frac{\partial \hat{\Psi}}{\partial x} \quad (11g)$$

$$\bar{v}' = \frac{\partial \bar{\Psi}'}{\partial x} = 0 \quad (11h)$$

The turbulent kinetic energy is

$$\hat{E}(x,y,t) = \frac{1}{2} \left[\left(- \frac{\partial \hat{\Psi}}{\partial y} \right)^2 + \left(\frac{\partial \hat{\Psi}}{\partial x} \right)^2 \right] \quad (12a)$$

The mean value is

$$\bar{E}(y,t) = \frac{1}{2L} \int_{-L}^L \hat{E}(x,y,t) dx \quad (12b)$$

and the normalized sum of turbulent kinetic energy over a domain extending from the upper to the lower wall and for one period of the basic disturbance is

$$\hat{E}(t) = \frac{1}{2} \int_{-1}^1 dy \left\{ \frac{1}{2L} \int_{-L}^L \hat{E}(x,y,t) dx \right\} \quad (12c)$$

Similarly, the kinetic energy in the mean flow is

$$E(y,t) = \frac{1}{2} \left[U(y) - \frac{\partial \bar{\Psi}'}{\partial y} \right]^2 \quad (13a)$$

and the normalized sum over the domain is

$$E(t) = \frac{1}{2} \int_{-1}^1 E(y,t) dy \quad (13b)$$

The normalized energy in the initial laminar flow is

$$E_\ell = \frac{1}{2} \int_{-1}^1 \frac{1}{2} U^2 dy = .600 . \quad (13c)$$

We can represent the periodic disturbance by means of a Fourier series as follows:

$$\psi'(x,y,t) = \sum_{n=-\infty}^{\infty} f_n(y,t) e^{-i n \alpha x} \quad (14a)$$

$$\zeta'(x,y,t) = \sum_{n=-\infty}^{\infty} g_n(y,t) e^{-i n \alpha x} \quad (14b)$$

with

$$f_n(y,t) = \frac{1}{2L} \int_{-L}^L \psi'(x,y,t) e^{in\alpha x} dx \quad (15a)$$

$$f_{-n} = f_n^*$$

$$g_n(y,t) = \frac{1}{2L} \int_{-L}^L \zeta'(x,y,t) e^{in\alpha x} dx \quad (15b)$$

$$g_{-n} = g_n^*$$

where $\alpha = \pi/L$, and superscript * denotes a complex conjugate. From 5b

$$g_n = f_n'' - (n\alpha)^2 f_n \quad (15c)$$

Notice that the mean value of the disturbance streamfunction and vorticity is simply

$$\overline{\psi'}(y,t) = f_0(y,t) \quad (16)$$

$$\overline{\zeta'}(y,t) = g_0(y,t) \quad (17)$$

The mean value of the turbulent kinetic energy is given by

$$\overline{E}(y,t) = \sum_{n=-\infty}^{\infty} E_n(y,t) - E_0(y,t) \quad (18)$$

where each of the components of the energy spectrum function, $E_n(y,t)$, is given by

$$E_n(y,t) = \frac{1}{2} \left(|f_n'|^2 + \left(\frac{n\pi}{L}\right)^2 |f_n|^2 \right) \quad (19)$$

The normalized total turbulent kinetic energy over the domain is

$$\hat{E}(t) = \sum_{n=-\infty}^{\infty} E_n(t) - E_0(t) \quad (19a)$$

where

$$E_n(t) = \frac{1}{2} \int_{-1}^1 E_n(y,t) dy \quad (19b)$$

4. The Numerical Model

A rectangular grid of dimensions $2 \times 2L$ is used with $M \times N$ grid points located as shown in Figure 2. For the calculations presented herein 64×201 grid points were used. The indices k , j , and l denote stations along x , y , and t respectively and δx , δy , δt are the corresponding intervals. The value of the disturbance streamfunction $\Psi'(x,y,t)$ is then denoted by $\Psi_{K,J}^l$. The use of the primes will be discarded from this point unless necessary for clarity. Equations 5a and 5b are expressed in finite difference form as follows

$$\begin{aligned} \frac{\zeta_{K,J}^{l+1} - \zeta_{K,J}^{l-1}}{2\delta t} = & 3 \frac{\Psi_{K+1,J}^l - \Psi_{K-1,J}^l}{2\delta x} - U_J \frac{\zeta_{K+1,J}^l - \zeta_{K-1,J}^l}{2\delta x} \\ & + J_{K,J}^l + \frac{1}{R_e} \overline{\Delta^2} \zeta_{KJ}^l \end{aligned} \quad (20a)$$

$$\begin{aligned} \zeta_{K,J}^l = \Delta^2 \Psi_{K,J}^l = & \frac{1}{\delta x^2} \left(\Psi_{K+1,J}^l - 2\Psi_{K,J}^l + \Psi_{K-1,J}^l \right) \\ & + \frac{1}{\delta y^2} \left(\Psi_{K,J+1}^l - 2\Psi_{K,J}^l + \Psi_{K,J-1}^l \right) \end{aligned} \quad (20b)$$

where $\overline{\Delta^2}$ represents the modified form of the Laplacian differential operator of DuFort and Frankel (1958) defined as

$$\begin{aligned} \overline{\Delta^2} \zeta_{K,J}^l = & \frac{1}{\delta x^2} \left[\zeta_{K+1,J}^l - (\zeta_{K,J}^{l+1} + \zeta_{K,J}^{l-1}) + \zeta_{K-1,J}^l \right] \\ & + \frac{1}{\delta y^2} \left[\zeta_{K,J+1}^l - (\zeta_{K,J}^{l+1} + \zeta_{K,J}^{l-1}) + \zeta_{K,J-1}^l \right] \end{aligned} \quad (21)$$

and $J_{K,J}^l$ is the total energy and mean square vorticity conservation form of the non-linear advection terms introduced by Arakawa (1966).
i.e.,

$$\begin{aligned} J_{K,J}^l = & \frac{1}{3} \left\{ \Delta_y \Psi_{K,J}^l \Delta_x \zeta_{K,J}^l - \Delta_x \Psi_{K,J}^l \Delta_y \zeta_{K,J}^l \right\} \\ & + \frac{1}{3} \left\{ \Delta_y (\Psi \Delta_x \zeta)_{K,J}^l - \Delta_x (\Psi \Delta_y \zeta)_{K,J}^l \right\} \\ & + \frac{1}{3} \left\{ \Delta_x (\zeta \Delta_y \Psi)_{K,J}^l - \Delta_y (\zeta \Delta_x \Psi)_{K,J}^l \right\} \end{aligned} \quad (23)$$

where Δ_x and Δ_y denote ordinary first central differences.

Equation 20a is solved explicitly for $\zeta_{K,J}^{l+1}$ at each time step from the known values of $\Psi_{K,J}^l$, $\zeta_{K,J}^l$, and $\zeta_{K,J}^{l-1}$. The corresponding values of the $\Psi_{K,J}^{l+1}$ are obtained from equation 20b. Equation 20b represents a set of simultaneous algebraic equations to be solved for the $\Psi_{K,J}^l$ $K = 1, 2, \dots, M$; $J = 1, 2, \dots, N$ at each time step. Because of the large number of mesh points used in this investigation, conventional techniques are not suitable and an alternative method is used. We express the variables $\zeta_{K,J}^l$ and $\Psi_{K,J}^l$ in terms of their discrete Fourier transforms as follows:

$$\psi_{K,J}^l = \sum_{n=1}^M f_{n,J}^l e^{-i \theta_{n,K}} \quad (24a)$$

$$\zeta_{K,J}^l = \sum_{n=1}^M g_{n,J}^l e^{-i \theta_{n,K}} \quad (24b)$$

with

$$f_{n,J}^l = \frac{1}{M} \sum_{k=1}^M \psi_{K,J}^l e^{i \theta_{n,K}} \quad (24c)$$

$$g_{n,J}^l = \frac{1}{M} \sum_{k=1}^M \zeta_{K,J}^l e^{i \theta_{n,K}} \quad (24d)$$

where

$$\theta_{n,K} = \frac{2\pi(n-1)(k-1)}{M} \quad k, n = 1, 2, \dots, M$$

Substituting equations 24 into equation 20b yields the following equation for the Fourier components of $\psi_{K,J}^l$:

$$f_{n,J+1}^* - \alpha_n^* f_{n,J}^* + f_{n,J-1}^* = \delta_y^2 g_{n,J}^* \quad (25)$$

$$n = 1, 2, \dots, M$$

$$J = 1, 2, \dots, N$$

where

$$\alpha_n^* = 2 \left[1 - (\delta y / \delta x)^2 (\cos \theta_{n,2} - 1) \right].$$

The transforms and inverse transforms defined by equations 24 are computed by the fast Fourier algorithm of Cooley and Tukey (1965) while equations 25 are tri-diagonal and are easily solved for the $f_{n,J}$'s by Gauss elimination.

The assumed periodicity in x is automatically satisfied through equations 24. The boundary conditions at the walls (equation 6) are solved by setting $\Psi_{K,1}^l = \Psi_{K,N}^l = 0$ for all times and the no slip condition is satisfied in the following way. We express $\Psi_{K,J}^l$ in terms of $\Psi_{K,1}^l$ through a Taylor series expansion about a point on the wall.

$$\begin{aligned}
 \Psi_{K,2}^l &= \Psi_{K,1}^l + A_1 \delta y + A_2 \delta y^2 + A_3 \delta y^3 + \dots \\
 \Psi_{K,3}^l &= \Psi_{K,1}^l + 2A_1 \delta y + 4A_2 \delta y^2 + 8A_3 \delta y^3 + \dots \\
 \Psi_{K,4}^l &= \Psi_{K,1}^l + 2A_1 \delta y + 9A_2 \delta y^2 + 27A_3 \delta y^3 + \dots \\
 &\vdots \\
 &\text{etc.}
 \end{aligned} \tag{26}$$

The no slip condition ($\partial \Psi' / \partial y = 0$) is satisfied if we require that $A_1 = 0$ which implies that (since $\Psi_{K,1}^l = 0$)

$$\Psi_{K,2}^l = \frac{1}{2} \Psi_{K,3}^l - \frac{1}{9} \Psi_{K,4}^l \tag{27a}$$

and

$$\Psi_{K,N-1}^l = \frac{1}{2} \Psi_{K,N-2}^l - \frac{1}{9} \Psi_{K,N-3}^l \tag{27b}$$

for all k and l . The Poisson equation (5b) is satisfied (to second order) at the walls by

$$\zeta_{K,1}^l = 2A_2 = \frac{1}{\delta y^2} \left\{ \frac{3}{2} \Psi_{K,3}^l - \frac{4}{9} \Psi_{K,4}^l \right\} \tag{28a}$$

$$\zeta_{K,N}^l = \frac{1}{\delta y^2} \left\{ \frac{3}{2} \Psi_{K,N-2}^l - \frac{4}{9} \Psi_{K,N-3}^l \right\} \tag{28b}$$

The length of the time increment, δt , is fixed by the semi-empirical stability limit

$$\delta t = f \delta x \delta y \sqrt{(U + u)_0^2 + v_0'^2} \delta x \quad (29)$$

where the velocity components $(U+u')_0$ to v_0' are the maximum absolute magnitudes of velocity selected from a large sample of grid points. Numerical experimentation has shown that for values of $f \leq .6$ consistent results are obtained. Values of f near unity may lead to catastrophic instability in this explicit technique.

Since equation 20a is not "self starting" (it requires three time levels), the computation procedure starts with the forward difference representation

$$\begin{aligned} \frac{\zeta_{K,J}^{l+1} - \zeta_{K,J}^l}{\delta t} = & \frac{1}{2} \left\{ 3 \frac{\psi_{K+1,J}^{l+1} - \psi_{K-1,J}^{l+1}}{2\delta x} - U_J \frac{\zeta_{K+1,J}^{l+1} - \zeta_{K-1,J}^{l+1}}{2\delta x} \right. \\ & \left. + J_{K,J}^{l+1} + \frac{1}{Re} \Delta^2 \zeta_{K,J}^{l+1} \right\} \\ & + \frac{1}{2} \left\{ 3 \frac{\psi_{K+1,J}^l - \psi_{K-1,J}^l}{2\delta x} - U_J \frac{\zeta_{K+1,J}^l - \zeta_{K-1,J}^l}{2\delta x} \right. \\ & \left. + J_{K,J}^l + \frac{1}{Re} \Delta^2 \zeta_{K,J}^l \right\} . \end{aligned} \quad (30)$$

Equation 30 is also used periodically during the calculations in order to suppress any instabilities associated with the central time differencing used in equation 20a.

The computation procedure can now be outlined step-by-step.

1. An initial distribution of $\psi_{K,J}^0$ is chosen and the corresponding $\zeta_{K,J}^0$ are computed from equation 20b.

2. The time increment, δt , is computed from equation 29.
3. The values of $\zeta_{K,J}^1$ are computed for all the interior points ($J = 3, 4, \dots, N-2$) by iteratively solving equation 30.
4. The Fourier coefficients, $g_{n,J}^1$ are computed from equation 24d, equation 25 is solved for the $f_{n,J}^1$ and the corresponding values for the $\psi_{K,J}^1$ found from equation 24a for the interior points ($J = 3, 4, \dots, N-2$).
5. The remaining grid points for $\psi_{K,J}^1$, $\zeta_{K,J}^1$; $J = 1, 2, N-1, N$) are computed from equations 27a, 27b, 28a,b and 20b.
6. For each time step the procedure in steps 3, 4, and 5 is repeated except the explicit central difference equation 20a is used in step 3 rather than equation 30.
7. Periodically, say every 50 time steps, a new time increment, δt , is computed (step 2) and a single time step using the implicit forward difference equation 30 is used.

For all of the computations presented in this paper a grid with dimensions $M = 64$, $N = 201$ was used which required a computation time of approximately 17 seconds per time step.

5. Linear Calculations

In an investigation such as this it is desirable to make some comparison between the results of our numerical computations and some known solution to the Navier Stokes equations. The imposed restraint of two dimensionality precludes any comparison with experimental data and, of course, there are no exact solutions to the non-linear equations of motion. The only alternative is to consider the limiting case of infinitesimal disturbances for which the results from linear theory

are available. For this reason, a rather thorough investigation of the linear solutions to equations 5a and 5b was undertaken. For small amplitude disturbances the non-linear terms in the vorticity transport equation are neglected and the equations of motion become

$$\frac{\partial \zeta'}{\partial t} + U \frac{\partial \zeta'}{\partial x} - 3 \frac{\partial \Psi'}{\partial x} = \frac{1}{R_e} \nabla^2 \zeta' \quad (31a)$$

$$\zeta' = \nabla^2 \Psi' \quad (31b)$$

The general solution to equations 31 can be expressed in the form

$$\Psi'(x, y, t) = \sum_{n=-\infty}^{\infty} \sum_{m=1}^{\infty} \Phi_{nm}(y) e^{-i(n\alpha x - \beta_{nm} t)} \quad (32a)$$

$$\zeta'(x, y, t) = \sum_{n=-\infty}^{\infty} \sum_{m=1}^{\infty} \Theta_{nm}(y) e^{-i(n\alpha x - \beta_{nm} t)} \quad (32b)$$

with

$$\Theta_{nm} = \Phi_{nm}'' - (n\alpha)^2 \Phi_{nm} \quad (32c)$$

$$\alpha = 2\pi/\lambda$$

where λ is the wavelength of the disturbance.

Substituting equation 32 into 31 results in the well known Orr-Sommerfeld equation for $\Phi_{nm}(y)$; i.e.,

$$\begin{aligned} \Phi_{nm}^{IV} - 2(n\alpha)^2 \Phi_{nm}'' + (n\alpha)^4 \Phi_{nm} + i n\alpha R_e \left[\left(U - \frac{\beta_{nm}}{n\alpha} \right) \left(\Phi_{nm}'' \right. \right. \\ \left. \left. - (n\alpha)^2 \Phi_{nm} \right) + U'' \Phi_{nm} \right] = 0 \end{aligned} \quad (33a)$$

with boundary conditions

$$\Phi_{nm} = \Phi'_{nm} = 0 \quad \text{at} \quad y = \pm 1. \quad (33b)$$

Solutions of 33a for $\Phi_{nm}(y)$ for given α , n , and R_e can be made to satisfy the homogeneous boundary conditions (33b) only for the discrete eigenvalues, β_{nm} , $1 \leq m \leq \infty$. For the given α , n , and R_e we are usually interested in determining if there exist corresponding β_{nm} 's which have negative imaginary parts. The corresponding disturbance, $\Phi_{nm}(y)$, then grows exponentially with time and the flow is unstable to disturbances at the specified α , n , and R_e .

For the present analysis we are interested in solutions to equation 20a; hence, we must consider the finite difference representation of the linearized equation. For small disturbances equation 20a becomes

$$\begin{aligned} \frac{\zeta_{K,J}^{l+1} - \zeta_{K,J}^{l-1}}{2\delta t} = 3 \frac{\psi_{K+1,J}^l - \psi_{K-1,J}^l}{2\delta x} - U_J \frac{\zeta_{K+1,J}^l - \zeta_{K-1,J}^l}{2\delta x} \\ + 1/R_e \overline{\Delta^2} \zeta_{K,J}^l \end{aligned} \quad (34)$$

Again we will consider solutions of the form (32); hence, we have

$$\begin{aligned} \psi_{K,J}^l = (\Phi_J)_{nm} e^{-i(n\alpha(k-1)\delta x - \beta_{nm} l \delta t)} \\ \zeta_{K,J}^l = (\Theta_J)_{nm} e^{-i(n\alpha(k-1)\delta x - \beta_{nm} l \delta t)} \end{aligned} \quad (35)$$

Substituting into 34 and 20b results in

$$\beta'_{nm} (\Theta_J)_{nm} = i n \alpha' \left[U_J (\Theta_J)_{nm} + 3 (\Phi_J)_{nm} \right] + \frac{1}{R_e \delta y^2} \left[(\Theta_{J+1})_{nm} + \omega (\Theta_J)_{nm} + (\Theta_{J-1})_{nm} \right] \quad (36a)$$

$$(\theta_J)_{nm} = \frac{1}{\delta y^2} \left[(\Phi_{J+1})_{nm} + \omega' (\Phi_J)_{nm} + (\Phi_{J-1})_{nm} \right] \quad (36b)$$

where

$$\omega = 2 \left((\delta y / \delta x)^2 \cos n\alpha \delta x \right) \quad (37a)$$

$$\omega' = -2 \left[1 + \left(\frac{\delta y}{\delta x} \right)^2 (1 - \cos n\alpha \delta x) \right] \quad (37b)$$

$$\alpha' = \sin n\alpha \delta x / n\delta x \quad (37c)$$

and

$$\beta'_{nm} = 2 \left[1 + 1/R_e \delta x^2 \right] \cos \beta_{nm} \delta t + i \frac{\sin \beta_{nm} \delta t}{\delta t} \quad (37d)$$

$$i = \sqrt{-1}$$

When expression 36b for $(\theta_J)_{nm}$ is substituted into equation 36a there results a homogeneous set of linear algebraic equations for the $(\Phi_J)_{nm}$. For given values of α , n , R_e , δx , δy , and δt we wish to determine the eigenvalues and eigenvectors of the matrix of coefficients of the $(\Phi_J)_{nm}$. In particular, we are interested in those eigenvalues β_{nm} for which the imaginary part of β_{nm} is negative and in the associated eigenvectors $(\Phi_J)_{nm}$. The effects of δx , δy , and δt on the linear solution are especially important for the present application.

The eigenvalues and eigenvectors have been computed for a number of Reynolds numbers and for a wide range of α 's using the QR algorithm (Wilkinson 1965 or Fair 1971). For more details on these calculations the reader is referred to O'Brien (1970) or to the report by Gawain and Clark (1971). In the latter report some of the eigenvalues (β_{nm}) and

eigenfunctions ($\phi_{nm}(y)$) are tabulated for the case $\alpha = 1.0$, $R_e = 6667$. In the limit as $\delta x, \delta t \rightarrow 0$, the problem is the same as that solved by Thomas (1953) although the methods used are quite different from those employed by Thomas. For the case $\alpha = 1.0$, $R_e = 6667$, and $\delta y = .01$ (in Thomas' notation this corresponds to $\alpha = 1.0$, $R_e = 10,000$, $\delta y = .01$) we have solved equations 36 for $n = 1, 2, 3$, and 4. Our solutions show that there is only one unstable eigenvalue and this unstable solution occurs for $n = 1$. We shall order the eigenvalues, β_{nm} , so that for a given n , the m 's are arranged according to the stability of the computed eigenvalues. Hence, for the case $\alpha = 1.0$, $R_e = 6667$, β_{11} is the unstable eigenvalue with the corresponding eigenfunction $\phi_{11}(y)$. Thomas gives a value of $\beta_{11} = .3653 - i .0055$ and the corresponding mode shape, $\phi_{11}(y)$ is tabulated in his Table V. (Using our non-dimensionalization, β_{11} is exactly 1.5 times the value given by Thomas.) Our calculations yield the value $\beta_{11} = .3593 - i .0041$ and the corresponding mode shape, $\phi_{11}(y)$, is shown in Figure 3 for comparison with that of Thomas.

Now consider the influence of the finite difference parameters δx , δy , and δt on the solutions to 36. The effect of δy on the growth rate (β_{11}) is illustrated in Figure 4. As δy increases the flow becomes more and more stable and when $\delta y = .05$, the phenomenon of linear instability has been completely obscured by the crude finite difference representation of the equations of motion. Indeed, calculations with $\delta y = .05$ for a wide range of Reynolds numbers and α 's have shown no indication of linear instability.

The effect of varying δx was investigated at $R_e = 6667$, $\alpha = 1.0$, $\delta y = .01$ and $\delta t < .02$. Figure 5 shows the variation with δx of the growth

rate ($\Im \beta_{11}$) and phase velocity ($\Re \beta_{11}$) for the unstable mode. For $\delta x < .8$ the changes in the disturbance profile ($\Phi_{11}(y)$) were insignificant.

Perhaps the most surprising discovery in this investigation of the linear behavior of the discrete representation of the equations of motion was the significance of the time interval, δt , on the disturbance growth rate ($\Im \beta_{11}$). The effects of δt on this parameter are shown in Figure 6. There are significant departures from the "exact" value of $\Im \beta_{11}$ for $\delta t > .04$ while the phase velocity and mode shape are not significantly changed. Hence, in addition to the usual stability constraint (29) on the time interval, δt , it is necessary that $\delta t < .04$ in the numerical integration scheme described in section 4.

We can now summarize the results presented in the preceding discussion. Increasing the y increment, δy , tends to make the flow more stable and for coarse grids ($\delta y > .05$) the phenomenon of linear instability is completely obscured. The linear solution is comparatively insensitive to changes in δx , at least, until the x -increment is approximately the same length as the channel half-width. The growth rate of the disturbance is strongly influenced by the δt increment (due to the DuFort-Frankel representation of the diffusion term) and for large δt the growth rate is much higher than that predicted by the "exact" linear solution.

6. Numerical Integration of the Vorticity Equation

(a) Small Amplitude Disturbances

We now return to the numerical integration of the vorticity equation using the techniques described in Section 4. As a check on the validity of the solution we first consider the limiting case of

small amplitude disturbances and compare the results obtained with the known results from the linear solution as described in the preceeding section. To be more explicit, for a given Reynolds number and initial disturbance streamfunction, $\Psi'(x,y,0)$, are the results from the numerical integration consistent with the values of β_{nm} and $\Phi_{nm}(y)$ predicted by linear theory?

A series of calculations were made at $R_e = 6667$ and the initial disturbance given by

$$\Psi'(x,y,0) = \epsilon \left\{ f_1(y,0) e^{-i\alpha x} + f_1^*(y,0) e^{+i\alpha x} \right\} \quad (38)$$

where ϵ is an amplitude factor. For ϵ sufficiently small the non-linear terms in equation 5a should be negligible and the numerical integration should give results which are in agreement with the linear theory. As a first test we choose $\alpha = 1.0$, $R_e = 6667$, $\epsilon = .005$ and the initial mode shape identical to the unstable mode computed from linear theory; i.e., $f_1(y,0) = \Phi_{11}(y)$, where $\Phi_{11}(y)$ was shown in Figure 3. The growth rate of the disturbance kinetic energy, $\hat{E}(t)$, as defined by equation 12c is shown in Figure 7. The computed growth rate gives a value of $\beta_{11} = .0050$ which is in good agreement with the value given by Thomas. From equation 14 we can determine the phase, $\phi_n(y,t)$, of any of the spectral components of $\Psi'(x,y,t)$ by

$$\phi_n(y,t) = \tan^{-1} \left(\frac{f_n}{\alpha f_n} \right) \quad (39)$$

The phase velocity, c_n , or rate of propagation, of any of the spectral components is then

$$c_n = \frac{1}{n\alpha} \frac{\partial \phi_n}{\partial t} \quad (40)$$

For these computations the grid length, $2L$, was set equal to the wavelength, λ , of the disturbance; so for the disturbance (primary) mode, $n = 1$, and in the linear range we can identify c_1 with $\alpha \beta_{11}$ from the linear theory. Figure 10 shows that c_1 is, indeed, a constant and the slope of this phase versus time plot shows that $c_1 = .363$ which is in excellent agreement with Thomas' value of $\alpha \beta_{11} = .3653$ and with our value of $\alpha \beta_{11} = 3593$.

Other short computations were carried out with, again, $\alpha = 1.0$, $R_e = 6667$, $\epsilon = .005$, but with the initial mode shape, $f_1(y,0)$, chosen to correspond to one of the stable modes computed from linear theory. These calculations were carried out by arbitrarily setting $f_1(y,0)$ equal to the mode ϕ_{17} , ϕ_{28} , and ϕ_{22}^* which are shown in Figure 9. The energy decay rates for these three cases are shown in Figure 10. From the energy decay rates and from the computed phase velocities (not shown here) the numerical integration technique yields the following values for the appropriate eigenvalues

$$\beta_{17} = 1.351 + i .138, \quad \beta_{28} = 1.425 + i .207$$

$$\beta_{22} = 1.456 + i .0764.$$

The linear matrix solution described in the preceeding section gave the values

$$\beta_{17} = 1.363 + i .136; \quad \beta_{28} = 1.403 + i .192;$$

$$\beta_{22} = 1.462 + i .0742.$$

* Since equation 33a is symmetrical in y it is possible to divide the solutions for $\phi_{nm}(y)$ into even and odd solutions. The boundary conditions are $\phi_{nm}(+1) = \phi'_{nm}(+1) = 0$, with $\phi'_{nm}(0) = \phi''_{nm}(0) = 0$ for even solutions and $\phi_{nm}(0) = \phi''_{nm}(0) = 0$ for odd solutions. For our numerical model with N lateral stations there are $N-2$ unknown $(\phi_j)_{nm}$'s; hence, $N-2$ eigenvalues are computed for each n , α , R_e . Of these $N-2$ eigenvalues, $\frac{N-1}{2}$ correspond to even solutions and $\frac{N-3}{2}$ correspond to odd solutions.

A more critical test of the numerical integration is the ability to predict the correct mode shape, $\Phi_{nm}(y)$, for a disturbance of known wavelength and at a fixed R_e . Suppose in equation 38 we choose $\alpha = 1.0$ but arbitrarily select the initial disturbance mode shape $f_1(y,0)$. The arbitrary function $f_1(y,0)$ can be expressed in terms of the eigenfunctions, $\Phi_{1m}(y)$, of the Orr-Sommerfeld equation (33a) for the chosen α and R_e (Schensted, 1961). i.e.,

$$f_1(y,0) = \sum_{m=1}^{\infty} A_m \Phi_{1m}(y) \quad (41a)$$

with

$$A_m = \int_{-1}^1 f_1(y,0) \chi_m(y) dy \quad (41b)$$

and

$$\chi_m(y) = \left(\frac{d^2}{dy^2} - \alpha^2 \right) \tilde{\Phi}_{1m}$$

where $\tilde{\Phi}_{1m}(y)$ is the solution to the adjoint of equation 33a. However, the linear solution tells us that only one of the Φ_{1m} in equation 41a is unstable; all other modes will decay with time. Hence, in the linear range only one mode, $\Phi_{11}(y)$, grows and will eventually dominate all the other terms in the expansion (41a). Therefore, the mode shape

$$f_1(y,t) \rightarrow \Phi_{11}(y) \quad \text{as } t \rightarrow \infty$$

where $\Phi_{11}(y)$ is as shown in Figure 3 for the case $\alpha = 1.0$, $R_e = 6667$. The initial shape chosen for $f_1(y,0)$ is shown in Figure 11. The disturbance kinetic energy, $\hat{E}(t)$, is given in Figure 12 and the mode shapes, $f_1(y,t)$, are shown for various times during the calculations.

As expected, the disturbance energy at first rapidly decreases then grows according to linear theory while the computed mode shape is clearly tending towards the predicted shape of $\Phi_{11}(y)$.

From the results discussed in this section and from calculations at other wavenumbers, α , we have found that the numerical integration scheme consistently gives results that are in excellent agreement with the linear theory. The agreement between the results of the numerical model and the predicted results for small amplitude disturbances is gratifying and gives some confidence in the non-linear calculations now to be discussed.

b) Finite Amplitude Disturbances

Before discussing the results of the non-linear aspects of this investigation it is appropriate to give a very brief outline of the features of the existing non-linear theories which predict equations of the form of equation 1. The following discussion is from the paper by Pekeris and Shkoller (1967) which in turn outlines Stuart's (1960) theory for finite amplitude disturbances. If the Fourier representations for the disturbance streamfunction, Ψ' , and vorticity, ζ' ; (equations 14 and 15) are substituted into the equation of motion (5a) the following equation for the modes results:

$$\frac{\partial g_n}{\partial t} = \frac{1}{R_e} (g_n'' - (n\alpha)^2 g_n) + i n \alpha \left[(U - f_0') g_n - (U'' - f_0'') f_n \right] \quad (42)$$

$$- i \alpha H_n \quad n = 0, 1, 2, \dots$$

where

$$g_n = f_n'' - (n\alpha)^2 f_n \quad (15c)$$

and

$$H_n = \sum_{s=1}^{\infty} \left\{ (n-s)(f_s' g_{n-s} - g_s' f_{n-s}) + (n+s)(f_s^{*'} g_{n+s} - g_s^{*'} f_{n+s}) \right\} \quad (42a)$$

If the parameter, $\epsilon_0^2 \equiv |\beta_{11}|$, is small (implying proximity to the neutral curve) then Stuart showed that in an approximation in which terms of order $\epsilon_0^{3/2}$ are retained, only the f_0 , f_1 , and f_2 in (14a) are significant. Now expand $f_1(y,t)$ in terms of the eigenfunctions, ϕ_{1m} , of the Orr-Sommerfeld equation as was done in equation (41a), so that

$$f_1(y,t) = \epsilon_0 \sum_{m=1}^{\infty} A_m(t) \phi_{1m} \quad (43)$$

Stuart's asymptotic analysis for small ϵ_0 shows that only the first term in (43) is important, i.e.,

$$f_1(y,t) \approx \epsilon_0 A_1(t) \phi_{11}(y) + O(\epsilon_0^3) \quad (44)$$

and that the terms f_0 and f_2 are of smaller order so that

$$f_0(y,t) = \epsilon_0^2 |A_1(t)|^2 G_0(y) + O(\epsilon_0^4) \quad (45)$$

$$f_2(y,t) = \epsilon_0^2 A_1^2(t) G_2(y) + O(\epsilon_0^4) \quad (46)$$

The functions G_0 and G_2 are determined from Pekeris and Shkoller's equations (22), (23), and (24). By substituting equations (44), (45), and (46) into (42) one can obtain an expression of the form (1) for the amplitude parameter, $|A_1(t)|^2$, i.e.,

$$\frac{d|A_1|^2}{dt} = k_1 |A_1|^2 + k_2 |A_1|^4 \quad (1)$$

The important point from our viewpoint is that according to the above analysis, the disturbance energy should be contained primarily in the $f_1(y,t)$ mode and that the growth of this energy should behave according to equation (1). Assuming that the disturbance streamfunction can be adequately represented by f_1 then we have from (44)

$$\psi'(x,y,t) = \epsilon_0 \left(A_1(t) \phi_{11}(y) e^{-i\alpha x} + A_1^*(t) \phi_{11}^*(y) e^{+i\alpha x} \right) \quad (47)$$

The disturbance kinetic energy as defined by equation (12c) (since we are neglecting the contribution from f_0 the "disturbance" and "turbulent" kinetic energies are the same) becomes

$$\hat{E}(t) = \epsilon_0^2 I |A_1(t)|^2 \quad (48)$$

where

$$I = \int_0^1 \left\{ |\phi'_{11}|^2 + \alpha^2 |\phi_{11}|^2 \right\} dy \quad (49)$$

It was pointed out in part 2 of this paper that the constant, k_1 , in (1) is related to the amplification factor of linear theory ($k_1 = -2\beta_{11}$) and if $k_2 < 0$ then the growth of an unstable disturbance is limited so that

$$|A_1|^2 \rightarrow k_1/k_2 \quad (50)$$

Pekeris and Shkoller found that these conditions are satisfied for α and R_e inside the lower portion of the neutral curve. For example, at $R_e = 6667$ and $\alpha = .90$ their calculations give

$$|A_1|^2 \rightarrow 1/9$$

Our solutions to the linear eigenvalue problem at $R_e = 6667$ and $\alpha = .875$ gives $\beta_{11} = -.00394$ and $I = 1.848$. Hence,

$$\hat{E}(t) \rightarrow (1.848)(.00394)/9.0 = 8.08 \times 10^{-4}$$

Figure 13 shows the energy growth for modes E_0 , E_1 , E_2 , and E_3 for a run with the initial disturbance given by (38) with $\alpha = .875$, $R_e = 6667$, $\epsilon = .005$, and $f_1(y,0) = \phi_{11}(y)$ where ϕ_{11} is the unstable eigenfunction for $\alpha = .875$. The disturbance is, indeed dominated by $E_1(t)$ and the mode shape, $f_1(y,t)$, normalized so that $f_1(0,t) = 1.0$, never departed from the initial shape given by $\phi_{11}(y)$. A longer calculation was made using the same initial conditions except in this case $\alpha = 1.0$. Again the energy remained predominately in the $n = 1$ mode and again the mode shape for $f_1(y,t)$ never departed from the initial $\phi_{11}(y)$ shape indicating that (44) and (47) do indeed adequately represent the flow as far as the overall disturbance energy is concerned.

Although this latter calculation required 34.5 hours of computer time, we can see that the energy growth is still within the linear range. This demonstrates that, as was pointed out in part 2, it is impractical using the present techniques to follow the disturbance through the linear and into the non-linear range of amplitudes. For this reason we have been unable to establish whether or not the "supercritical" equilibrium states as predicted by (1) and (50) do, in fact, exist for our exact treatment. Our calculations, as shown in Figures 13 and 14, do indicate, however, that there is no significant

difference between cases for which $\alpha = .875$ or $\alpha = 1.0$ in equation (38). The calculation of Pekeris and Shkoller, however, show that "super-critical" equilibrium states are possible for $\alpha = .875$ but not for $\alpha = 1.0$. All our calculations for both low and high amplitude disturbances have shown no strong dependence on α as far as the final result is concerned.

Although this last run was entirely within the linear energy growth range we will see that there were very interesting non-linear features to the calculations. The appearance of energy in modes E_0 , E_2 , and E_3 as shown in Figure 14 is, of course, due to the presence of the non-linear terms in equation (5a). In identical calculations for which the non-linear terms in (5a) were deliberately omitted the primary ($n=1$) mode grew according to linear theory while the energy in the other modes remained constant or decreased and the energy levels (due to numerical "noise") were twelve to fifteen orders of magnitude lower than that of the primary mode. Figure 14 shows that the energy in the other modes ($n = 0, 2, 3$) grows very rapidly at first and then seems to follow an exponential growth rate, i.e.,

$$E_n(t) \sim e^{2\beta_n t} \quad n = 0, 1, 2, 3$$

for large t . From the data shown in Figure 14 the values for β_n are $\beta_0 = .0114$, $\beta_1 = .0050$, $\beta_2 = .0080$, and $\beta_3 = .0117$.

The most interesting feature is the shape of the modes, f_2, f_3 , with respect to y^* . These shapes are shown in Figure 15 where the modes are normalized so that $f_n(0,t) = 1.0$ for even modes and for odd modes the maximum real and imaginary parts of $f_n(y)$ are unity. The phase velocities for these modes averaged between $t = 65$ and $t = 71$ were $c_2 = .362$ and $c_3 = .363$. These phase velocities are the same as the phase velocity of the primary mode predictable from linear theory (i.e. $\beta_{11} = .363$).

The striking feature is the strong resemblance between these modes and the modes calculated from the Orr-Sommerfeld equation. Indeed, it appears that the non-linear solution has spontaneously generated modes that can be predicted from the linear theory even though the linear solution indicates that these are stable modes and would decay with time. This means that if we represent each mode by an expression of the form of (43) i.e.,

$$f_n(y,t) = \sum_{m=1}^{\infty} A_m(t) \phi_{nm}(y) \quad (51)$$

*From equation (15c) we see that g_n has the same symmetry or anti-symmetry as does f_n ; i.e. if $f_n(y)$ is an even function of y then g_n is also even. Then from equation (42) we can establish that if $\psi'(x,y,0)$ is given by (38) and $f_1(y,0)$ is even in y then $f_0(y,t)$ is odd, $f_2(y,t)$ is odd, $f_3(y,t)$ is even, $f_4(y,t)$ is odd, etc. Likewise if $f_1(y,0)$ is odd then $f_0(y,t)$ is odd, $f_2(y,t)$ even, $f_3(y,t)$ odd, $f_4(y,t)$ is even, etc. For example, let $f_1(y,0)$ be even. Then since $f_n(y,0) = 0$ $n \neq 1$

$$\frac{\partial g_2}{\partial t} \Big|_{t=0} = -i \alpha H_2 \Big|_{t=0} = -i \alpha [f_1' g_1 - g_1' f_1]$$

= odd function of y .

At the next time step, $t = \delta t$

$$g_2(y, \delta t) = \left(\frac{\partial g_2}{\partial t} \right) \delta t = \text{odd function of } y$$

then one mode seems to dominate the expansion. It is interesting to notice that in each case the dominant mode is one for which there exist a step gradient near the wall. Most of the stable modes that we have computed from linear theory are similar to the ones shown in Figure 9 which have a detailed structure near the center of the channel rather than near the wall.

A series of higher energy runs with various initial disturbance amplitudes was made at $R_e = 6667$ using as initial conditions a disturbance with wave number $\alpha = 1.0$ and that mode shape given by Thomas (see Figure 3). The total energy growth (or decay) is shown in Figure 16 for several different initial energy levels. A further energy breakdown is given in Figure 17 for the cases $\epsilon = (.05)\sqrt{5}$. For this case the total energy remains almost constant while there is a continual exchange of energy between the mean flow and the turbulence. The turbulent kinetic energy oscillates about a value of $\hat{E}(t) = .03$ which is roughly ten times the equilibrium value predicted from equation 50. From Figure 14a it seems that there is a tendency towards some common energy equilibrium state for the different initial conditions. A more detailed inspection of the flow structure shows that there are significant differences between the three flows. Starting with the high energy run we summarize the structure of the flow by presenting plots of the mean velocity profile, Reynolds stresses, and energy spectrum at various times throughout the run (Figures 18, 19, and 20). Also, in Figure 21 the shape of the primary ($n = 1$) mode at the end of the calculations is shown for each of the three energy levels. For the high energy run (although the time parameter is comparatively small) there are drastic

alterations of the mean velocity profile and primary mode shape and considerable energy transfer from the primary mode to the higher harmonics. For the two lower energy runs there is little alteration of the parabolic velocity profile and only small amounts of energy transfer to higher wave numbers. For the lowest initial energy level ($\epsilon = .05 / \sqrt{2}$) the primary mode shape remains essentially unchanged throughout the entire calculation. More details of this low energy run are shown in Figure 22 where the growth of the total turbulent energy in the first three spectral components (equation 19b) is shown. The phase velocities (equation 40) were computed near the end of the run and are summarized below:

$$c_1 = .492, \quad c_2 = .484, \quad c_3 = .473$$

The measured C_n were independent of y and all are roughly 40% higher than the wave velocity ($R\beta_{11}$) of the primary unstable mode predicted by linear theory. This low energy run has some qualitative similarities to the predictions of the non-linear theory which was outlined at the beginning of this section. That is, there appears to be an asymptotic energy level, the primary mode shape is only slightly altered and the energy in the primary mode remains dominant.

In order to investigate the influence of initial wavenumber on the flow two runs were made at $R_e = 6667$ with $\alpha = .875$ (near the lower branch of the neutral curve) and with $\alpha = 1.05$ (near the upper branch). For both cases the initial mode shape was determined from the eigenvalue solution to the linear equations and the initial energy was chosen to be slightly lower than that of the run ($\epsilon = .05/\sqrt{5}$,

Figure 16) which seemed to remain in an energy equilibrium state. The energy variation for these cases is shown in Figure 23. There is no obvious qualitative difference between the three wavenumbers; the initial high energy level, however, apparently causes oscillations of the disturbance kinetic energy and makes any direct comparison with non-linear theory rather difficult.

Another important question which arises in the consideration of non-linear aspects in the stability of plane Poiseuille flows is whether or not a flow which is stable to infinitesimal disturbances might be unstable to disturbances of some finite amplitude. Such instabilities are generally referred to as "subcritical" instabilities. To investigate this aspect of the problem several runs were made using as initial conditions a disturbance that is known to be stable in the linear range. The case chosen was for $\alpha = .78$, $R_e = 6667$ for which $\beta_{11} = .249 + i .00124$ for the least stable eigenfunction determined from the linear solution described in Section 5. Again the initial disturbance was given by equation 38 with the function $f_1(y,0) = \phi_{11}(y)$ determined from the linear solution. For a small amplitude disturbance ($\epsilon = .005$) the disturbance energy decreased with time according to linear theory while for a larger amplitude ($\epsilon = .0635$). The energy variation was as shown in Figure 24. The familiar oscillation of the turbulent kinetic energy which is associated with an initially high disturbance energy is present in this case; while the total kinetic energy appears to remain approximately constant after an initial decrease.

We now address ourselves to the question posed at the end of Section 2 concerning the character of a two dimensional "turbulence"

in channel flows. For all the runs discussed above the computational grid length ($2L$) was equal to the wavelength of the initial unstable disturbance (i.e. $2L = 2\pi/\alpha$). In any finite difference representation of the equations of motion there are only discrete wavelengths available to be excited by the non-linear interactions. Recall from equation 24a that the streamfunction is expressed as

$$\Psi_{K,J} = \sum_{n=1}^M f_{n,J} e^{-i\theta_{n,k}} \quad (24a)$$

and since $\Psi_{K,J}$ is real

$$\Re f_{n,J} = \Re f_{M-n+2,J}$$

$$\Im f_{n,J} = -\Im f_{M-n+2,J}$$

i.e., $\Re f_{n,J}$ is even and $\Im f_{n,J}$ is odd over the interval $n = 1, 2, \dots, M/2, \dots, M$. Therefore, there are $M/2$ distinct Fourier modes "available" to the solution of the equations of motion. When the grid length equals the wavelength of the initial disturbance there is only one lower mode available to be excited; namely, the zero mode, $f_{0,J}$. It is known that two-dimensionality constrains the transfer of energy between the modes of which the disturbance is composed. For an isotropic two-dimensional turbulence there can be no systematic transfer of energy from lower to higher wave numbers without a corresponding transfer to still lower wavenumbers (Lilly (1968), Kraichnan (1967)). Hence, one may suspect that our discrete representation in which there are no available modes at lower wave numbers could force the disturbance energy to remain in the primary initial mode. The first

alternative to this dilemma would seem to be to increase the grid length, $2L$, thereby allowing modes with both higher and lower wave numbers to fit into the available grid length. However, if the initial disturbance energy is contained in, say, wave number n then the non-linear interaction of this mode with itself will initially excite wave numbers 0 and $2n$; later modes $0, 2n, 3n, 4n$, etc. The modes that can be excited will be separated by a spacing of n in wave number space, resulting in a spectrum with "holes" or regions in which no energy can appear. Clearly, this is not a realistic case. The alternative to this situation is to initially perturb the flow with a disturbance in which at least two contiguous (in the discrete wave number space) modes are present. For example, if the initial disturbance contains modes n and $n+1$ then the non-linear interaction will, at first, excite modes $0, 1, 2n, 2n+1, 2n+2$; these in turn will excite modes $0, 1, n-1, 2n-1, 4n$, etc. until all possible wave numbers have been excited.

It seems reasonable to require that the wavelengths of these two initial modes should both fall within the unstable region in the $(\alpha-R_e)$ plane. If we set the grid length so that $2L=16\pi$ (or $\alpha = 1/8$) then modes with wavenumbers 7α and 8α will both fall within the unstable region. Hence

$$\Psi'(x,y,0) = \epsilon \left\{ f_7 e^{-i7\alpha x} + f_8 e^{-i8\alpha x} + f_7^* e^{+i7\alpha x} + f_8^* e^{+i8\alpha x} \right\}$$

A lengthy numerical integration of the vorticity equations using the initial conditions just described is summarized in Figures 25 and 26 which show the turbulent kinetic energy time variation and the energy spectrum at various times during the run. For this run the turbulent kinetic energy initially grows and then appears to vary randomly about a value of $\hat{E}(t) = .019$. The energy spectrum is quite different from the other cases presented in that there is a gradual transfer of significant amounts of energy to other wavenumbers. Although it is not shown here, the mean velocity profile again differed only slightly from the parabolic distribution. Although, there are significant differences between this run and the others presented, all the examples that have been discussed are qualitatively similar in that most of the energy remains in modes whose wavelength approximately equals that of the primary (unstable) mode.

7. Conclusion

Our numerical technique for integrating the vorticity equation has been shown to be stable and predicts results that are consistent with linear solutions to the vorticity equation.

The influence of the finite difference representation on the linear eigenvalue solution to the equations of motion was investigated and some interesting conclusions resulted. The size of the δy increment significantly influences the stability of the equations and for grids with $\delta y > .05$ (approximately) the equations are stable to all disturbance. Because of the DuFort-Frankel representation of the diffusion term, the growth rate of an unstable disturbance is strongly influenced by the δt increment. The growth rate increases

rapidly with δt even though the time step increment may still be small enough to satisfy ordinary numerical stability requirements. The δx increment has the smallest effect on the linear solution and seems to be significant only when δx is approximately equal to the channel half-width.

Because of the long computing time required we were unable to follow the growth of an unstable disturbance through the linear and into the non-linear range of disturbance amplitudes. This precluded any direct comparison of our results with those predicted by the non-linear theories of Stuart and Watson and Reynolds and Potter. We can, however, make some general comparisons. We find qualitative agreement in the sense that the unstable primary mode dominates the disturbance and there is little distortion of the mean flow. The calculations presented indicate the existence of a disturbance energy equilibrium state which seems to be common (for a given Reynolds number) to all unstable disturbances despite their initial energy or wavenumber. Indeed, we have found no outstanding differences in the behaviour of disturbances with varying initial wave numbers (at a constant R_e) which is not in agreement with the non-linear theories. The distortion of the primary mode shape is significant when the initial energy is high enough to be well beyond the linear range but for lower initial energies the distortion of the mode shape is less important.

The computed flows which have been discussed in this paper show little resemblance to actual turbulent shear flows. In a true three dimensional flow one would expect an initial unstable disturbance

with a length scale approximately 2π times the channel half width to grow in amplitude and through non-linear interactions the energy of the disturbance would be transferred to higher wavenumbers with length scales comparable to the channel half width. The corresponding situation for a two dimensional turbulent channel flow is not clear. However, for two dimensional homogeneous turbulence the energy would cascade to the lower wavenumbers while mean square vorticity is transferred to higher wavenumbers when the turbulent energy is continually fed into the flow in a narrow band of spectral components. Neither of these processes was observed for the present calculations.

One can speculate that our calculated "quasi-equilibrium" states in which most of the energy remains in one or two spectral components with little alteration of the parabolic velocity profile represent two dimensional solutions to the equations of motion which are, in some sense, highly unstable flows and, for this reason, are not observed experimentally.

REFERENCES

1. Arakawa, A., 1966 "A Computational Design for Long Term Numerical Integration of the Equations of Fluid Motion: Two Dimensional Incompressible Flow, Part 1." J. Comp. Physics, 1, 1, pp. 119-143.
2. Cooley, J. W. and Tukey, J. W., 1965. "An Algorithm for the Machine Calculation of Complex Fourier Series," Math Comp., 19, 90, pp. 297-301.
3. DuFort, E. G. and Frankel, S. P., 1953. "Stability Conditions in the Numerical Treatment of Parabolic Differential Equations," Math Tables and Other Aids to Computation, 7, pp. 135-152.
4. Emmons, H. W., 1970. "Critique of Numerical Modeling," in Annual Review of Fluid Mechanics, Vol 2, Palo Alto, California: Annual Reviews, Inc.
5. Fair, G., 1971. "Allmat: A TSS/360 Fortran IV Subroutine for Eigenvalues and Eigenvectors of a General Complex Matrix," NASA TN D-7032.
6. Gawain, T. H. and Clark, W. H., 1971. "Tables of Eigenvalues and Eigenfunctions of the Orr-Sommerfeld Equation," to be published as Naval Postgraduate School Report, Monterey, California.
7. Kraichnan, R. H., 1967. "Inertial Ranges in Two-Dimensional Turbulence," Phys Fluids. 10, 7.
8. Lilly, D. K., 1970. "The Numerical Simulation of Three-Dimensional Turbulence with Two Dimensions." V. VII, SIAM-AMS Proceedings, American Mathematical Society, pp. 41-53.
9. O'Brien, G. D., 1970. "A Numerical Investigation of Finite-Amplitude Disturbances in a Plane Poiseuille Flow," Naval Postgraduate School, Ph.D. thesis.
10. Pekeris, C. L. and Shkoller, B., 1967. "Stability of Plane Poiseuille Flow to Periodic Disturbances of Finite Amplitude in the Vicinity of the Neutral Curve," JFM 29, 1.
11. Reynolds, W. C. and Potter, M. C., 1967. "Finite Amplitude Instability of Parallel Shear Flows," JFM 27, 3.
12. Schensted, I. V., 1961. "Contributions to the Theory of Hydrodynamic Stability," University of Michigan, Ph.D. Thesis.

13. Stuart, J. T., 1960. "On the Non-linear Mechanics of Wave Disturbances in Stable and Unstable Parallel Flows," part 1. JFM 9, 2.
14. Thomas, L. H., 1953. "The stability of Plane Poiseuille Flow," Phys Rev., 91, 4, pp. 780.
15. Watson, J., 1960. "On the Non-linear Mechanics of Wave Disturbances in Stable and Unstable Parallel Flows," part 2. JFM 9, 2.
16. Wilkinson, J. A., 1965. The Algebraic Eigenvalue Problem, pp. 485-569, Clarendon Press.

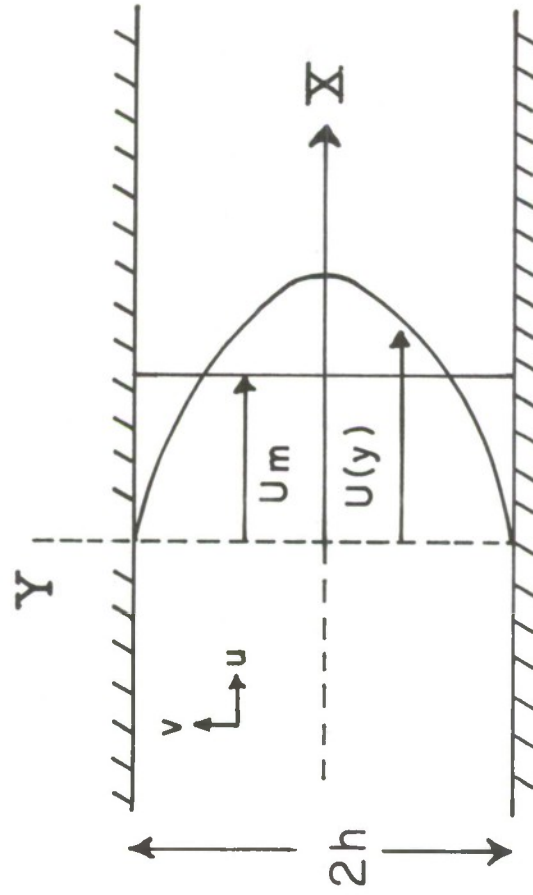


Figure 1. $R_e = U_m h / \nu$; $y = Y/h$, $x = X/h$
 $U(y) = 3/2 (1 - y^2)$

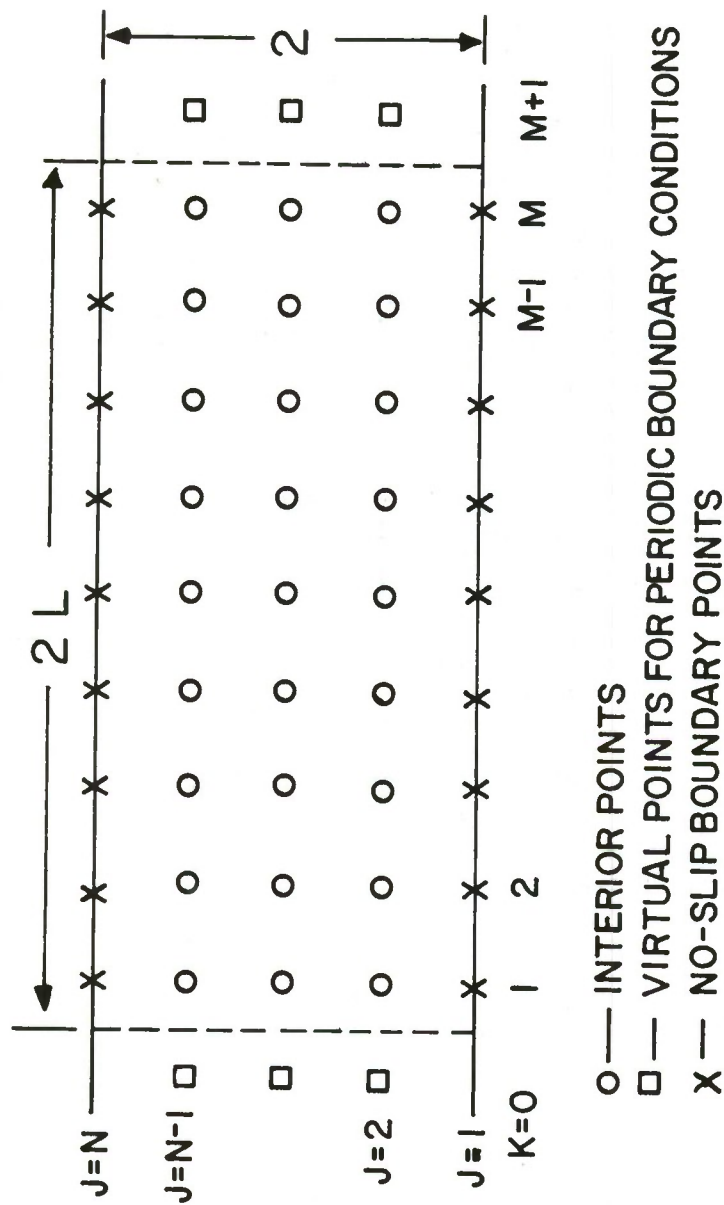


Figure 2. Finite Difference Mesh

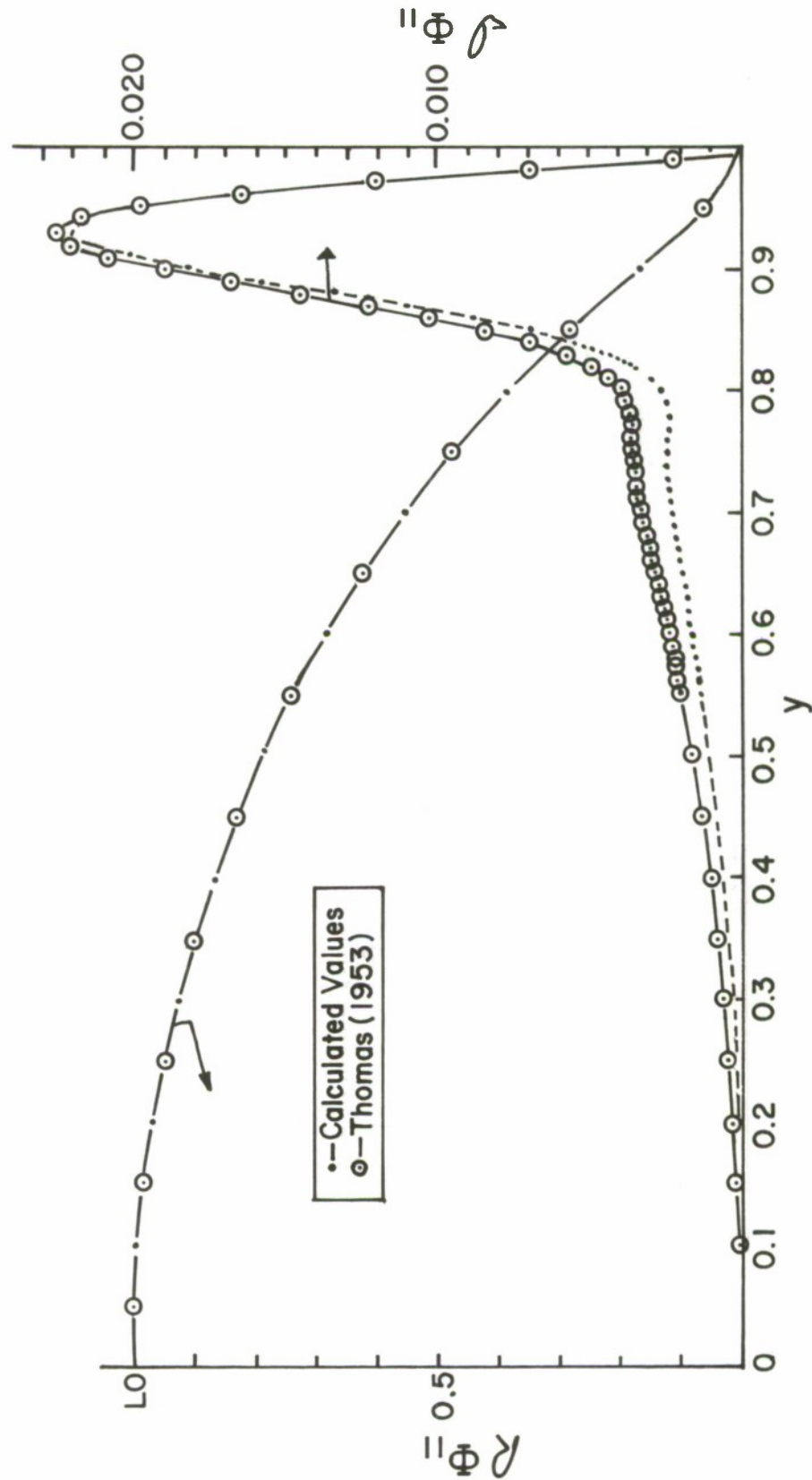


Figure 3. Comparison of the Eigenfunction, Φ_{11} , for $R_e = 6667$, $\alpha = 1.0$.

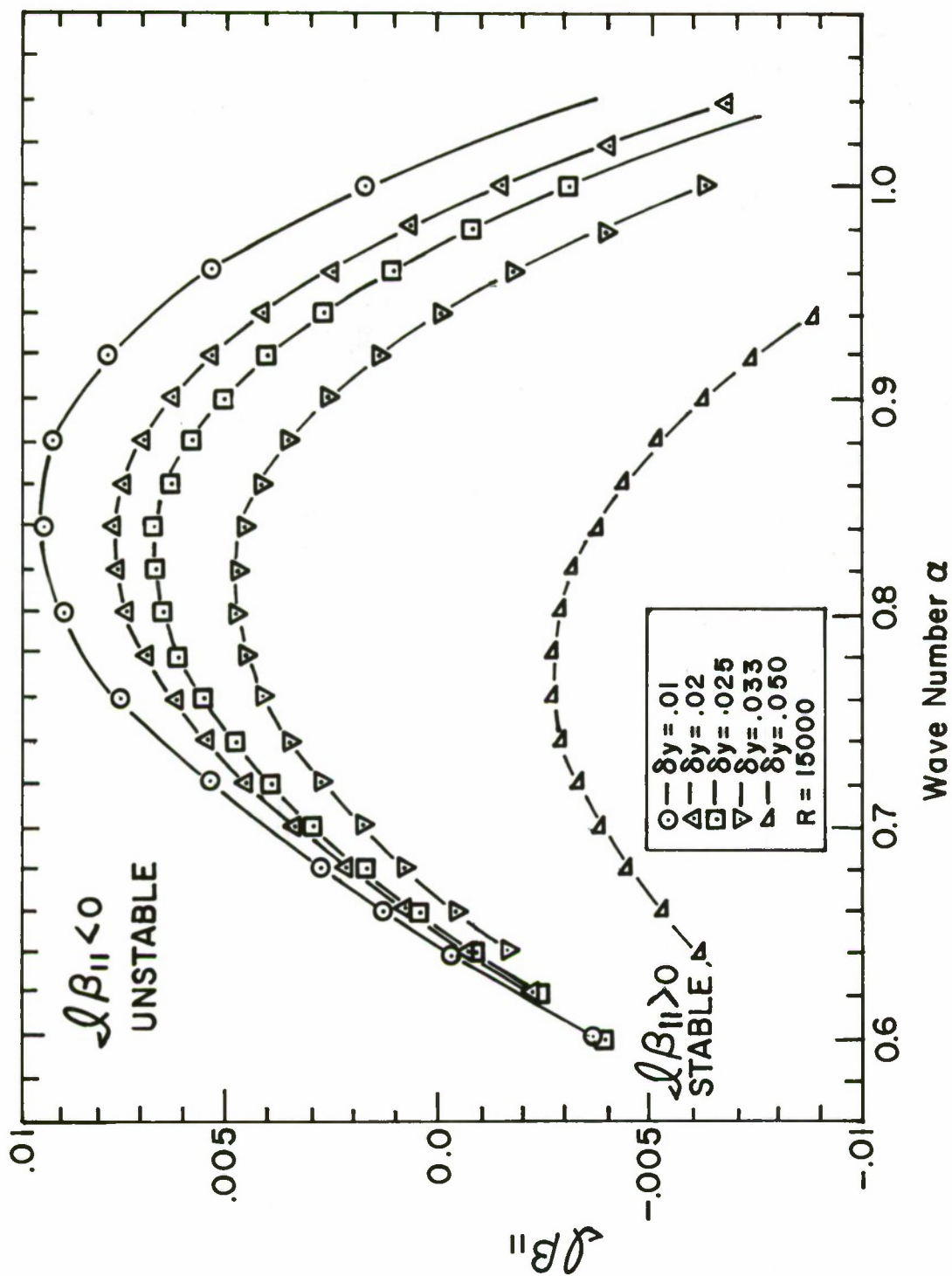


Figure 4. Effect of Grid Parameter, δy , on the Disturbance Growth Rate

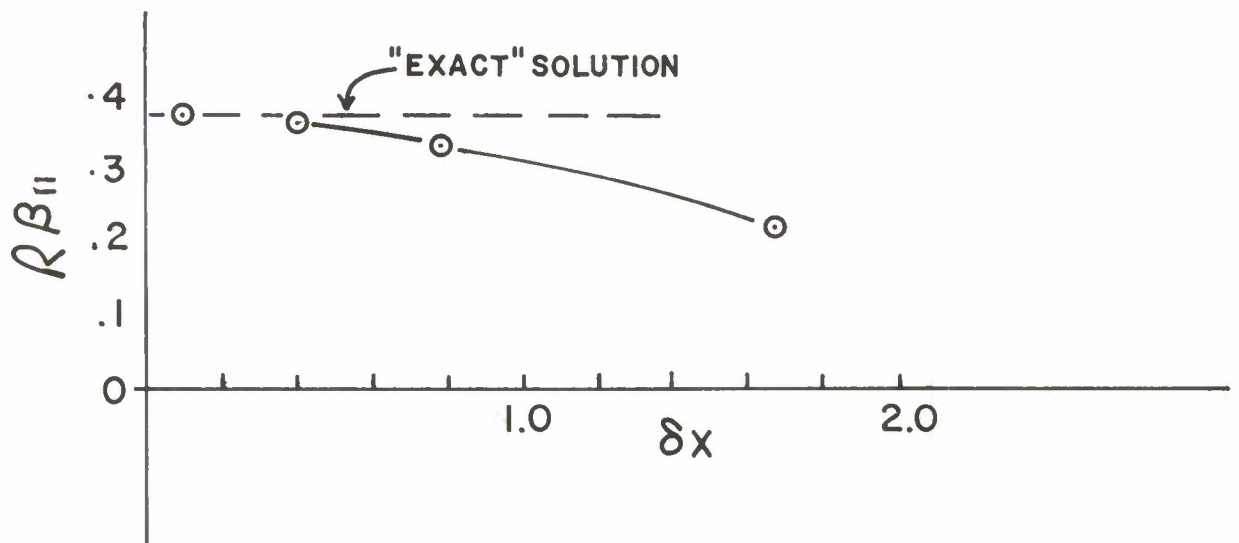
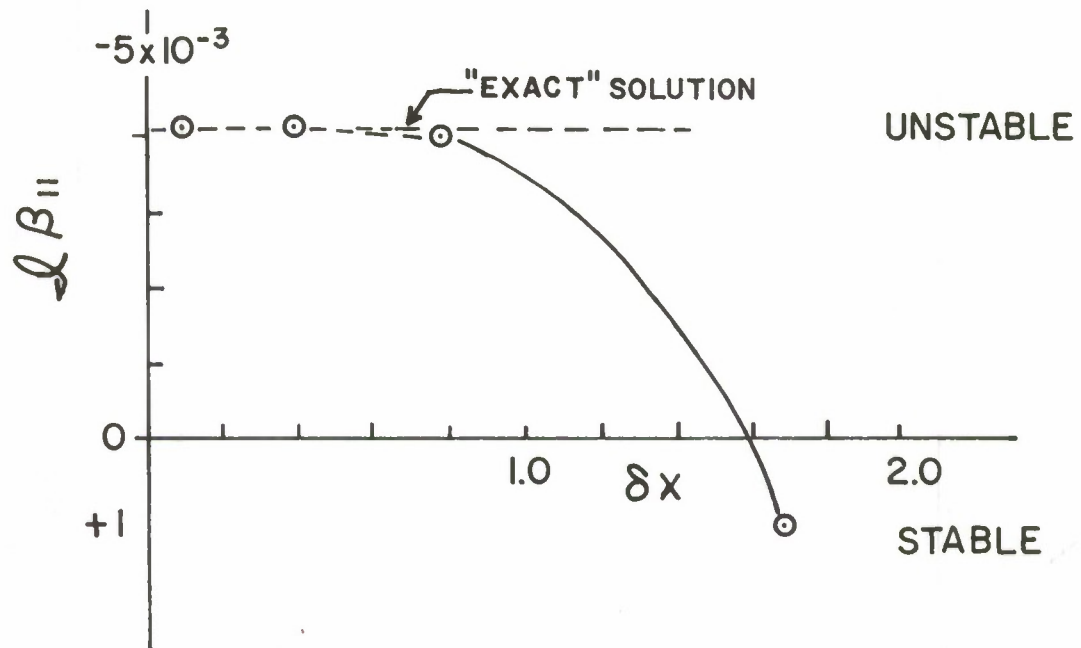


Figure 5. Effect of Grid Parameter, δx , on the Eigenvalue, β_{11}

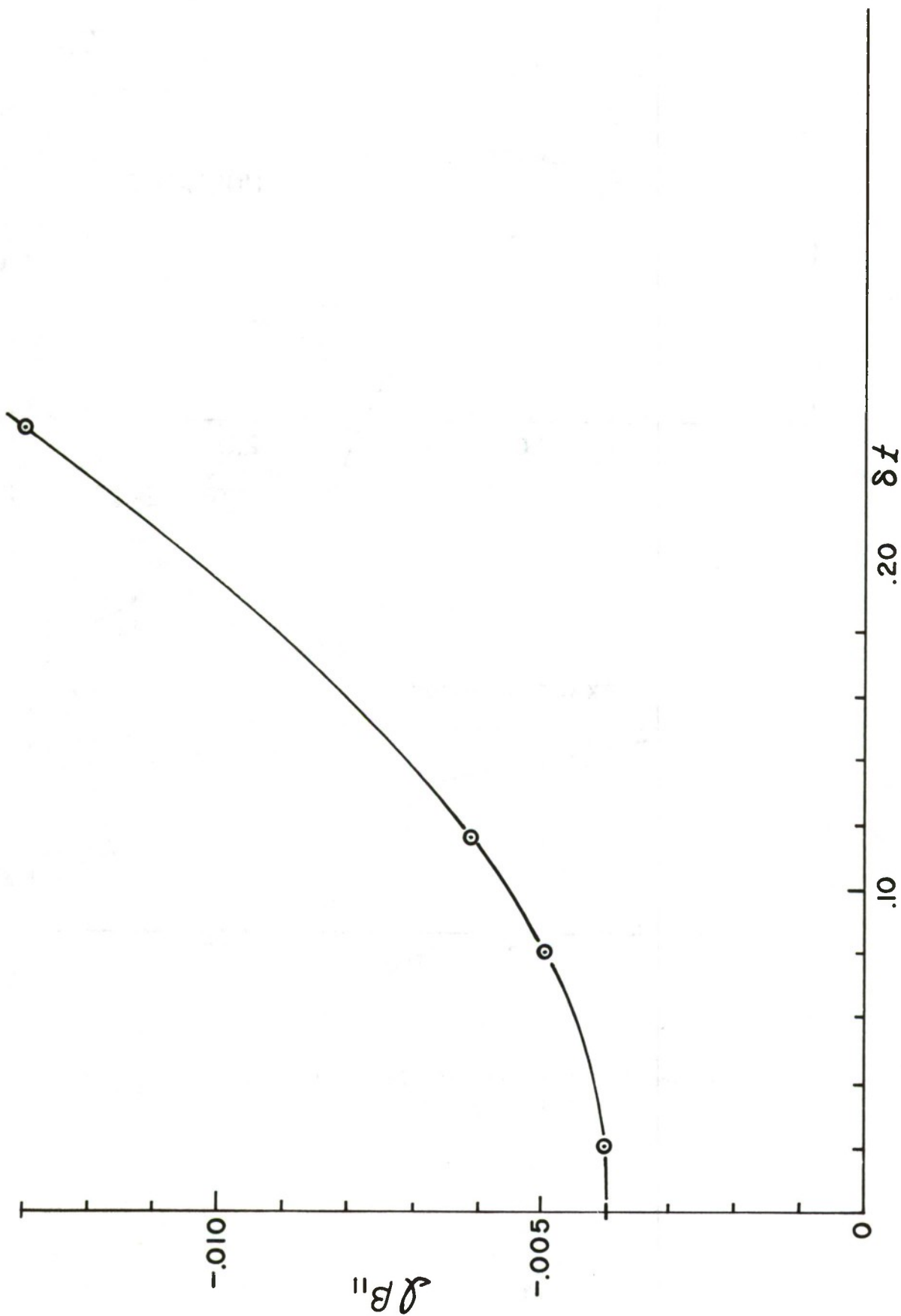


Figure 6. Effect of Grid Parameter, δt , on the Disturbance Growth Rate

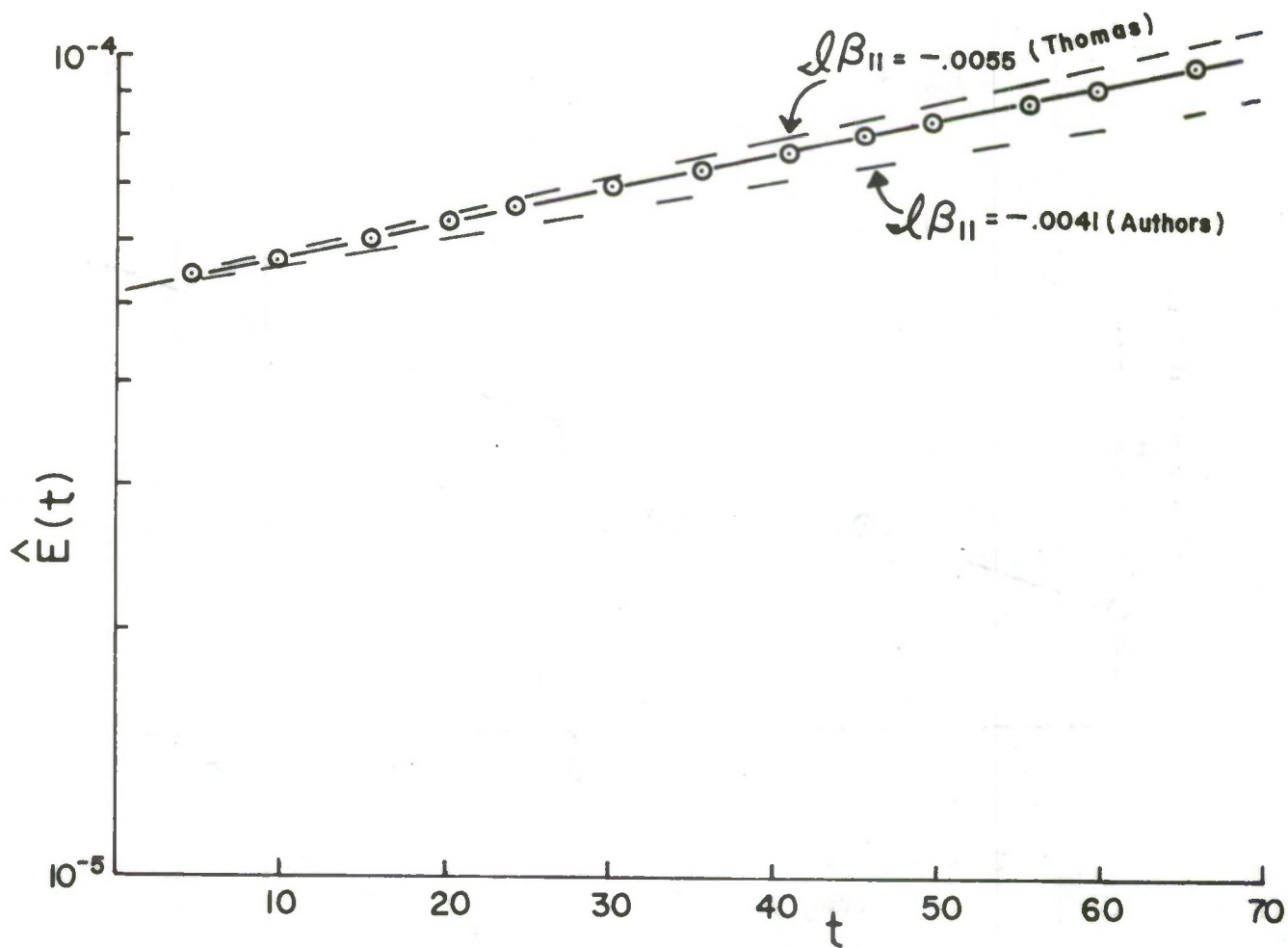


Figure 7. Energy Growth for a Low Amplitude Run.
 $R_e = 6667$, $\alpha = 1.0$

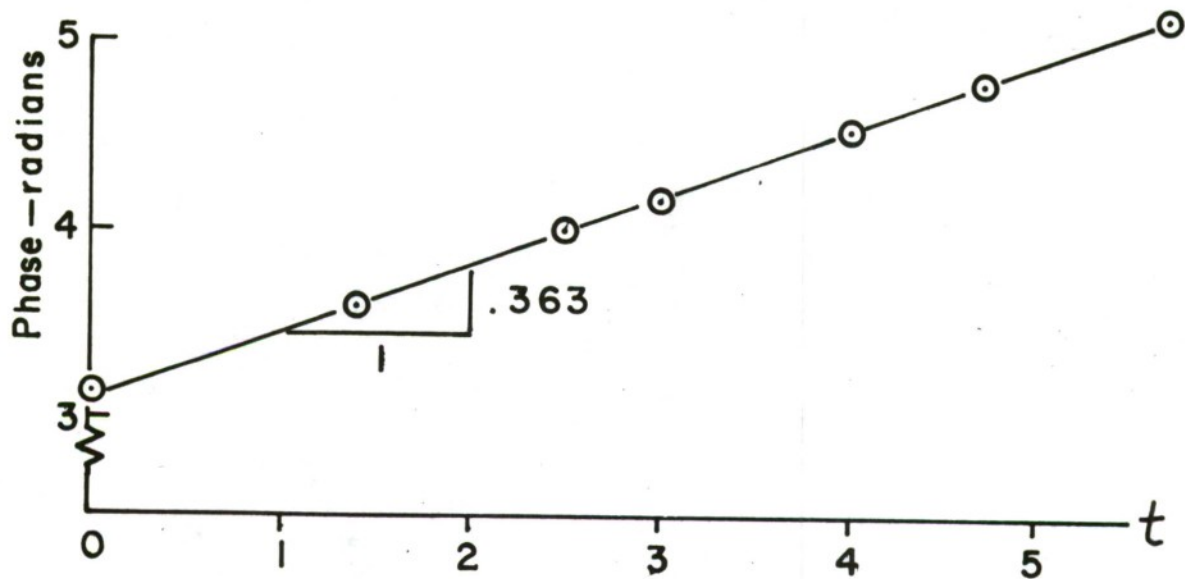


Figure 8. Phase, ϕ_1 , Variation for a Low Amplitude
Run. $R_e = 6667$, $\alpha = 1.0$

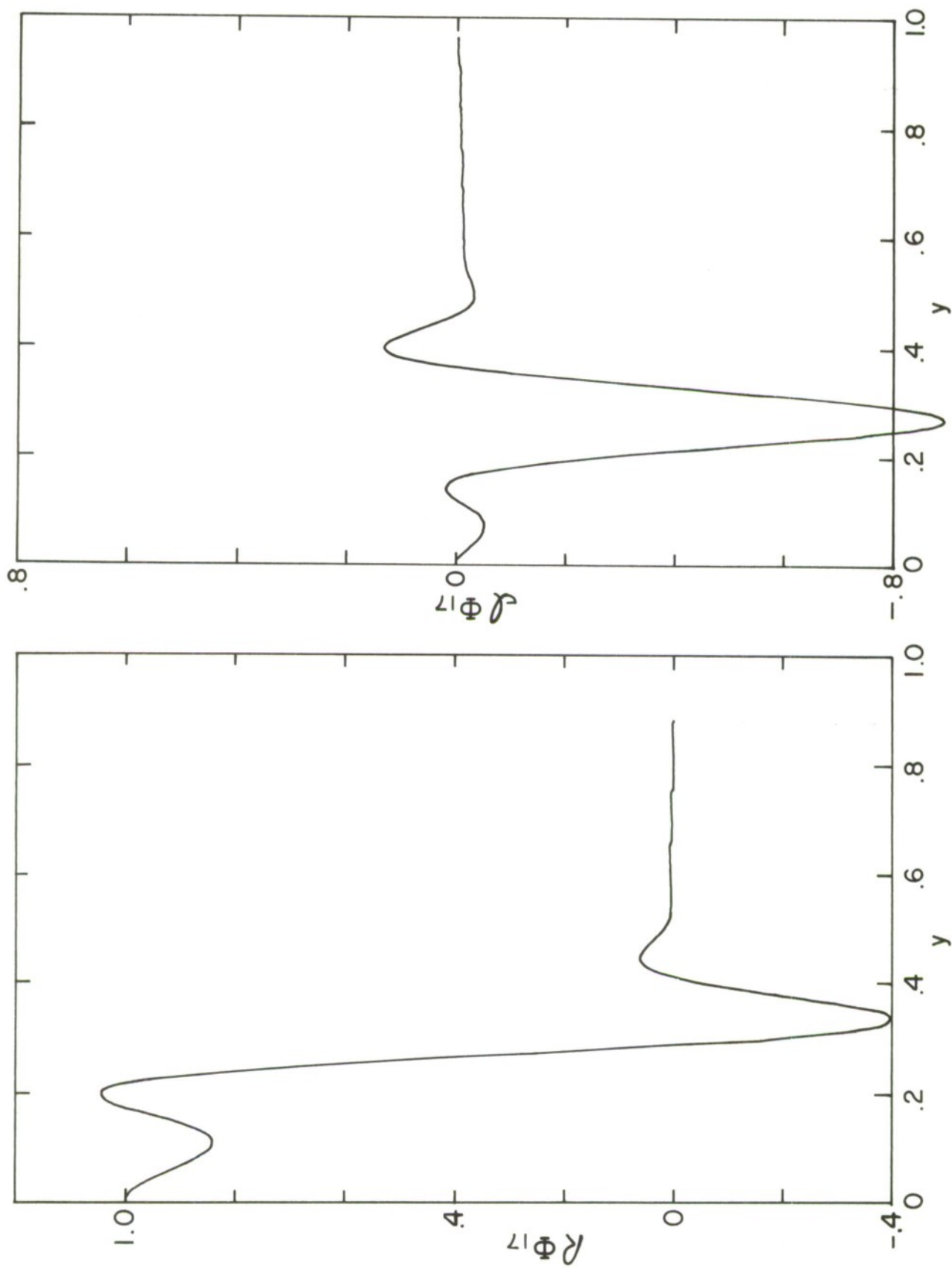


Figure 9a. Eigenfunction, $\Phi_{17}(\text{even})$, for $Re = 6667$,
 $\alpha = 1.0$

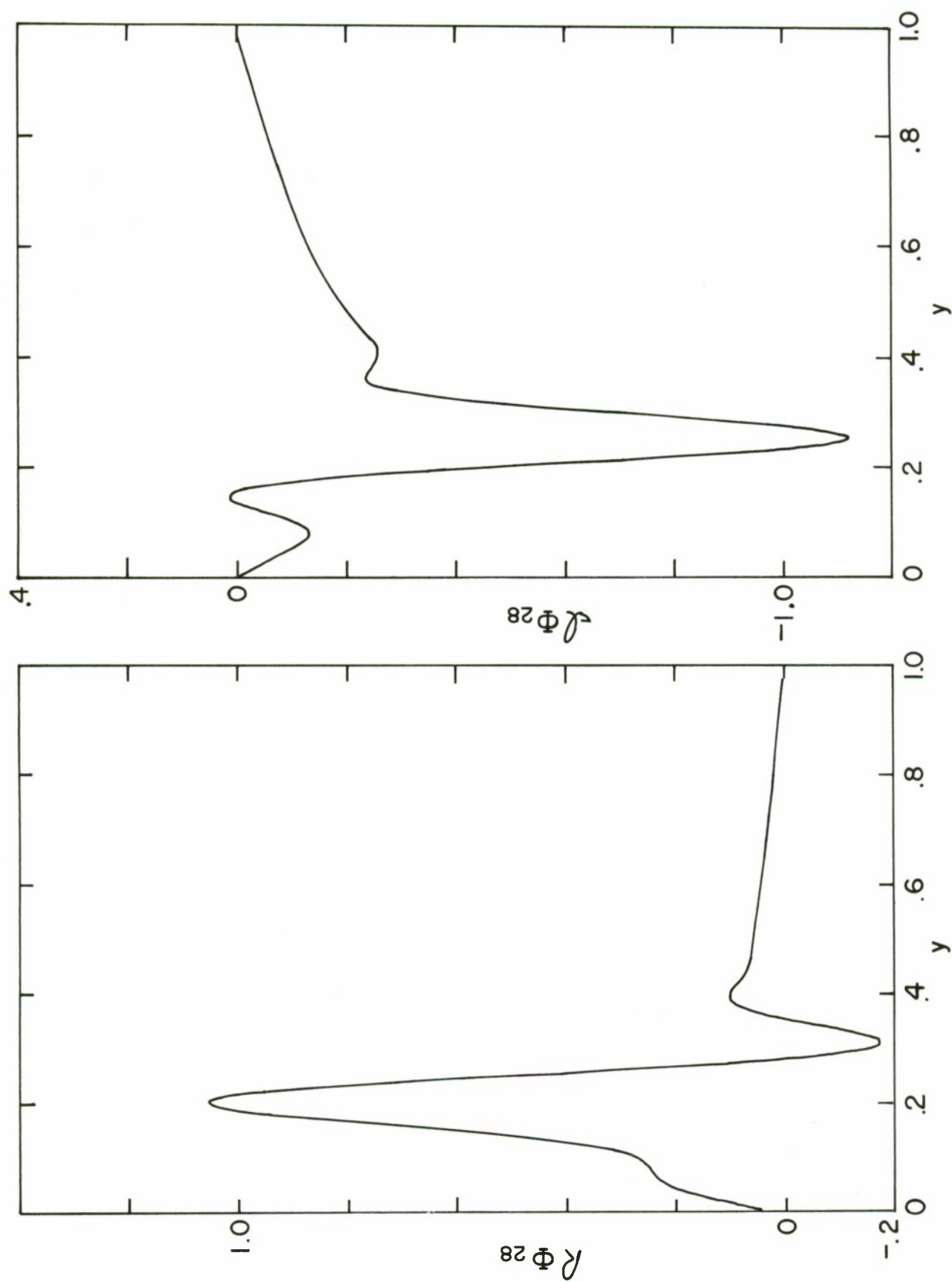


Figure 9b. Eigenfunction, $\Phi_{28}(\text{odd})$, for $R_e = 6667$,
 $\alpha = 1.0$

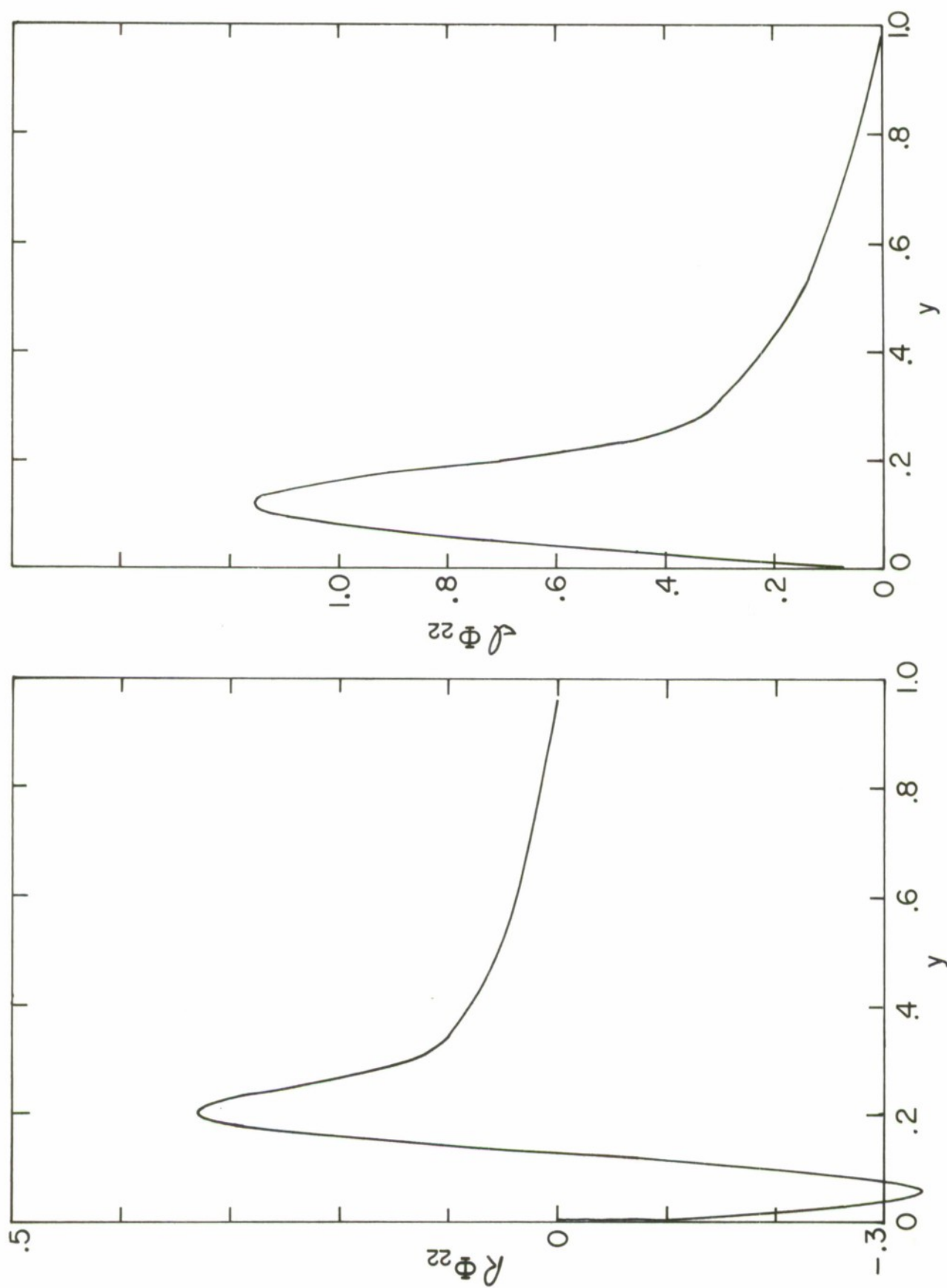


Figure 9c. Eigenfunction, $\rho_{22}(\text{odd})$, for $R_e = 6667$,
 $\alpha = 1.0$

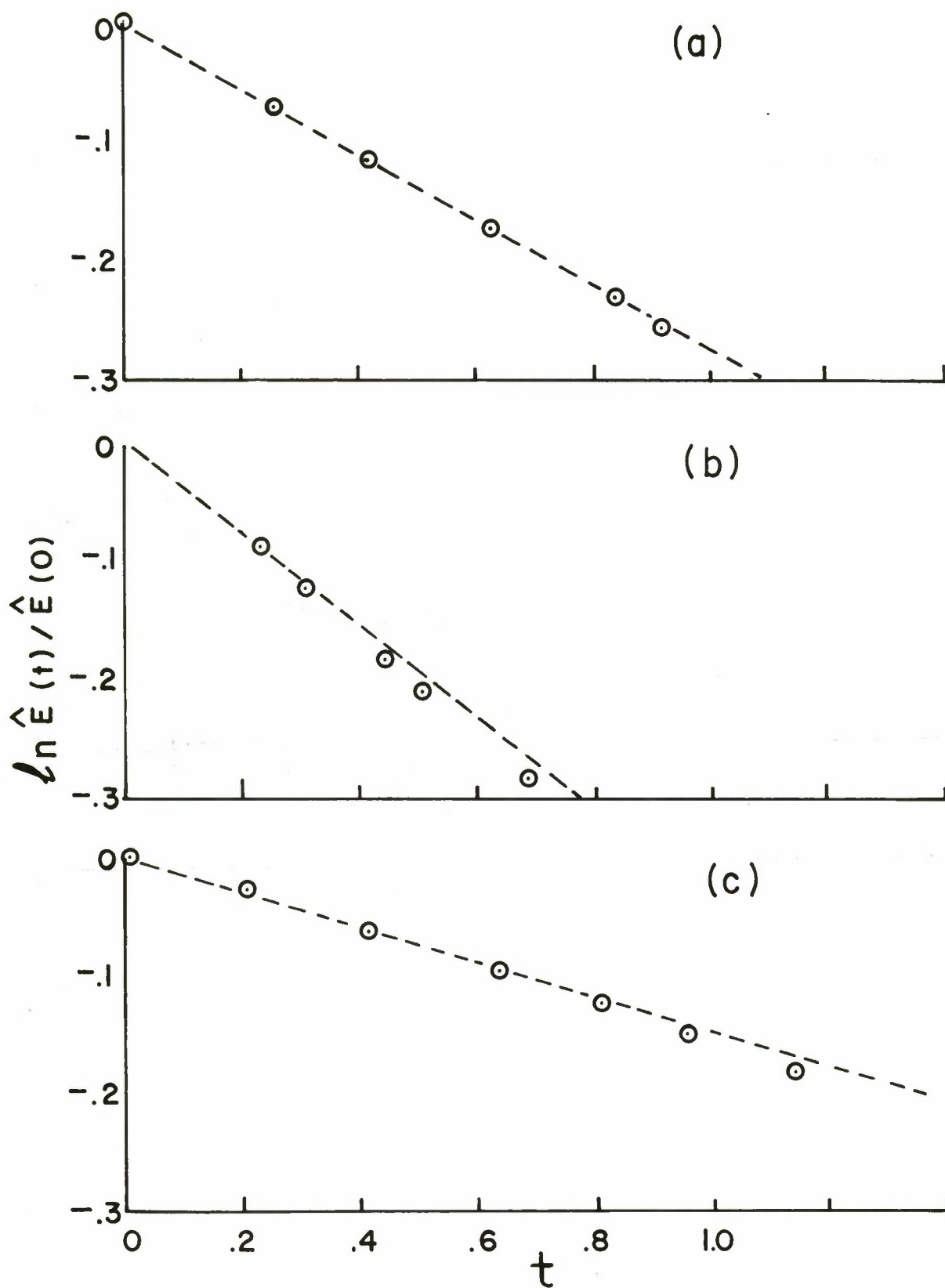


Figure 10. Computed Energy Decay for (a) $\hat{\epsilon}_{17}$, (b) $\hat{\epsilon}_{28}$, (c) $\hat{\epsilon}_{22}$. Dashed line represents decay rate predicted from linear theory

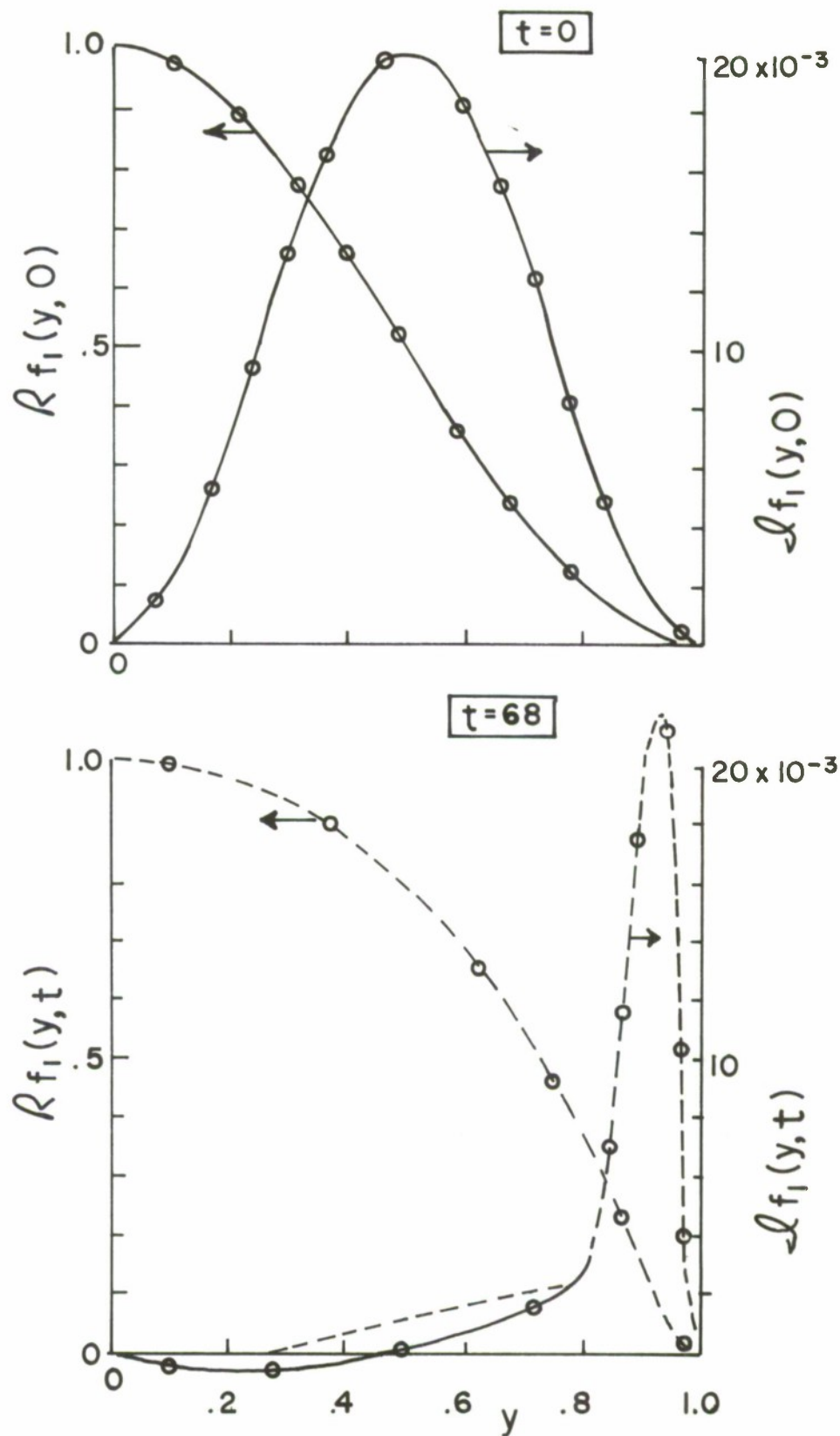


Figure 11. Primary Mode Shape, f_1 , for a Low Energy (Linear) Run at Times $t=0$ and $t=68$. Dashed Line Represents Φ_{11}

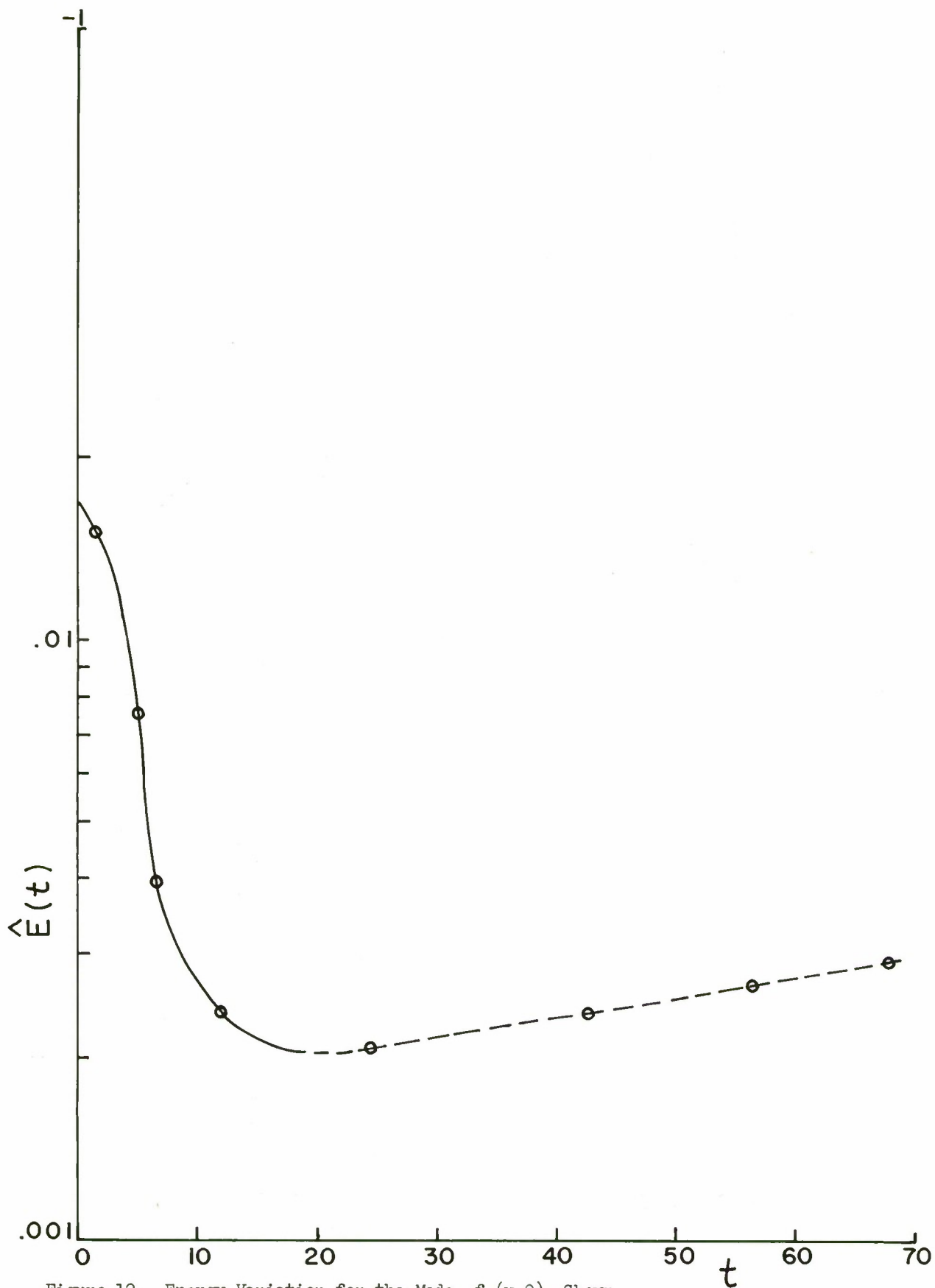


Figure 12. Energy Variation for the Mode, $f_1(y,0)$, Shown in Figure 11. Dashed Line Represents Predicted Growth Rate for ϕ_{11}

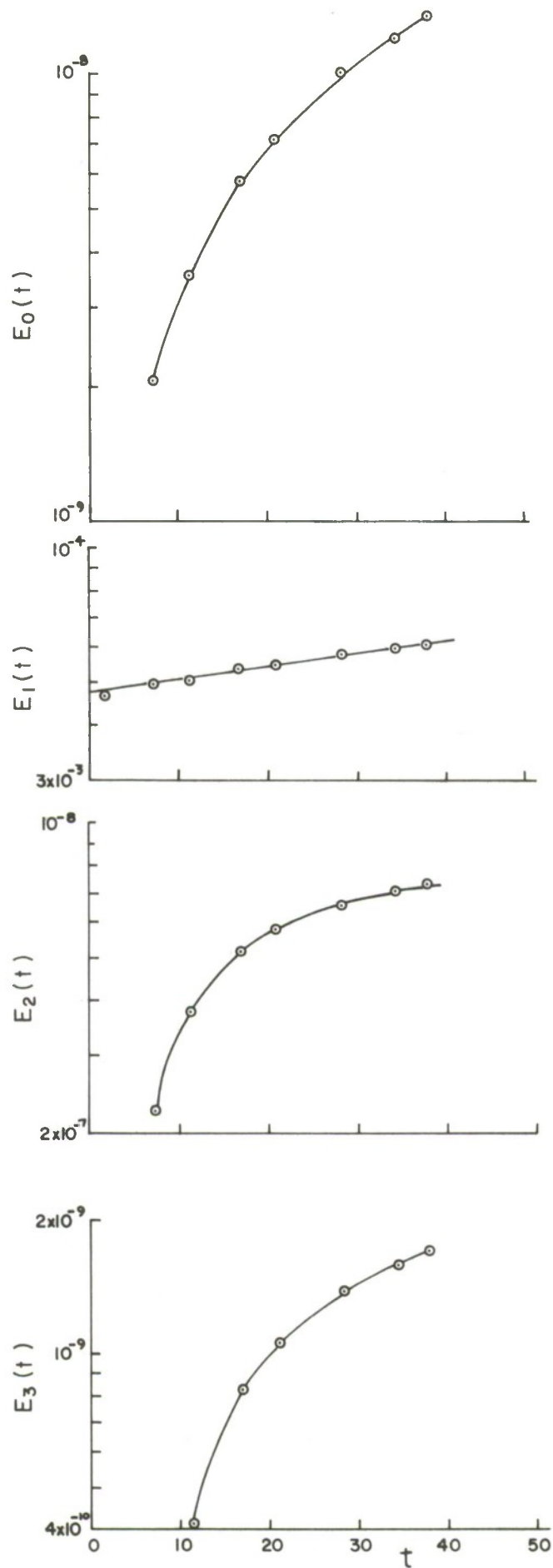


Figure 13. Energy Variation for the Modes E_0, E_1, E_2 and E_3 . $R_c = 6667$, $\alpha = .875$

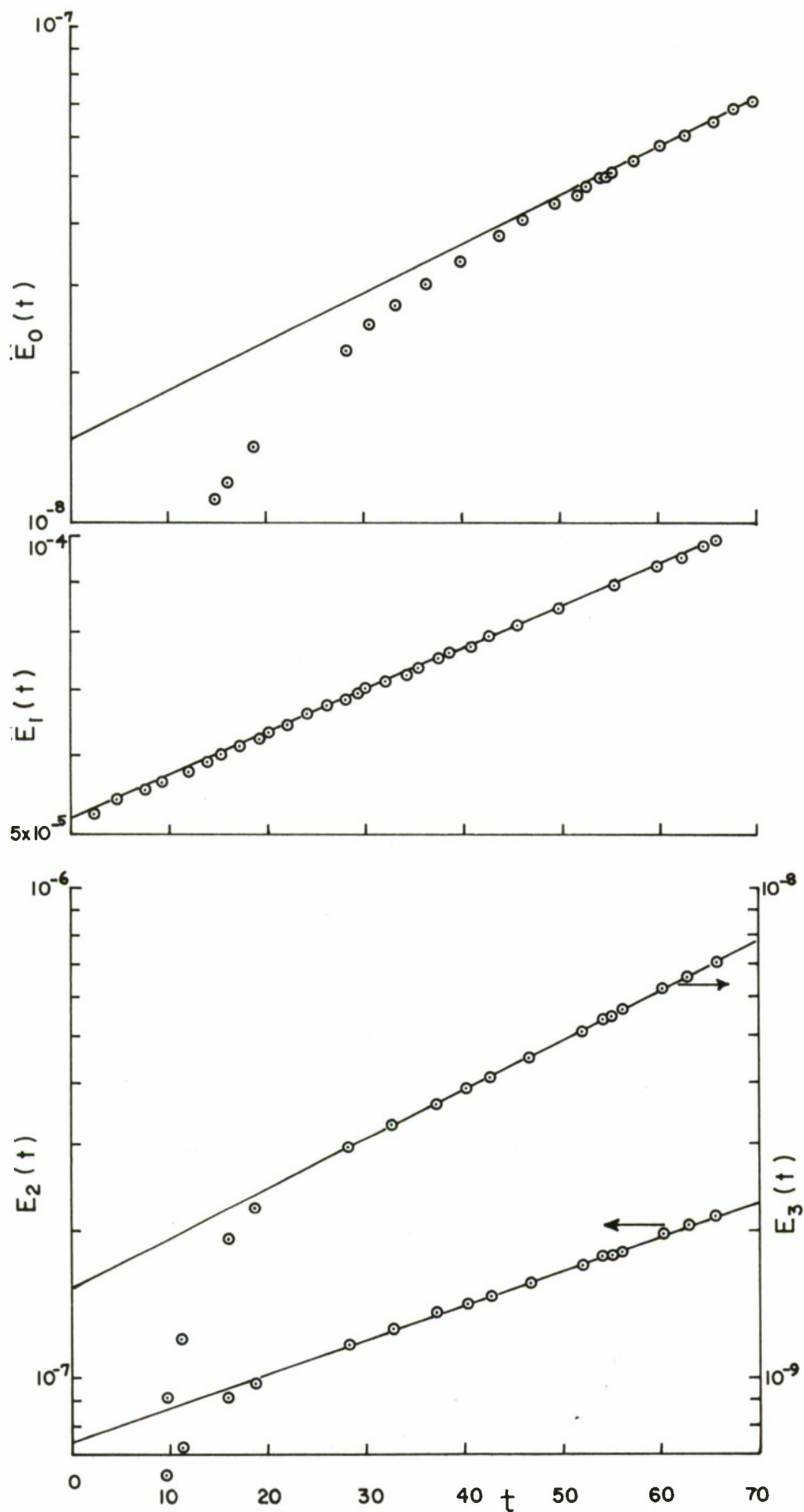


Figure 14. Energy Variation for the Modes E_0 , E_1 , E_2 and E_3 , $R_0 = 6667$, $\alpha = 1.0$

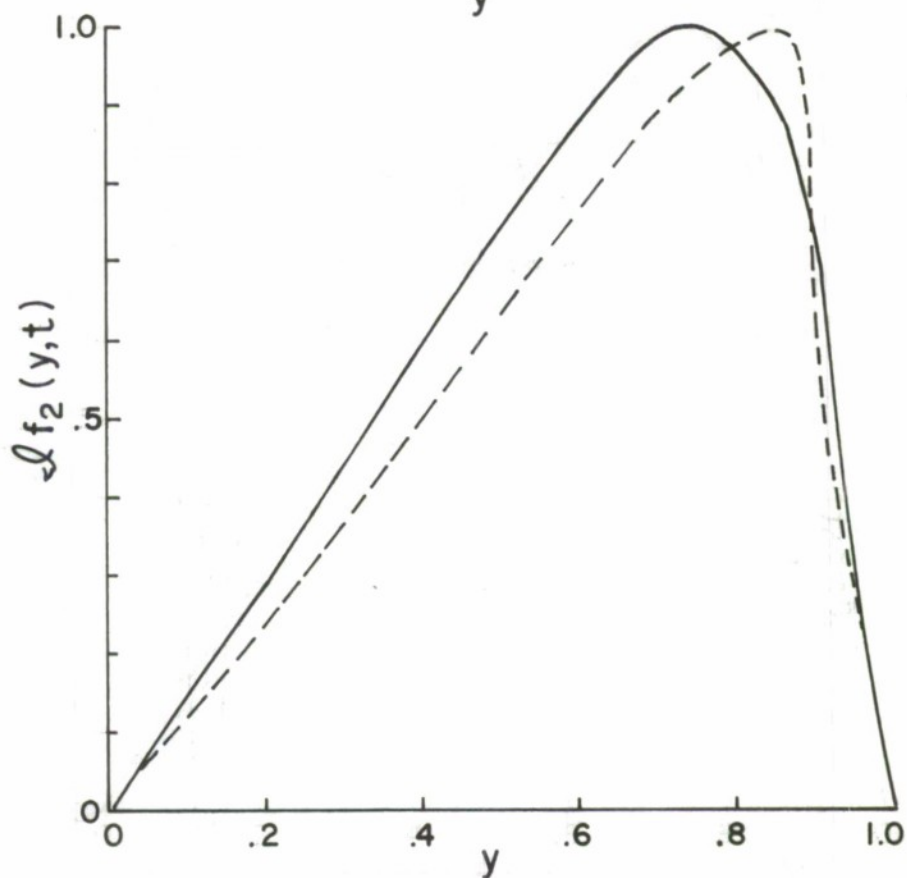
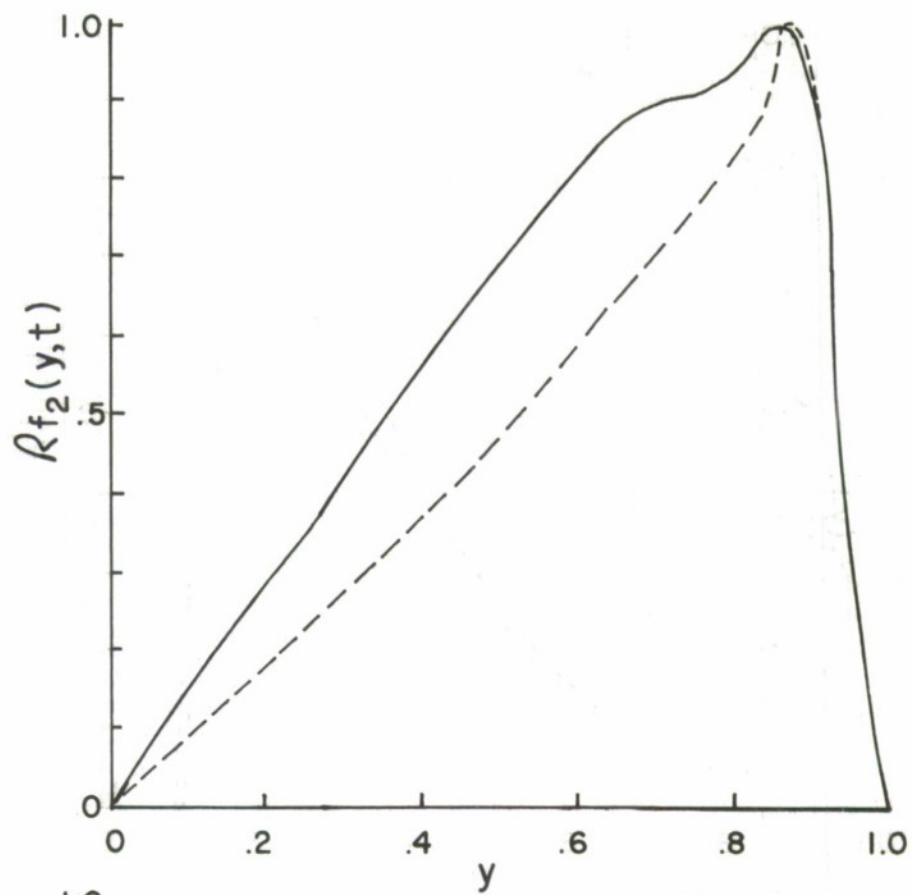


Figure 15a. Mode Shape for $f_2(\text{odd})$ at $t = 85$. $\alpha = 1.0$,
 $Re = 6667$.
 Dashed Line Represents $\phi_{26}(\text{odd})$

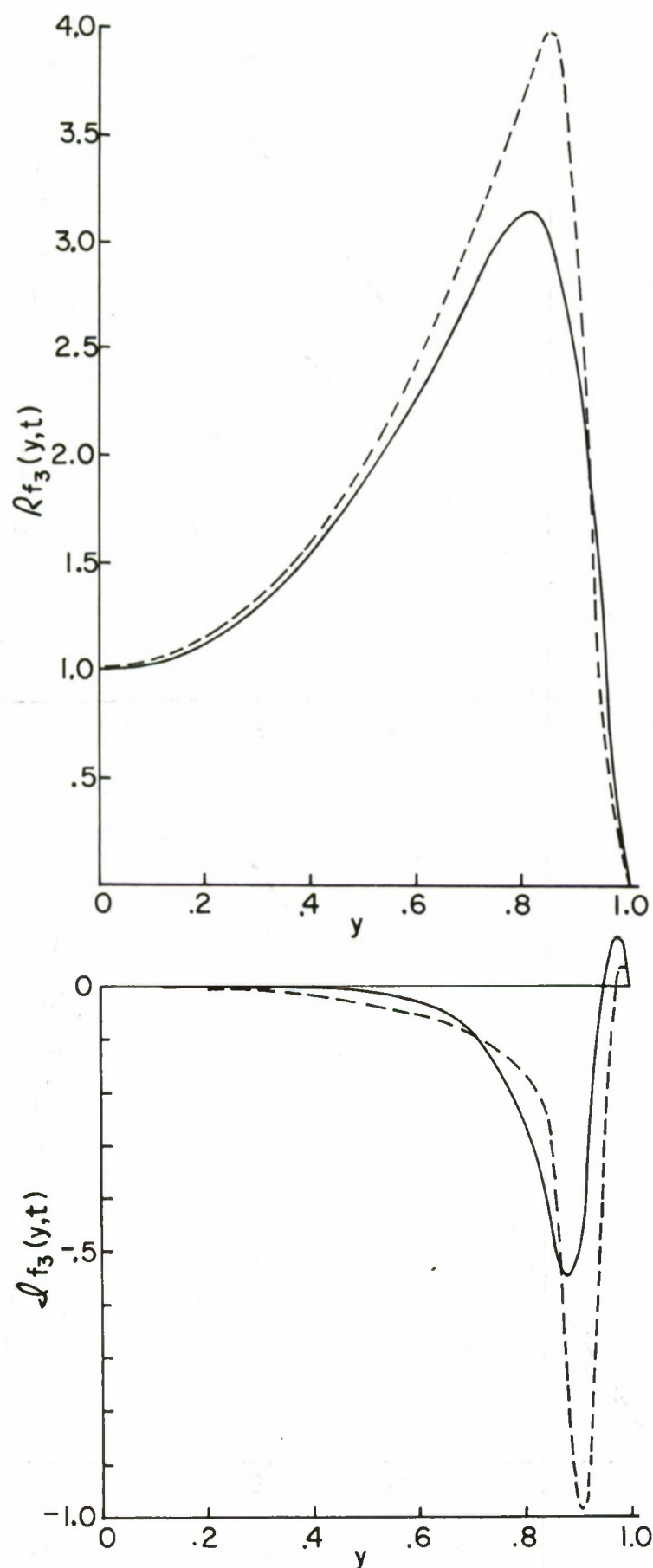


Figure 15b. Mode Shape for $f_3(\text{even})$ at $t = 85$. $\alpha = 1.0$,
 $Re = 6667$.
 Dashed Line Represents $f_{33}(\text{even})$

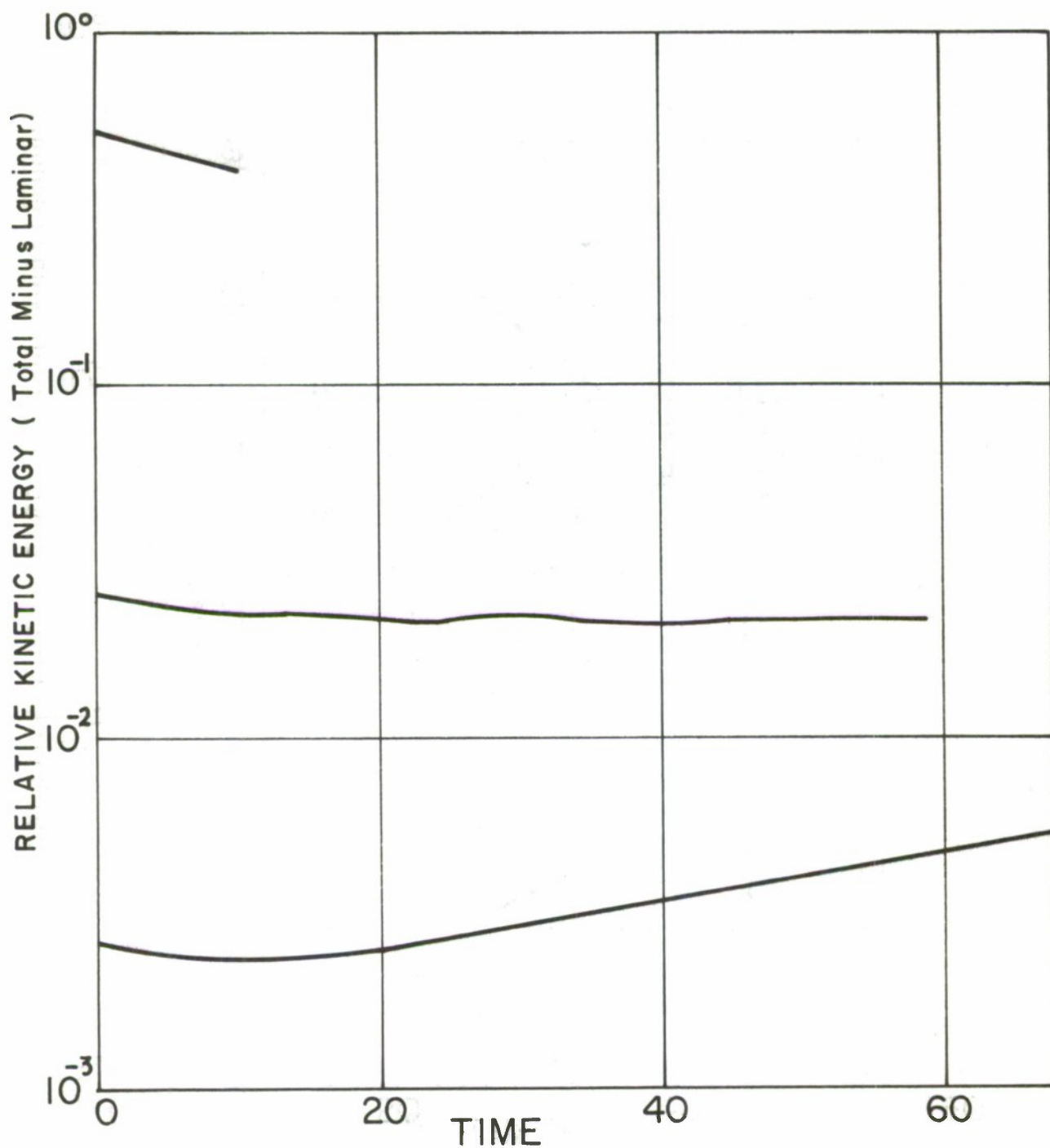


Figure 16. Total Kinetic Energy (Mean plus Turbulent) for Three Different Initial Energy Levels. The Laminar Energy (.600) has been Subtracted for Convenience.

Top Curve, $\epsilon = .5$
 Middle Curve $\epsilon = .05\sqrt{5}$
 Bottom Curve $\epsilon = .05/\sqrt{2}$

$\alpha = 1.0, R_e = 6667$

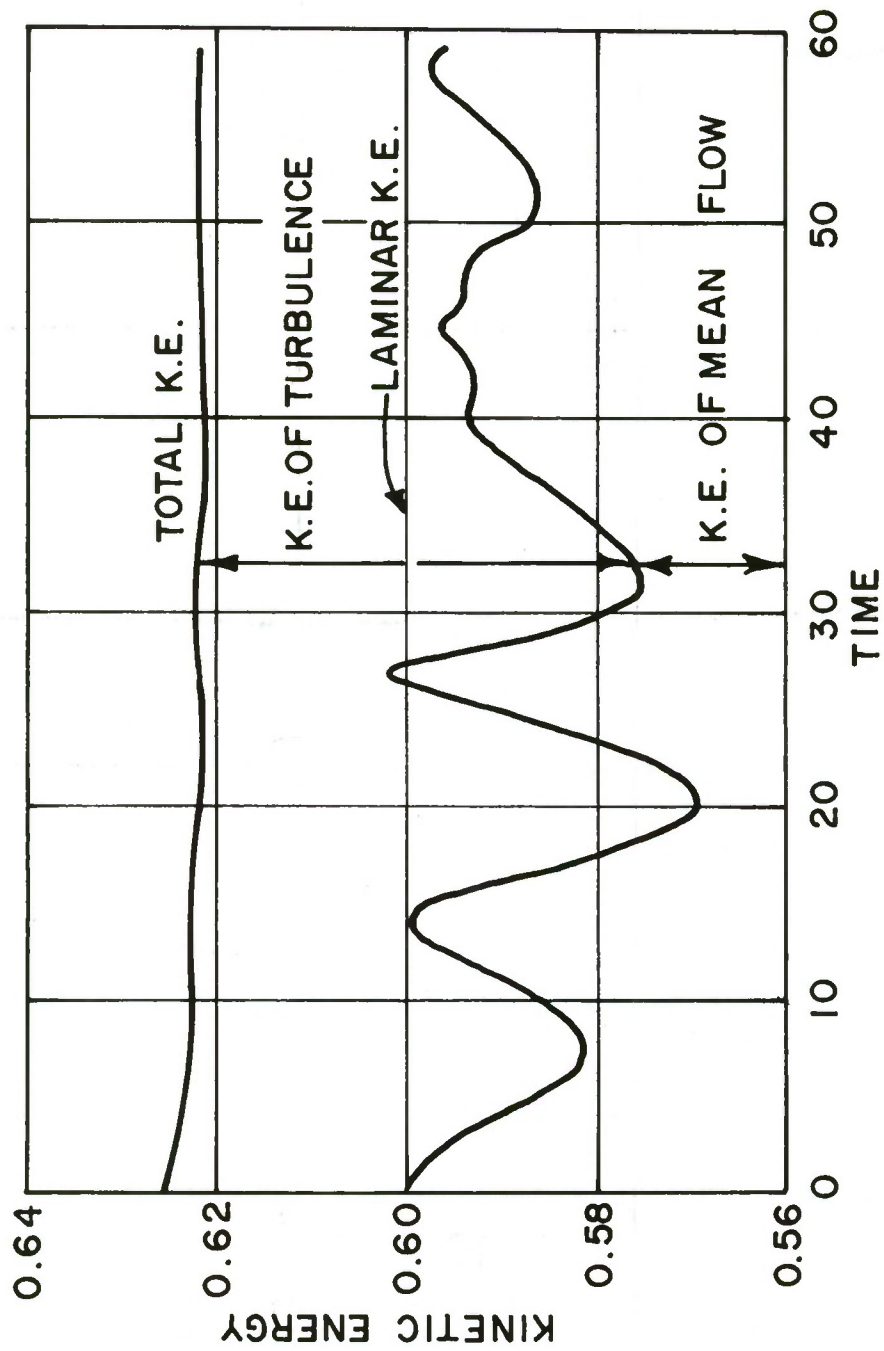


Figure 17. Energy Variation for the Run $\epsilon = .05 \sqrt{5}$

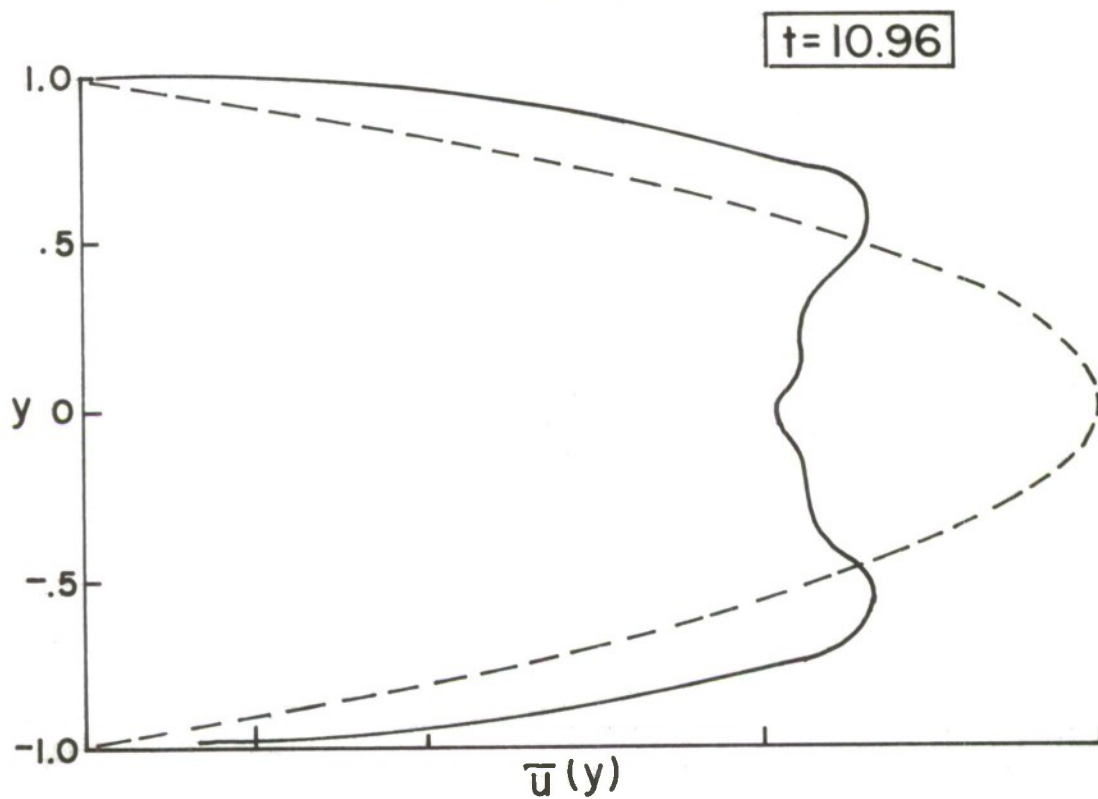
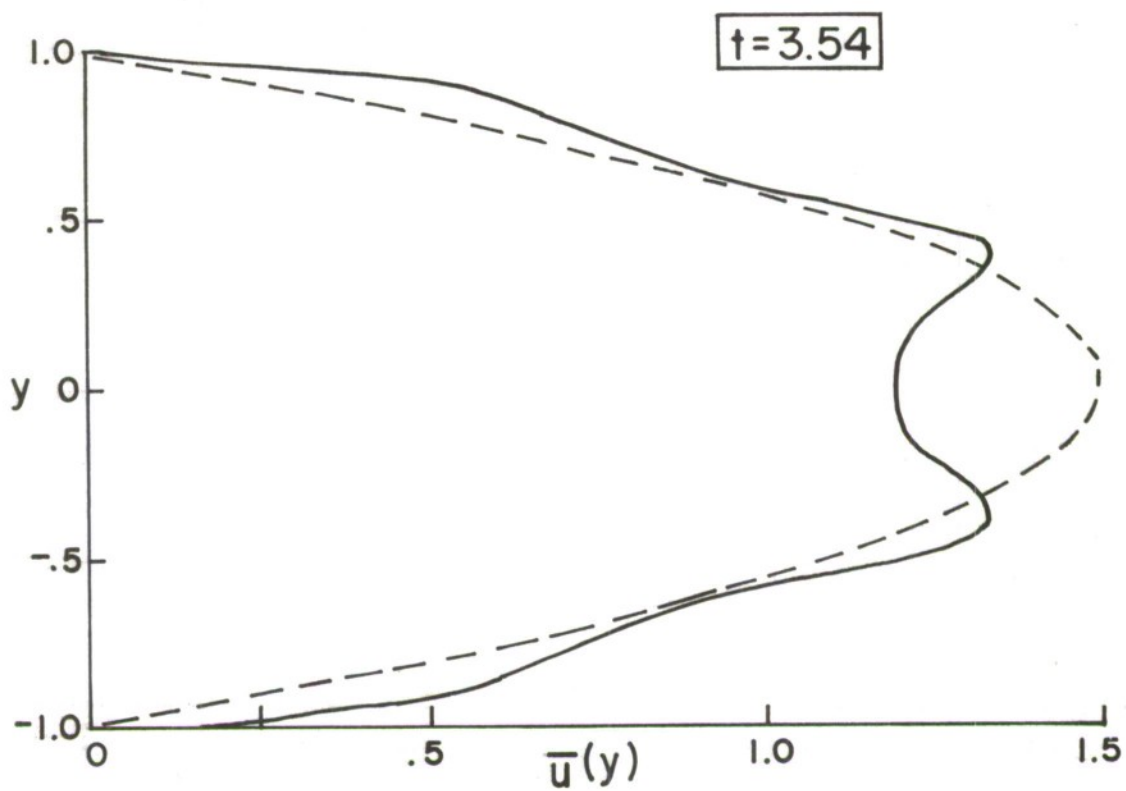


Figure 18a. Mean Velocity Profiles for the Run $\epsilon = .5$,
 $\alpha = 1.0$, $R_e = 6667$
 Dashed Line is $U(y) = \frac{3}{2}(1 - y^2)$

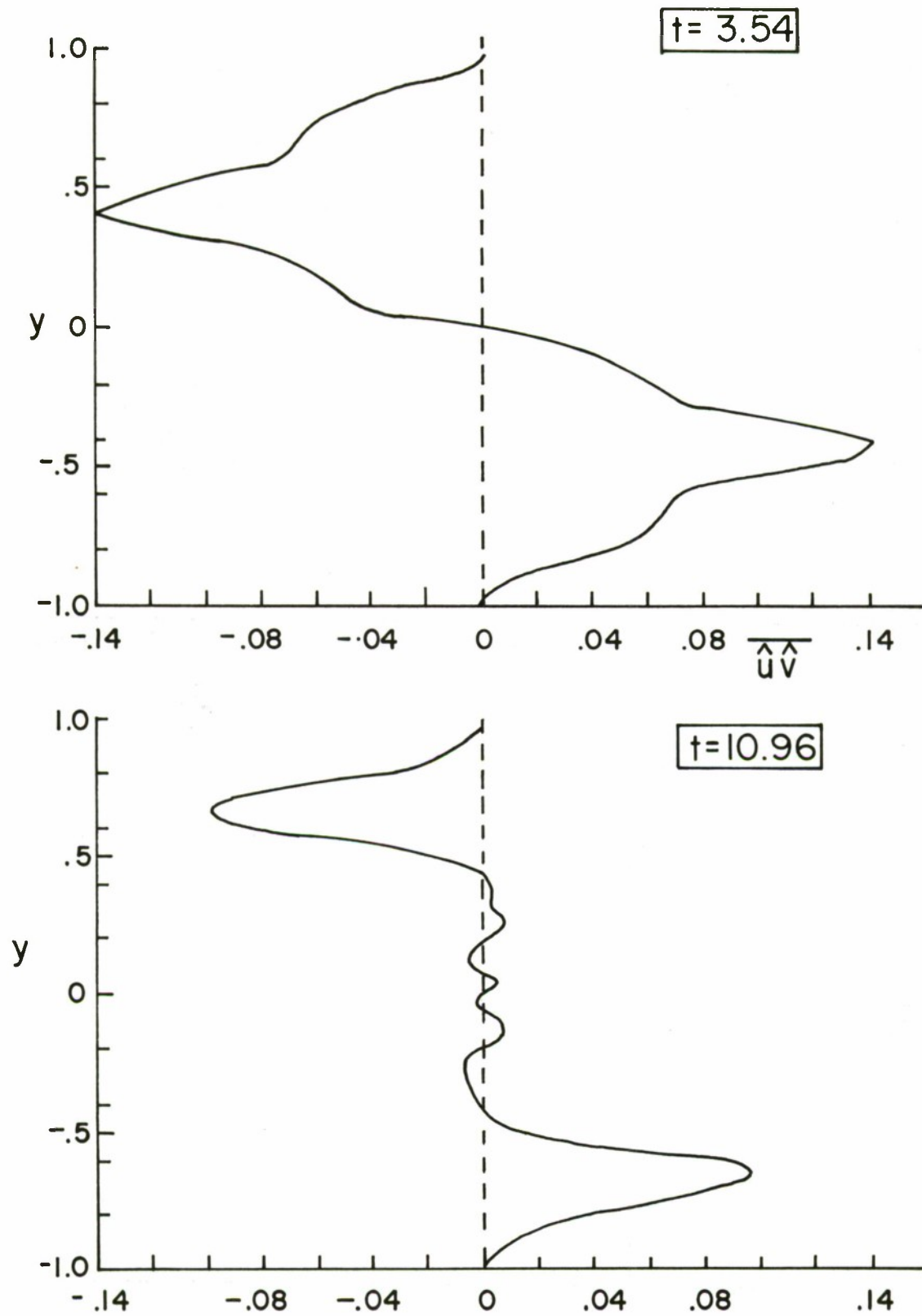


Figure 18b. Reynolds Stresses for the Run $\epsilon = .5$, $\alpha = 1.0$
 $R_e = 6667$

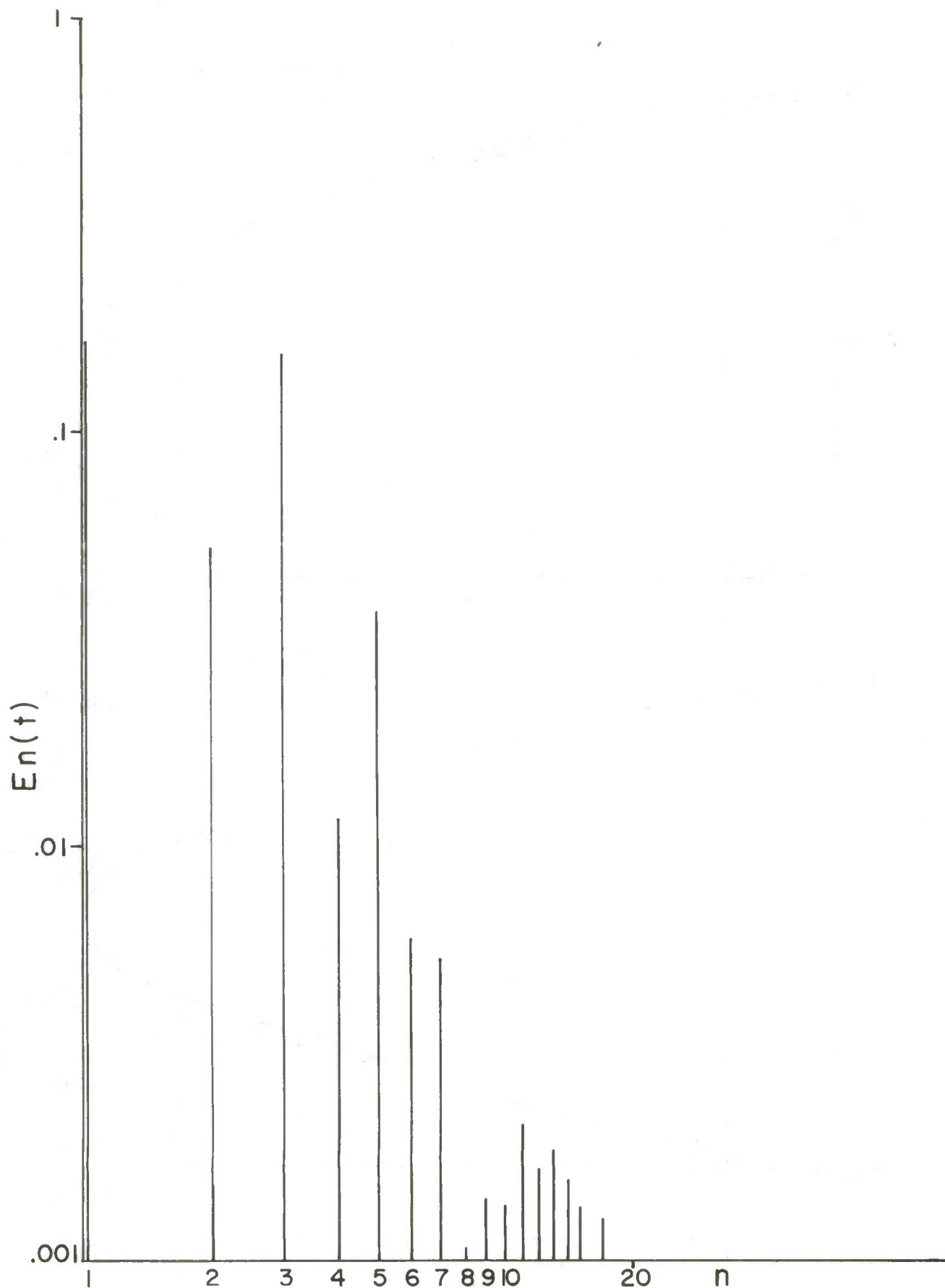


Figure 18c. Energy Spectrum for the Run $\epsilon = .5$, $\alpha = 1.0$,
 $R_e = 6667$ at $t = 11$

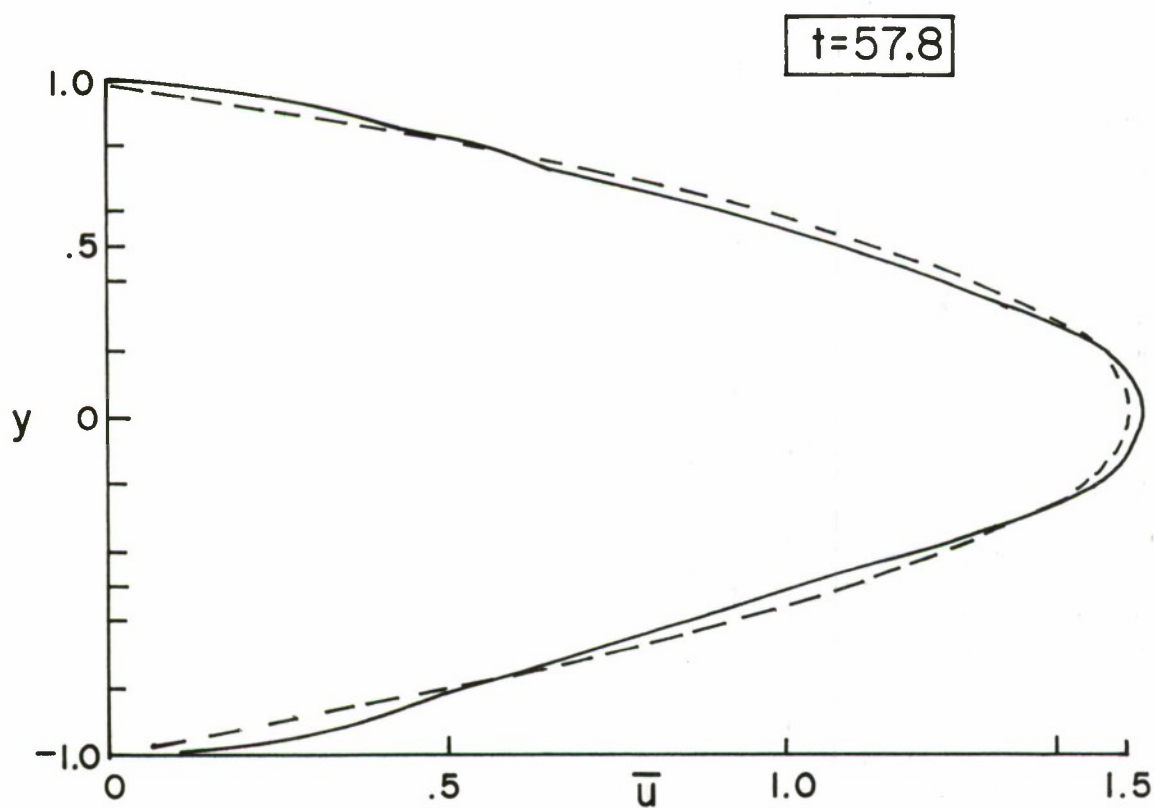
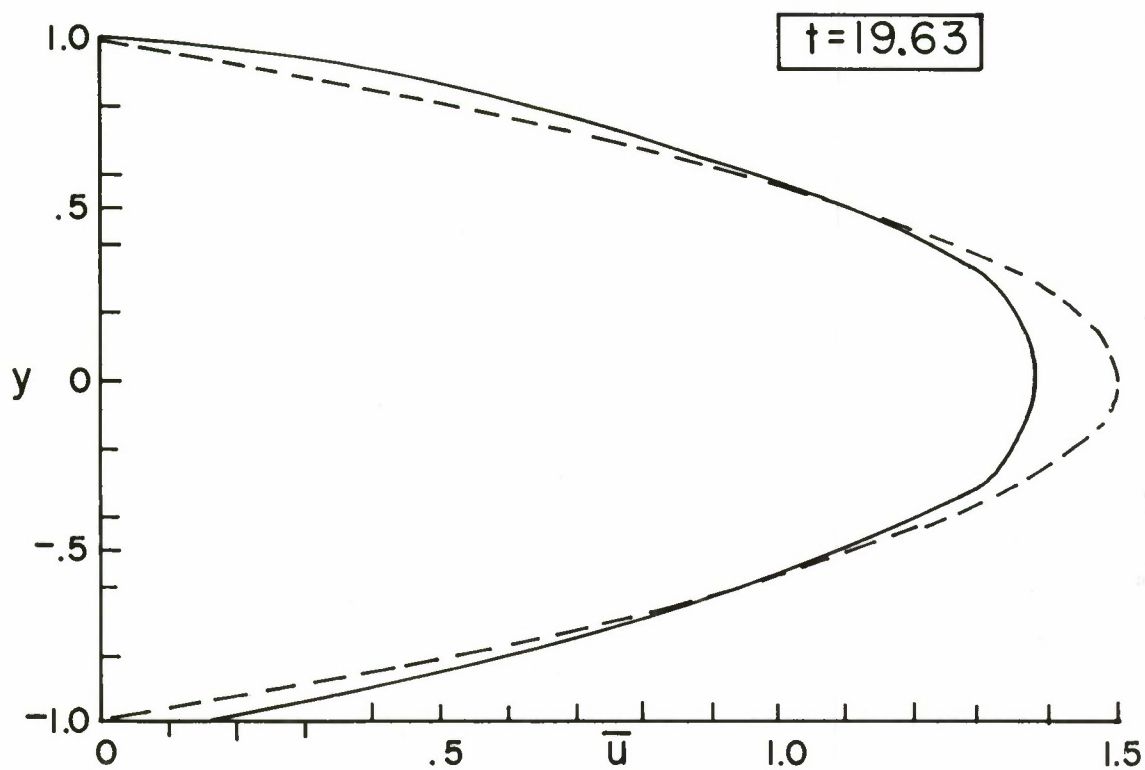


Figure 19a. Mean Velocity Profiles for the
 Run $\epsilon = .05\sqrt{5}$, $\alpha = 1.0$, $R_e = 6667$
 Dashed Line is $U(y) = 3/2(1-y^2)$

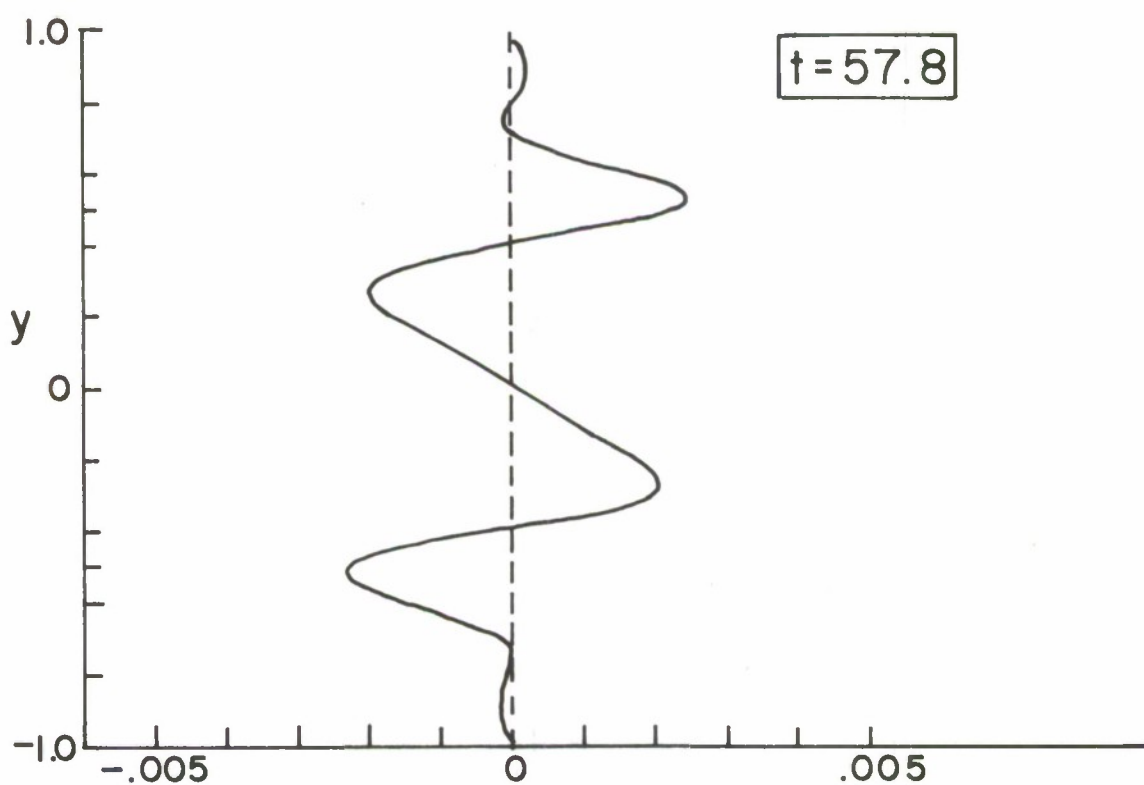
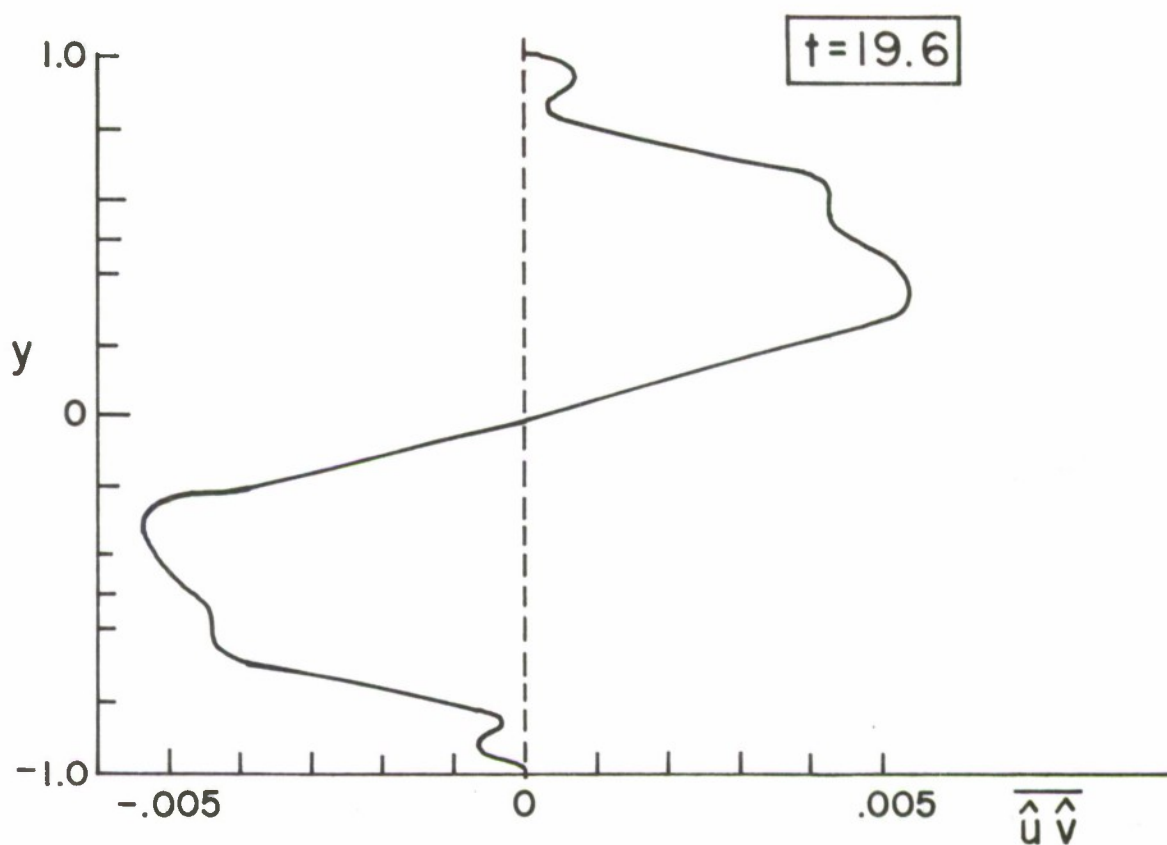


Figure 19b. Reynold's Stresses for the Run
 $\epsilon = .05\sqrt{5}$, $\alpha = 1.0$, $R_e = 6667$

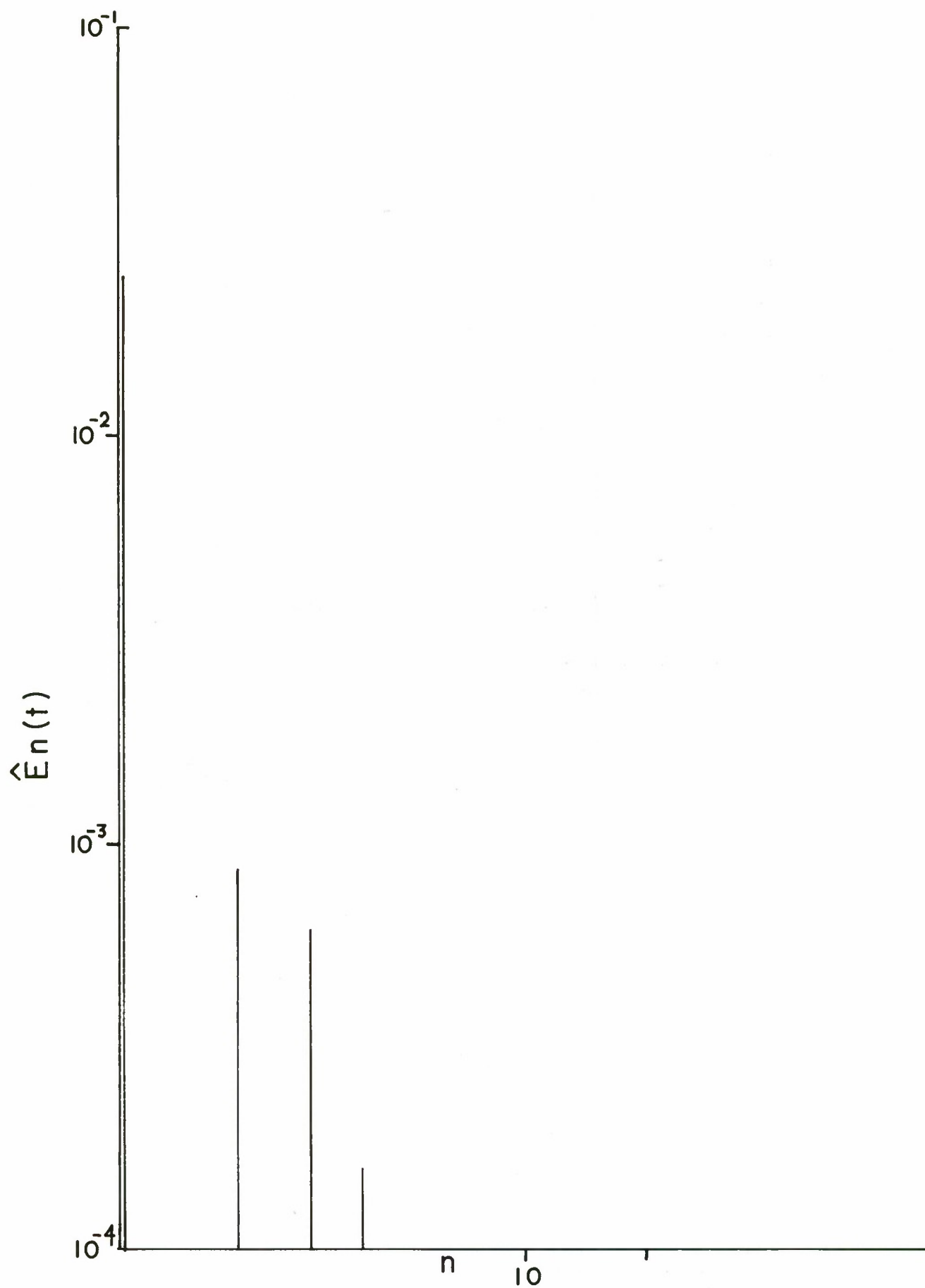


Figure 19c. Energy Spectrum for the Run $\epsilon = .05\sqrt{5}$,
 $\alpha = 1.0$, $R_e = 6667$ at $t = 59$

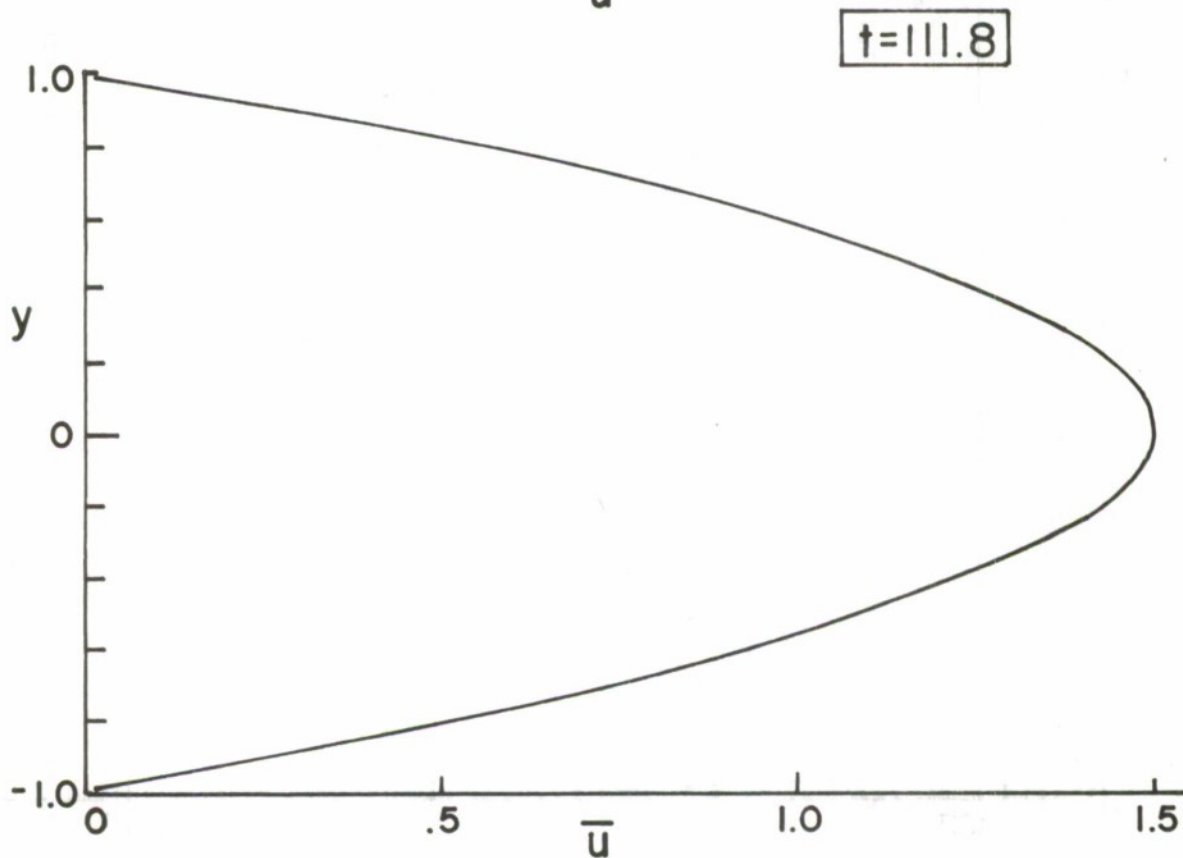
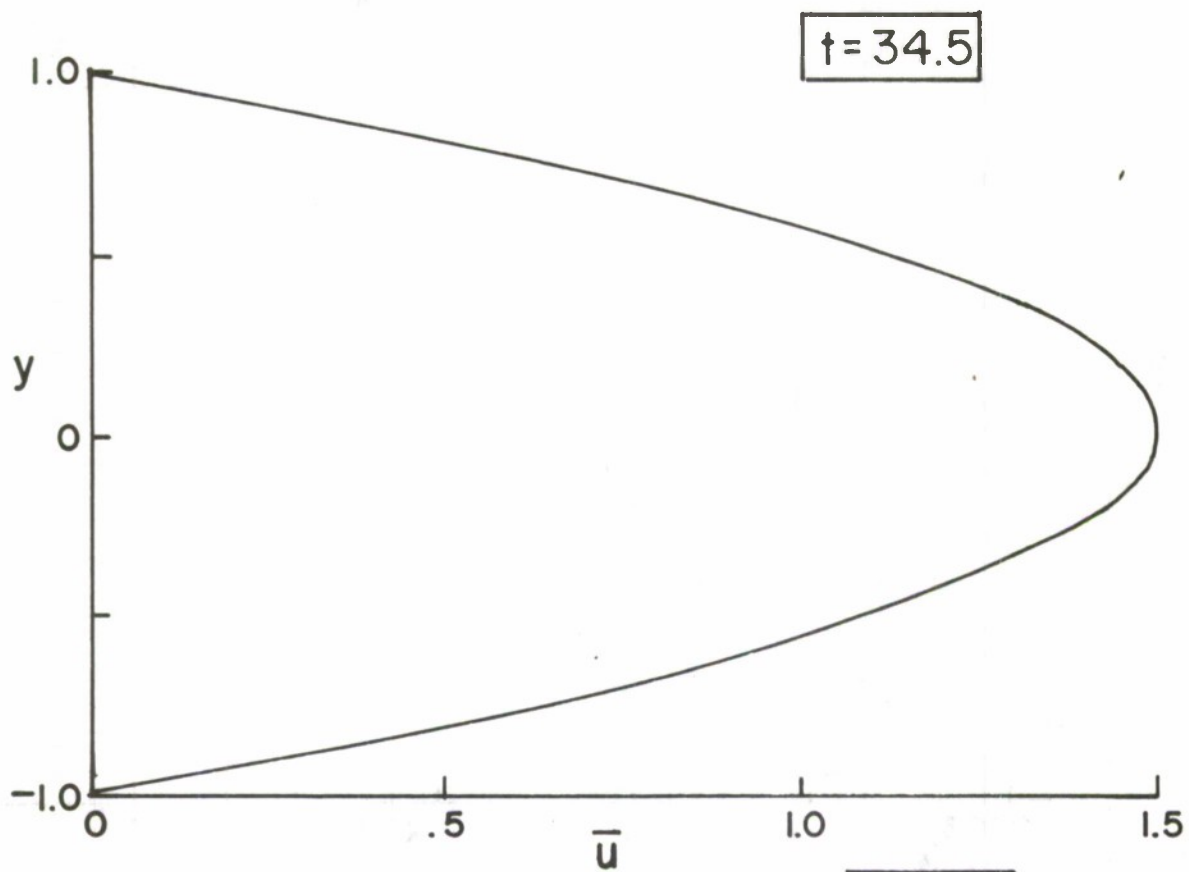


Figure 20a. Mean Velocity Profiles for the Run
 $\epsilon = .05/\sqrt{2}$, $\alpha = 1.0$, $R_e = 6667$

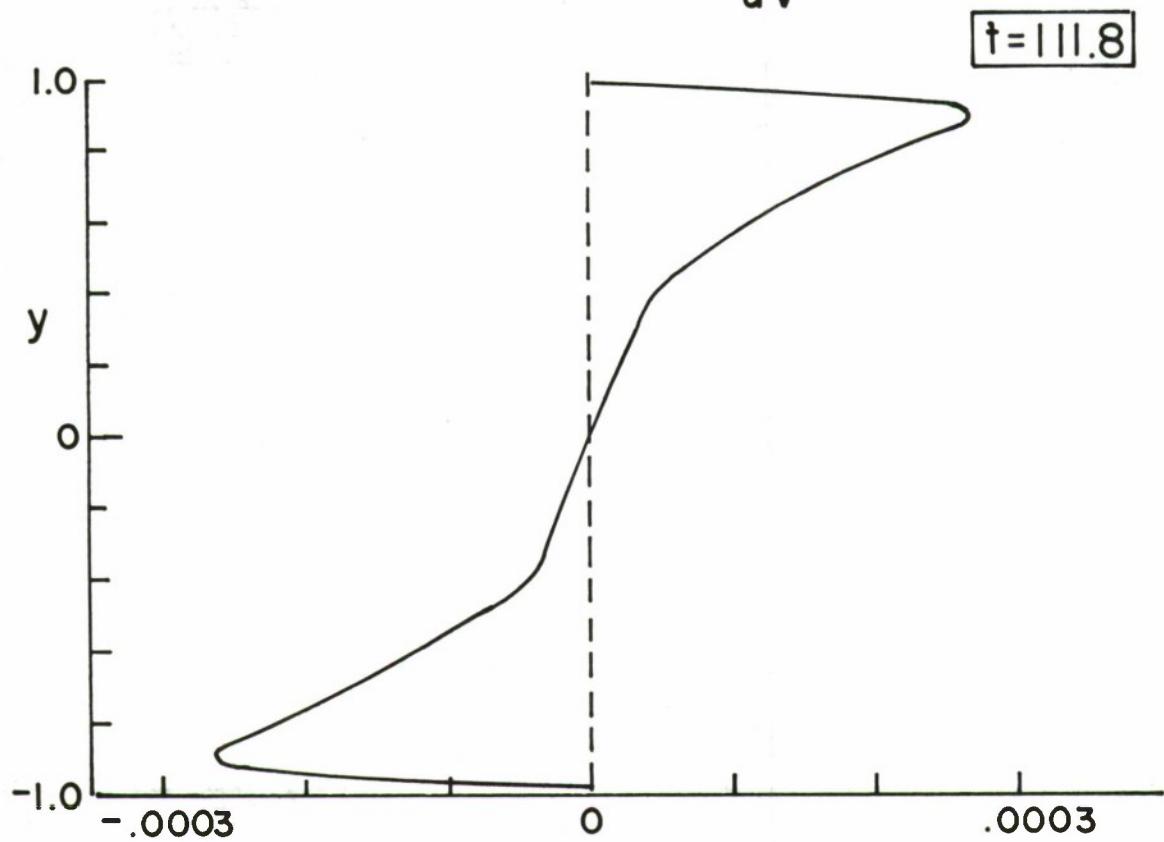
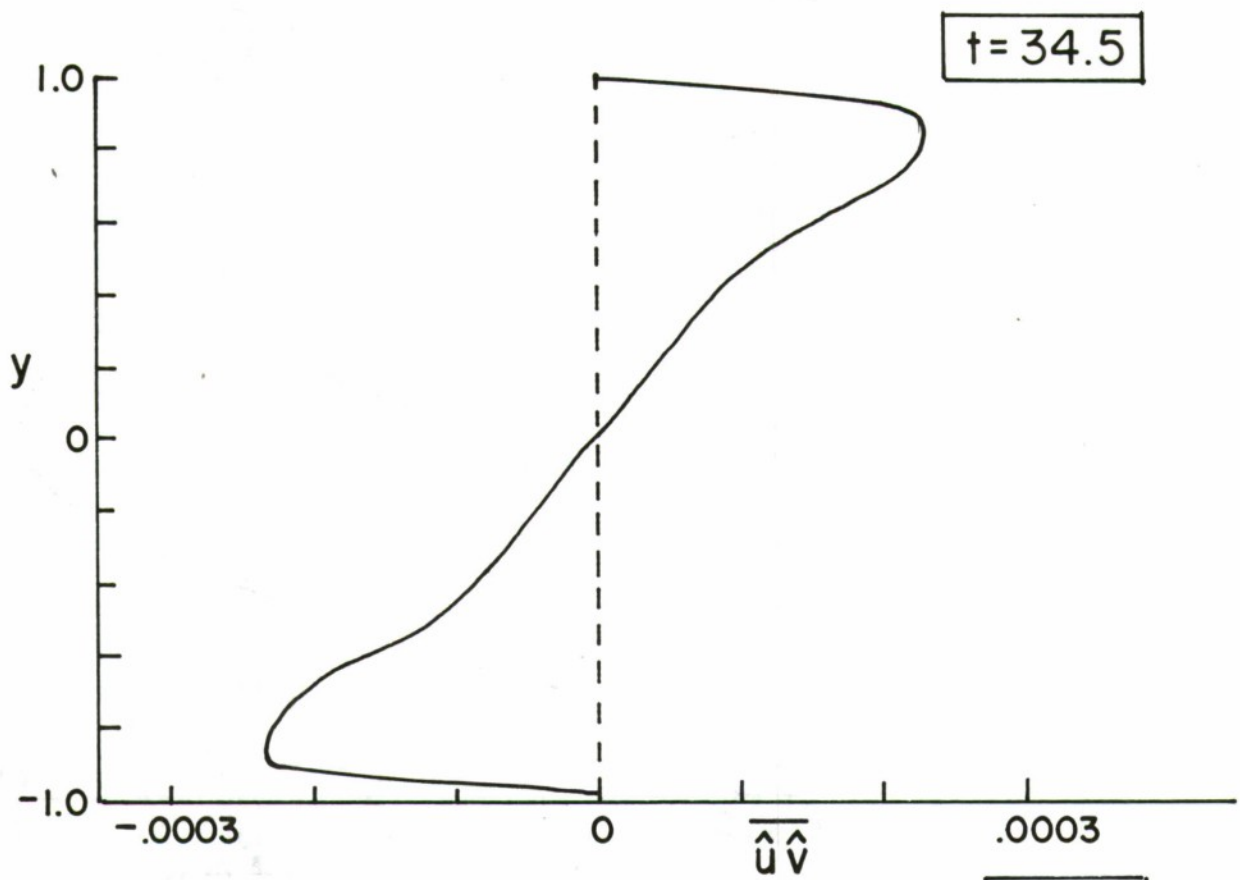


Figure 20b. Reynold's Stresses for the Run $\epsilon = .05/\sqrt{2}$
 $\alpha = 1.0$, $R_e = 6667$

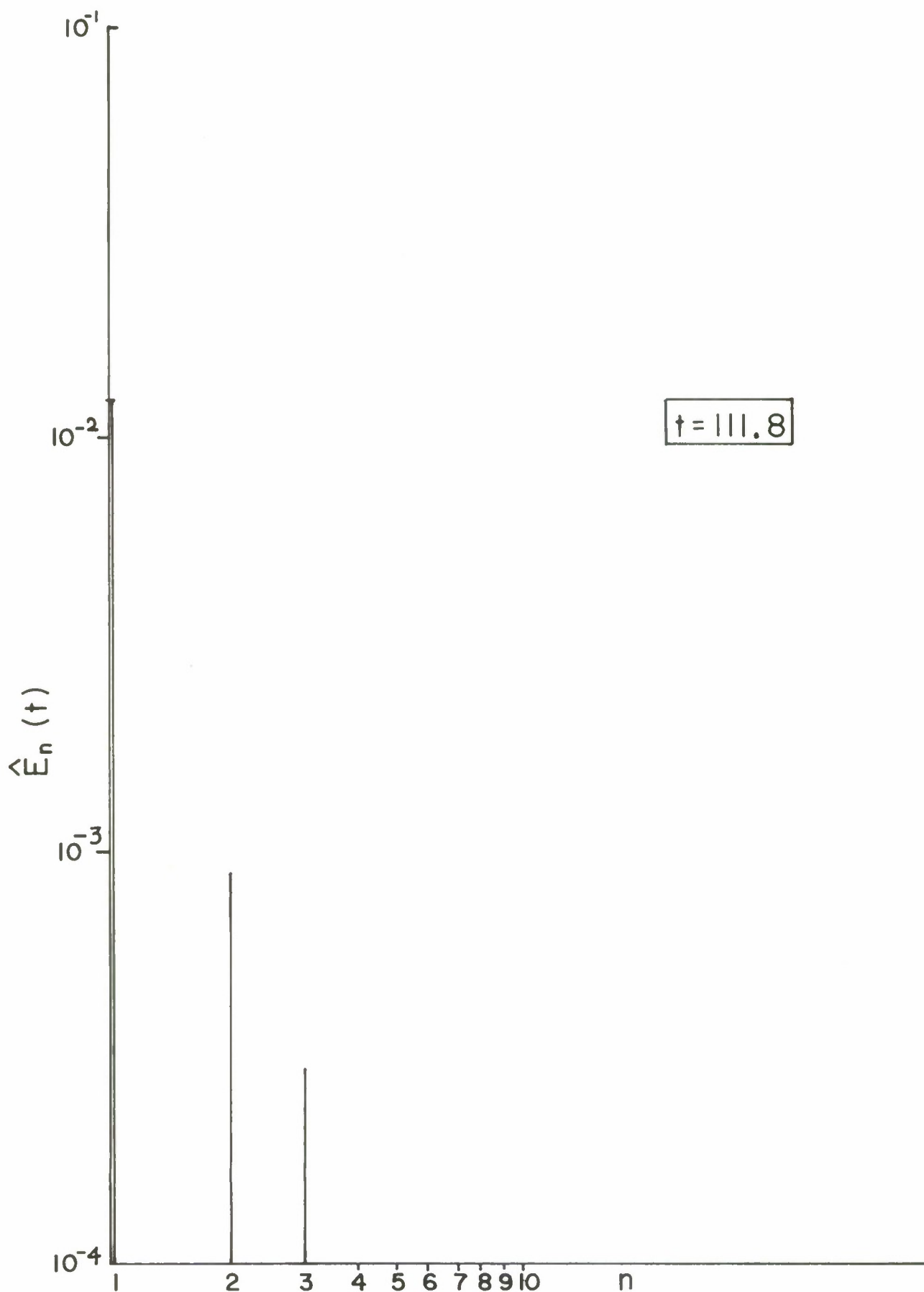


Figure 20c. Energy Spectrum for the Run $\epsilon = .05/\sqrt{2}$,
 $\alpha = 1.0$, $R_e = 6667$ 69

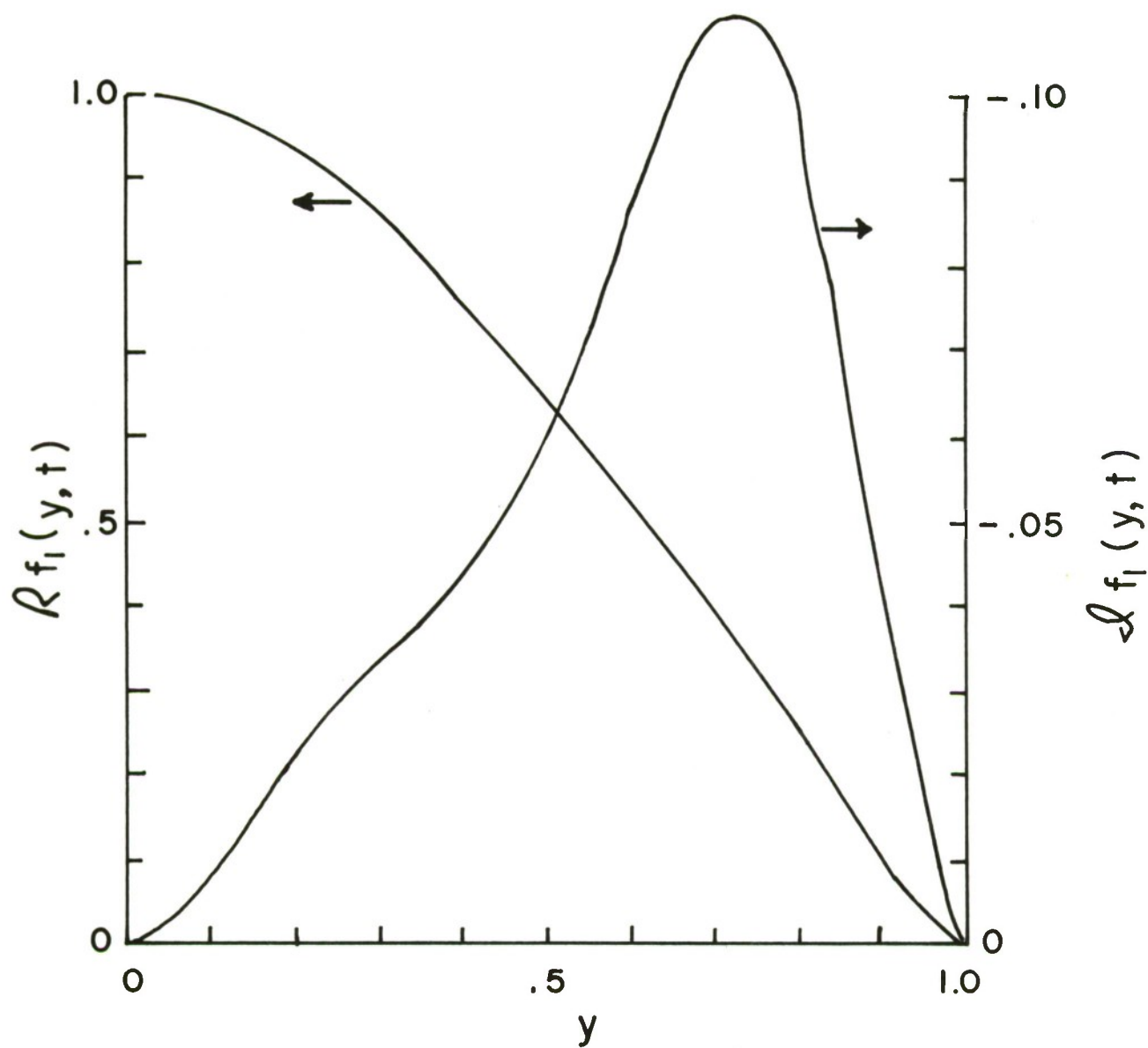


Figure 21a. Primary Mode Shape, f_1 , for the Run $\epsilon = .5$
at $t = 11$

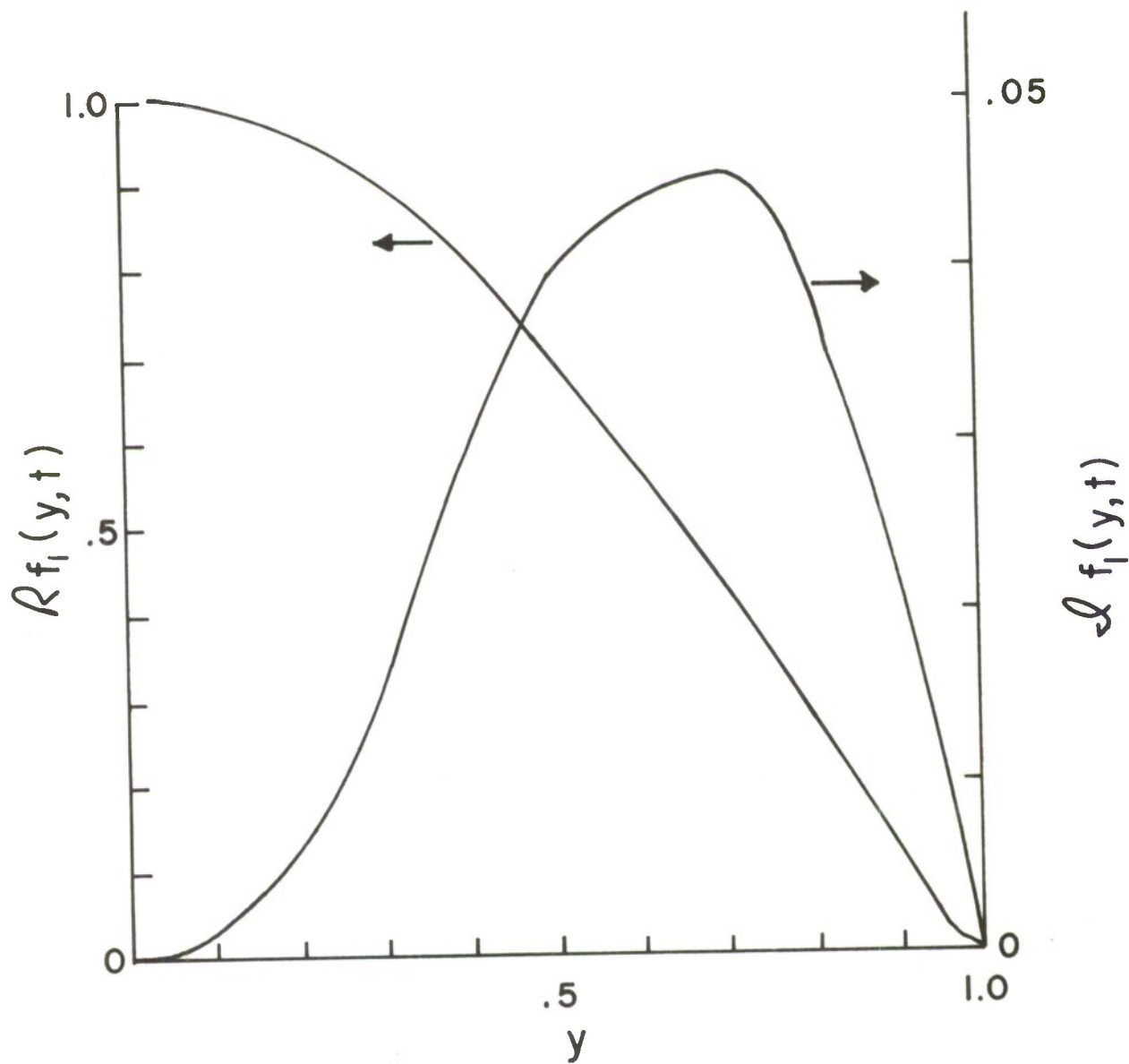


Figure 21b. Primary Mode Shape, f_1 , for the Run
 $\epsilon = .05\sqrt{5}$ at $t = 59$

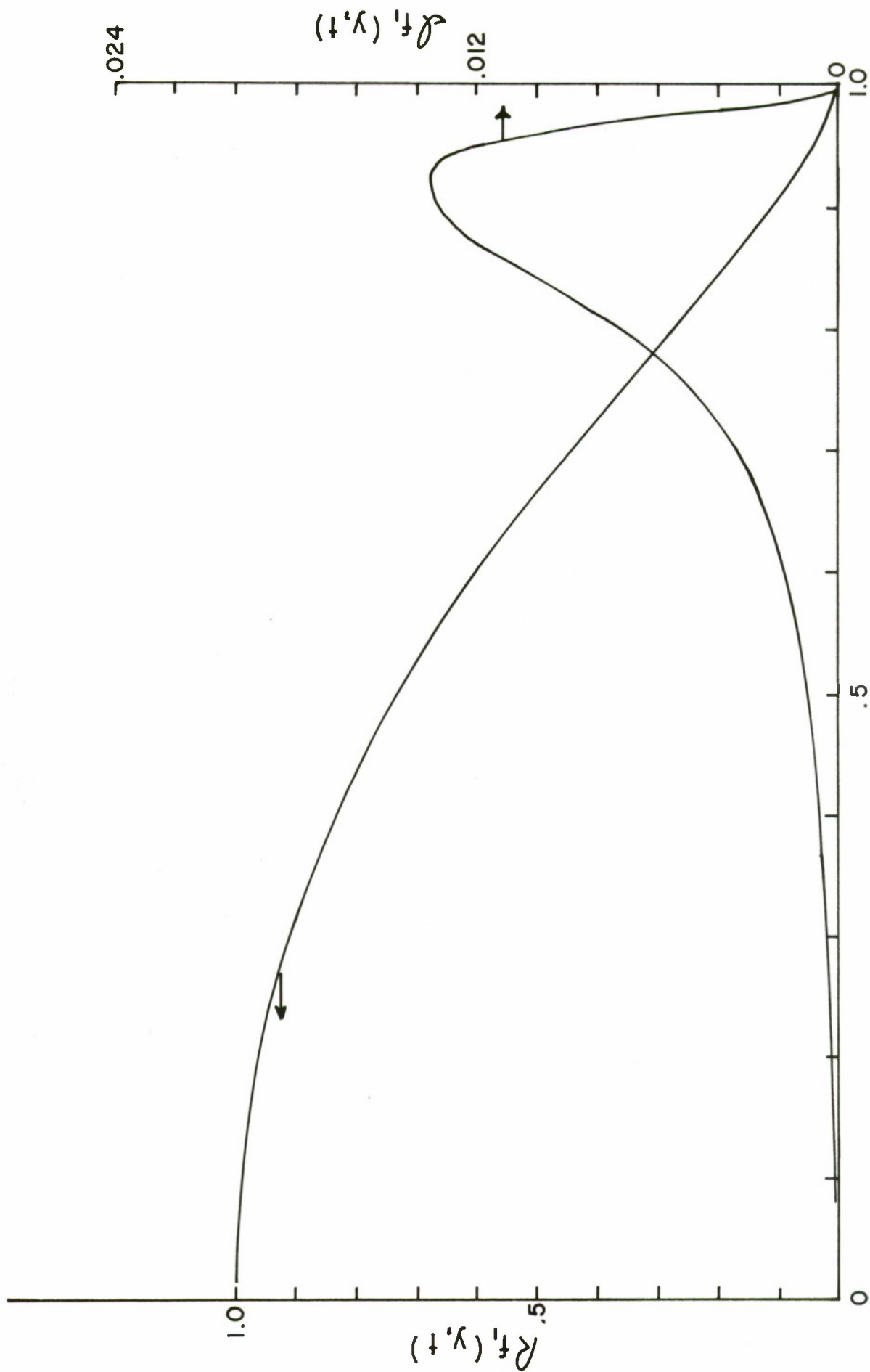


Figure 21c. Primary Mode Shape, f_1 , for the Run
 $\epsilon = .05/\sqrt{2}$ at $t = 112$

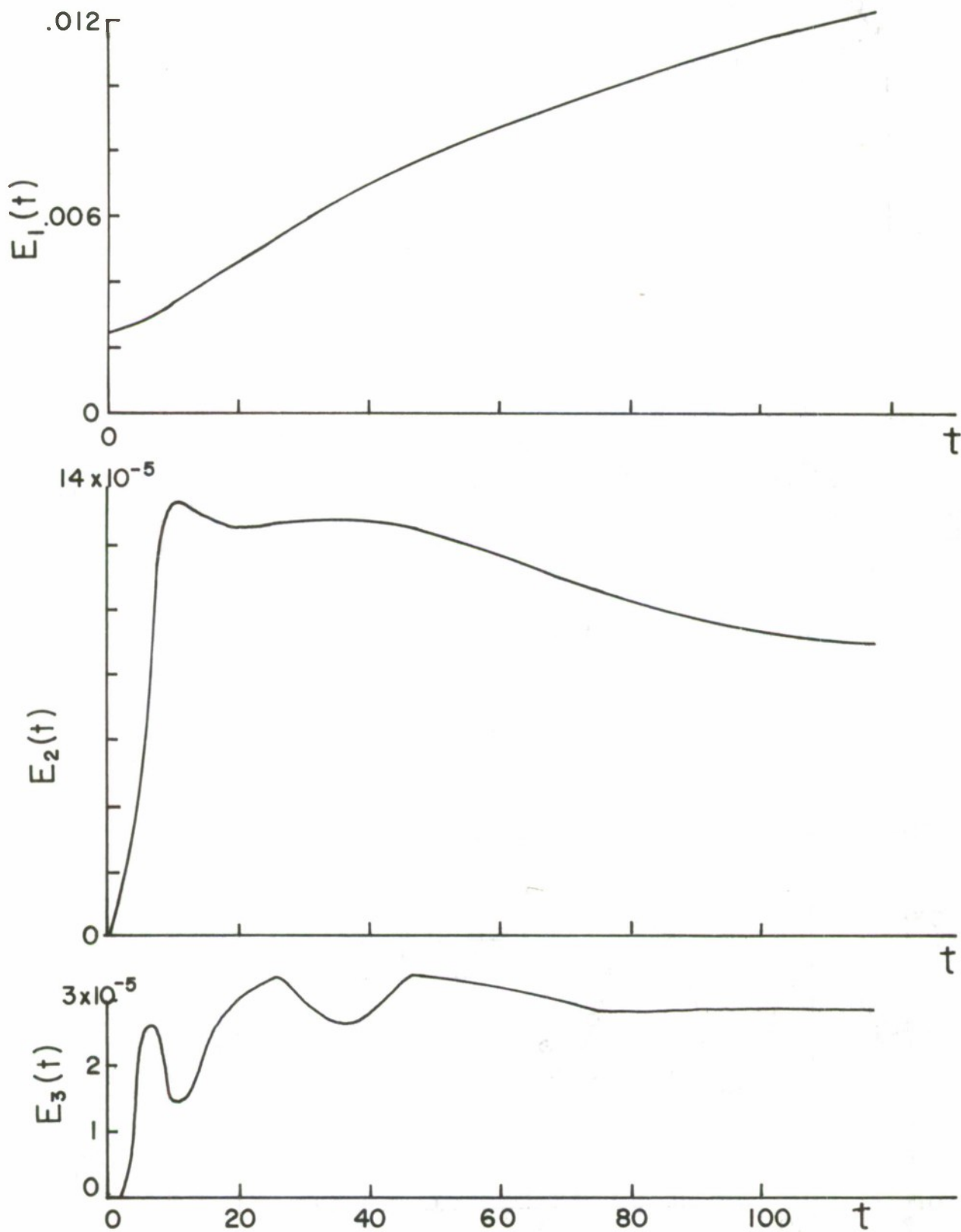


Figure 22. Energy Variation in E_1 , E_2 , and E_3 for the
Run $\epsilon = .05/\sqrt{2}$

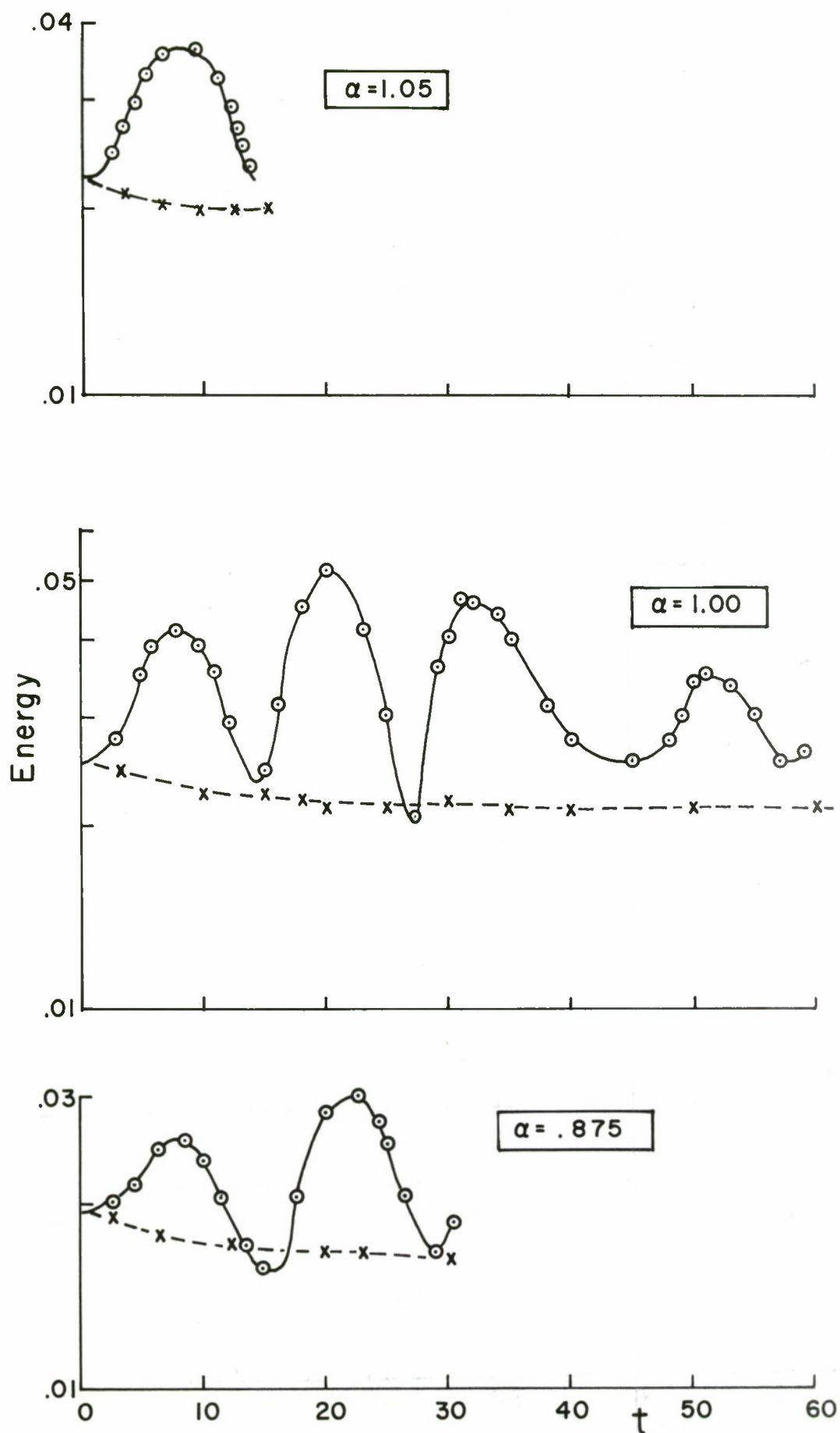


Figure 23. Energy Variation at $Re = 6667$ for Three Different Wavenumbers.
 -○- Turbulent Kinetic Energy
 -x- Total Kinetic Energy

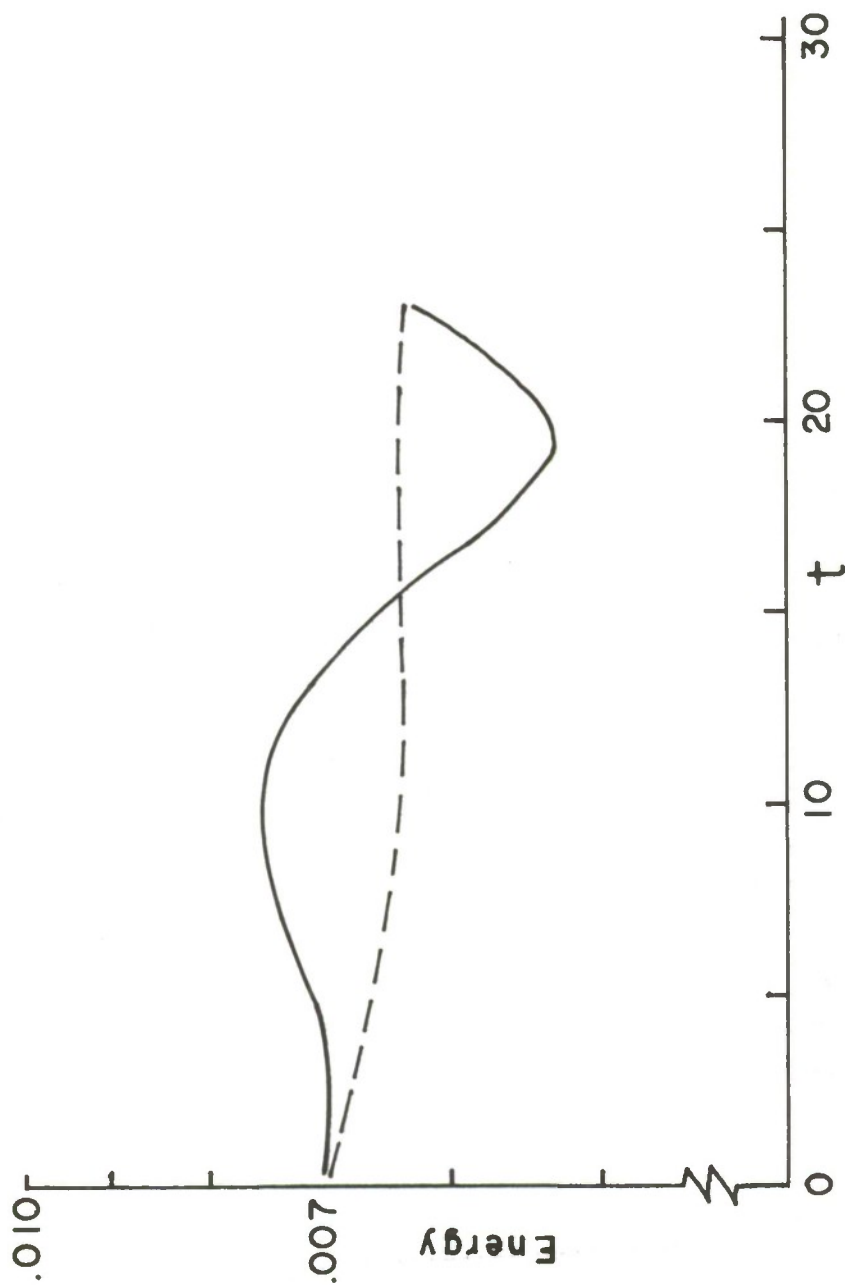


Figure 24. Energy Variation for $\alpha = .78$
 $R_e = 6667$, $\epsilon = .0635$. Dashed
 line is the total kinetic energy
 while solid line is turbulent
 kinetic energy.

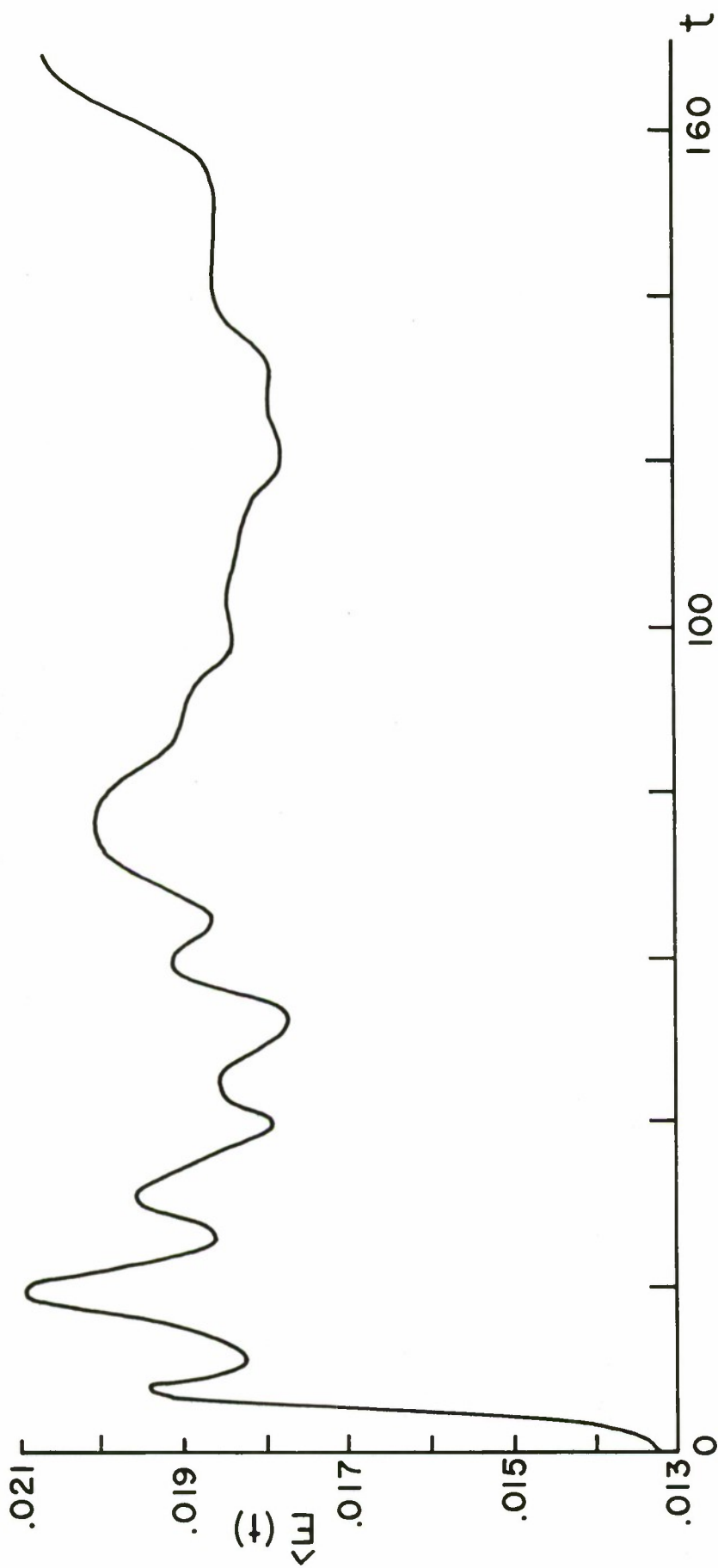


Figure 25. Turbulent Kinetic Energy for the Run with Modes f_7 and f_8 Initially Present $R_e = 6667$, $\epsilon = .059$

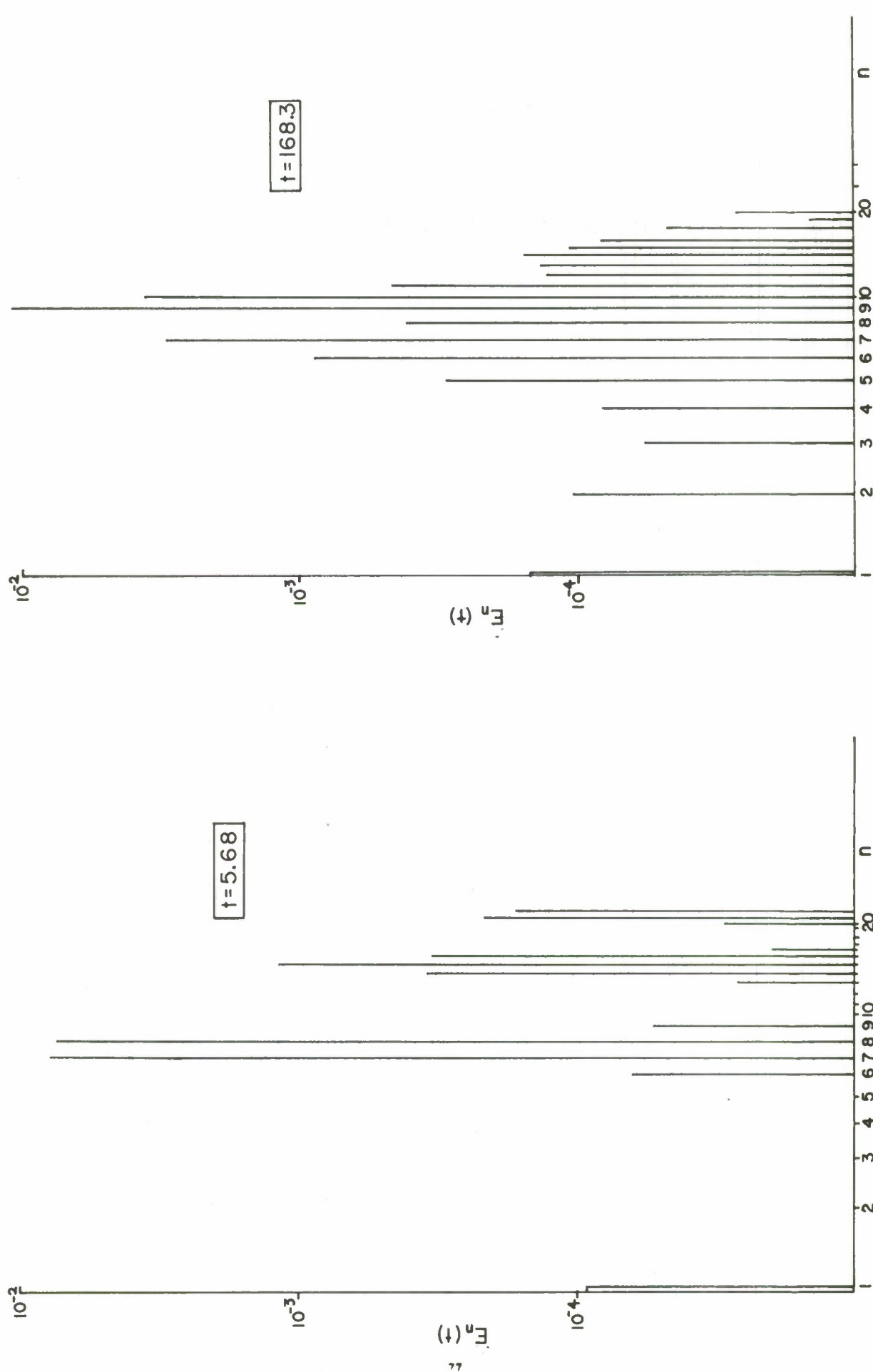


Figure 26. Energy Spectrum for the Run with Modes r_7 and r_8 Initially Present, $R_e = 6667$, $\epsilon = .059$

APPENDIX

LISTING OF THE FORTRAN CODE

```

COMMON / FIELDS / PHI,GAMA,FG,GAMOLD
COMMON / VECTOR / T,A,S,XALPHA,PHMEAN,GAMEAN,UMEAN,TEMP,TURBKE,
1 U,PHILAM,FF,ETA,GA,X,Y
COMMON / ARRAYS / IPO,IMO,INV,IAO,IAP,MM(3)
COMMON / PARAMS / N,M,NP1,NP2,NM1,NM2,NM3,NM4,NH,MP1,MP2,MP3,MM1,
1 M2M,MH,MHP,NPROB,ICOUNT,ITEL,INT,KSTEP,ISTART,
2 MSCIP,ITAPE,NITER,NITOT,NITMAX,IFIG,MCOMP,
3 KINT
COMMON / FACTOR / DX,DX2,DXSQR,DXSQR4,DXSQR8,DY,DY2,DYSQR,R,RSQR,
1 RSQRP,REYNLD,REY,FRACEL,XLAMDA,TIME,DT,DTT,PI,H,
2 EKMEAN,EKTURB,UVBAR,ATERM,BTERM,ALPHA,BETA,XM,XN,
3 XNM1,UMNFLO,UFO,TOL,FA,FB,FC,F1,F2,F3,F4,F5,F6
COMMON / SYMBOL / DOT,BLANK,XXX
DOUBLE PRECISION
1 DX,DX2,DXSQR,DXSQR4,DXSQR8,DY,DY2,DYSQR,R,RSQR,
2 RSQRP,REYNLD,REY,FRACEL,XLAMDA,TIME,DT,DTT,PI,H,
3 EKMEAN,EKTURB,UVBAR,ATERM,BTERM,ALPHA,BETA,XM,XN,
COMMON MRLOAD,NCYCLS,LINR
COMMON MRLOAD,PHY(64,201),GAMA(64,201),FG(64,201),GAMOLD(64,201)
1 UMEAN(201),TEMP(201),TURBKE(201),U(201),
2 PHILAM(201),T(201),A(128),S(32),XALPHA(64),
3 PHMEAN(201),GAMEAN(201),X(64),Y(201),FF(32),
DIMENSION
1 IPO(64),IMO(64),INV(32),IAO(64),IAP(64)
2 REAL*4 TITL(24)/'INITIAL VALUES OF PHI.'/
3
* * * * *
N =NUMBER OF POINTS IN Y DIRECTION
M =NUMBER OF POINTS IN X DIRECTION
NCYCLS=NUMBER OF TIME STEPS
MSCIP =NUMBER OF TIME STEPS BETWEEN CALLS CF S.R. PRINT
ISCIPI=NUMBER OF TIME STEPS BETWEEN CALLS CF S.R. PLOT
TOL =CONVERGENCE TOLERANCE FOR SOLUTION OF DELSQUARE PHI=GAMA
OMEGA =RELAXATION FACTOR
NITMAX=MAXIMUM NUMBER OF ITERATIONS IN RELAXATION
REYNLD=REYNOLDS NUMBER
FRACEL=DT*(UMAX*DY+VMAX*DX)/(DX*DY) --- CONTROLS DT
XLAMDA=4.*DT/(DX*DY*REYNLD) --- LIMITS DT
LINR IF LINR=1 THEN NON-LINEAR TERMS ARE ZEROED OUT
DATA CARDS
1 NPROB,NCYCLS ----- 2110
IF NPROB < 0 PROGRAM EXECUTES RESTART MODE ---- NO OTHER
DATA REQUIRED
2 N,M,NITMAX,ISCIPI,MSCIP ----- 5110
3 TOL,OMEGA,REYNLD,FRACEL,XLAMDA ----- 5F12.0

```

CCCCCCCCCCCCCCCCCCCCCCCCCCCCCCCC

```

* * * * * DIMENSIONS OF ARRAYS
* * * * * PHI,GAMA,FG,GAMOLD --- MXN
* * * * * UMEAN,TEMP,TURBKE,U,PHILAM,T,PHMEAN,GAMEAN,Y --- N
* * * * * XALPHA,X,IPO,IMO,IAO,IAIP --- M
* * * * * S,INV --- M/2
* * * * * A --- 2M
* * * * *
* * * * * THE FOLLOWING ARRAYS CONTAIN FIXED QUANTITIES AND SHOULD NEVER
* * * * * BE USED FOR TEMPORARY STORAGE.
* * * * *
* * * * * U,PHILAM,S,XALPHA,X,Y,IPO,IMO,INV,IAP,IAO
* * * * *
* * * * * CTHET ARRAYS MAY BE USED FOR TEMPORARY STORAGE AT CERTAIN PARTS
* * * * * OF THE PROGRAM. ARRAYS T AND A ARE MOST SUITABLE FOR THIS
* * * * * PURPOSE.
* * * * *
* * * * *
* * * * * FUNCTION
* * * * *
* * * * * SUBROUTINE
* * * * *
* * * * * SETUP
* * * * * REMAIN VALUES OF VARICUS QUANTITIES WHICH
* * * * * START ESTABLISH CONSTANT THROUGHOUT THE INTEGRATION
* * * * * TITLE AND VORTICITY INITIAL VALUES OF STREAM FUNCTION
* * * * * STEP WRITES OUTPUT TITLE
* * * * * ADVANC TIME STEP BY MODIFIED EULER IMPLICIT TIME
* * * * * PRESUR DIFFERENCING
* * * * * TRISOL TIME STEP BY DUFORT FRANKEL CENTRAL DIFFERENCING
* * * * *
* * * * * TIMER SOLUTION OF A SPECIAL TRIANGONAL SYSTEM OF
* * * * * MEANS LINEAR EQUATIONS BY GAUSS ELIMINATION.
* * * * * ENERGY CALLED BY SUBROUTINE PRESUR
* * * * *
* * * * * CALL EDDYS(+1) --- PUTS PHI-PHMEAN IN FG

```


CC

STRESS PRINT PLOT	CALL EDDYS(-1) --- PUTS GAMA-GAMEAN IN FG COMPUTES TURBULENT REYNOLDS STRESS PRINTS OUTPUT LINE	00C0C990 00001000 00001010 00001020 00001030 00001040 00001050 00001060 00001070 00001080 00001090 00001100 00001110 00001120 00001130 00001140 00001150 00001160 00001170 00001180 00001190 00001200 00001210 00001220 00001230 00001240 00001250 00001260 00001270 00C01280
SPCTRM	TURBULENCE SPECTRAL DENSITY OF MEAN VELOCITY, VORTICITY COMPUTES SPECTRAL DENSITY OF TURBULENT KINETIC ENERGY OR SQUARED VORTICITY AS FUNCTIONS OF Y, AND THE MEAN OVER Y. CALLED BY PRESUR	00001020 00001030 00001040 00001050 00001060 00001070 00001080 00001090 00001100 00001110 00001120 00001130 00001140 00001150 00001160 00001170 00001180 00001190 00001200 00001210 00001220 00001230 00001240 00001250 00001260 00001270 00C01280
Modes	CALL SPCTRM(1) --- KINETIC ENERGY CALL SPCTRM(-1) --- SQUARED VORTICITY COMPUTES AND PRINTS MODAL VECTORS CALL MODES(MOD1,MOD2,1) PRINTS VECTORS FOR FOURIER MODES MOD1 AND MOD2 NORMALIZED SO THAT AT Y=0 REAL PART = 1, AND IMAGINARY PART=0. CALL MODES(MOD1,MOD2,2) PRINTS MODULUS AND PHASE	00001020 00001030 00001040 00001050 00001060 00001070 00001080 00001090 00001100 00001110 00001120 00001130 00001140 00001150 00001160 00001170 00001180 00001190 00001200 00001210 00001220 00001230 00001240 00001250 00001260 00001270 00C01280
PLOTSP	PRINTS ONLINE GRAPHS --- GENERAL CALL PLOTSP(A,B,N) PRINTS GRAPHS OF POSITIVE N-DIMENSIONAL VECTORS A AND B	00001020 00001030 00001040 00001050 00001060 00001070 00001080 00001090 00001100 00001110 00001120 00001130 00001140 00001150 00001160 00001170 00001180 00001190 00001200 00001210 00001220 00001230 00001240 00001250 00001260 00001270 00C01280
CPlot Output	PRINTS TWO DIMENSIONAL ARRAYS. CALL OUTPUT(1) --- PRINTS PHI CALL OUTPUT(2) --- PRINTS GAMA CALL OUTPUT(3) --- PRINTS FG	00001020 00001030 00001040 00001050 00001060 00001070 00001080 00001090 00001100 00001110 00001120 00001130 00001140 00001150 00001160 00001170 00001180 00001190 00001200 00001210 00001220 00001230 00001240 00001250 00001260 00001270 00C01280
LOAD RELOAD DHARM	READS DATA FROM TAPE OR DISC WRITES DATA ON TAPE OR DISC COMPUTES FINITE FOURIER TRANSFORM. DHARM IS INCLUDED IN THE IBM SCIENTIFIC LIBRARY OF PRE COMPILED PROGRAMS AVAILABLE AT NPS.	00001020 00001030 00001040 00001050 00001060 00001070 00001080 00001090 00001100 00001110 00001120 00001130 00001140 00001150 00001160 00001170 00001180 00001190 00001200 00001210 00001220 00001230 00001240 00001250 00001260 00001270 00C01280
PRMTRS	COMPUTES LATERAL STATIONS OF PHASES OF FIRST FIVE MODES AT SEVERAL STATIONS	00001020 00001030 00001040 00001050 00001060 00001070 00001080 00001090 00001100 00001110 00001120 00001130 00001140 00001150 00001160 00001170 00001180 00001190 00001200 00001210 00001220 00001230 00001240 00001250 00001260 00001270 00C01280
LOGICAL ICOUNT INT	NUMBER OF COMPLETED TIME STEPS CONTROLS DETAILED OUTPUT---WHEN ICOUNT=INT MAIN CALLS PRINT, PRESUR CALLS SPCTRM ETC.	00001290 00001300 00001310 00001320 00001330 00001340 00001350 00001360 00001370 00001380 00001390 00001400 00001410 00001420 00001430 00001440
ISCIP MCOMP	INCREMENT FOR INT CONTROLS SINGLE LINE OUTPUT---WHEN ICOUNT=MCOMP MAIN CALLS PRINT	00001290 00001300 00001310 00001320 00001330 00001340 00001350 00001360 00001370 00001380 00001390 00001400 00001410 00001420 00001430 00001440
MSCIP KSTEP	INCREMENT FOR MCOMP CONTROLS CALL OF SUBROUTINE STEP. IF ICOUNT= KSTEP TIME STEP IS PERFORMED BY STEP	00001290 00001300 00001310 00001320 00001330 00001340 00001350 00001360 00001370 00001380 00001390 00001400 00001410 00001420 00001430 00001440
KINT	INCREMENT FOR KSTEP. IF KINT=1 THEN INTEGRATION IS BY MOD EULER TIME DIFFERENCING.	00001290 00001300 00001310 00001320 00001330 00001340 00001350 00001360 00001370 00001380 00001390 00001400 00001410 00001420 00001430 00001440


```

C C C C C C C
MRLOAD      CCNTRLS  FREQUENCY AT WHICH DATA IS WRITTEN ON DISK
              THIS IS INCLUDED AS A PRECAUTION TO PREVENT LOSING
              A LENGTHY COMPUTATION DUE TO MACHINE FAILURE NEAR
              END OF COMPUTATION
* * * * *
1  READ(5,11) NPROB, NCYCLS, LINR
   ITAPE=10
   CALL ERRSET(255,1000,-1,1)
   IF(NPROB.LT.0) GO TO 2
   READ(5,12) N,M,ISCIP,MSCIP
   READ(5,13) REYNLD,FRACEL,XLAMDA
   READ(5,19) DOT,BLANK,XXX
   INT=0
   ISTART=0
   KSTEP=0
   MCOMP=0
   TIME=0.
   NITOT=0
   MRLOAD=200
   CALL SETUP
   CALL START
   WRITE(6,14) NPROB, NCYCLS, N, M, NITMAX, ISCIP, MSCIP
   GO TO 3
2  CALL LOAD
   MCOMP=ISTART
   ISCIP=55
   CALL TITLE
   WRITE(6,15)
   WRITE(6,16)
   IFIG=1
   CALL PRINT
   CALL PLOT
3  DO 10 ICOUNT=ISTART, NCYCLS
   IF(ICOUNT.NE.MCOMP) GO TO 5
   MCOMP=MCOMP+MSCIP
4  CALL PRINT
5  IF(ICOUNT.NE.INT) GO TO 7
6  INT=INT+ISCIP
   CALL PLOT
7  CALL ADVANC
   IF(ICOUNT.NE.MRLOAD) GO TO 8
   MRLOAD=MRLOAD+200
   ISTART=ICOUNT+1
   CALL RELOAD
8  CONTINUE

```

```

00001450
00001460
00001470
00001490
00001500
00001510
00001520
00001530
00001540
00001550
00001560
00001570
00001580
00001590
00001600
00001610
00001620
00001630
00001640
00001650
00001660
00001670
00001680
00001690
00001700
00001710
00001720
00001730
00001740
00001750
00001760
00001770
00001780
00001790
00001800
00001810

```

```

00001820
00001830
00001840
00001850
00001860
00001880
00001890
00001900
00001910
00001920
00001930
00001940
00001950
00001960
00001970
00001980

CCCONTINUE
I$TART=NCYCCLS+1
CALL PRINT
WRITE(6,17)
WRITE(6,18)
FCFORMAT(3,110)
FCFORMAT(5,110)
FCFORMAT(5G12,0)
FCFORMAT(7,110)
FCFORMAT(10X,'INITIAL VALUES OF STREAM FUNCTION'//)
FCFORMAT(10X,'INITIAL VALUES OF VORTICITY'//)
FCFORMAT(10X,'STREAM FUNCTION'//)
FCFORMAT(10X,'VORTICITY'//)
FCFORMAT(3A1)
CALL RELOAD
STOP
END

```

[illegible]

UUUU

C

PI=3.1415926535898
H=3.1415926535898

C C

ALPHA=1.D0
H=H/ALPHA
KINT=50
NITMAX=15
NP2=N+2
NPI=N+1
NM1=N-1
NM2=N-2
NM3=N-3
NM4=N-4
NH=N/2+1
NM(1)=M
MM(2)=0
MM(3)=0
N=2**M
MH=M/2
MHP=MH+1
MPI=M+1
MP2=M+2
MP3=M+3
M2M=M+M-1
MM1=M-1
XN=DFLOAT(N)
XNM1=DFLOAT(NM1)
XM=DFLOAT(M)
DX=2.D0*H/XM
DX2=2.D0*DX
DXSQR=DX*DX
DXSQR4=4.D0*DXSQR
DXSQR8=8.D0*DXSQR
DY=2.D0/XNM1
DY2=2.D0*DY
DYSQR=DY*DY
R=DX/DY
RSQR=R*R
RSQRP=RSQR+1.D0
REY=1.D0/REYNLD
TOL=.00002DC
ATERM=1.D0/(2.D0*DYSQR)
BTERM=XM*DX2*DY2
FA=1.D0/(XM*XM)
FB=1.D0/(DY2**2)
FC=1.D0/(8.D0*(XM*DY)**2)

00002280
00002290
00002300
00002310
00002330

00002350
00002360
00002370
00002380
00002390
00002400
00002410
00002420
00002430
00002440
00002450
00002460
00002470
00002480
00002490
00002500
00002510
00002520
00002530
00002540
00002550
00002560
00002570
00002580
00002590
00002600
00002610
00002620
00002630
00002640
00002650
00002660
00002670
00002680
00002690
00002700
00002710
00002720
00002730
00002740
00002750


```

100 C C C C C
    THETA=2.00*PI/XM
    WRITE(6,100)R,RSQR,RSQRP
    FORMAT(8X,F12.8,3X,F12.8,3X,F12.8)

    SET UP PERIODIC COUNTERS
    SET UP INDEXING COUNTERS, IAU & IAP.

    JC=0
    DO 10 I=1,M
      IPO(I)=I+1
      IMO(I)=I-1
      IAO(I)=I+JC
      IAP(I)=IAO(I)+1
      JC=JC+1
    CONTINUE
    IPO(M)=1
    IMO(1)=M
10 C C C C C

    SET UP COORDINATES

    DO 20 J=1,N
      Y(J)=DFLOAT(J-1)*DY-1.00
    CONTINUE
    DO 30 I=1,M
      X(I)=DFLOAT(I-1)*DX-H+DX/2.00
    CONTINUE
30 C C C C C

    SET UP MODAL CONSTANTS. --- ALPHA & FF .

    ALPHA=DYSQR/DXSQR
    XALPHA(1)=2.00
    FF(1)=0.00
    DO 35 I=2,MH
      IM=I-1
      IA=IAP(IM)
      IP=IA+1
      XNN=DFLOAT(IM)
      XALPHA(IA)=2.00*(1.00-ALPHA*(DCOS(THETA*XNN)-1.00))
      XALPHA(IP)=XALPHA(IA)
      FF(I)=1.00/DXSQR*(DSIN((2.00*PI*XNN)/XM))**2
    CONTINUE
35 C C C C C

    XNN=DFLOAT(MH)
    XALPHA(M)=2.00*(1.00-ALPHA*(DCOS(THETA*XNN)-1.00))

    SET UP S AND INV TABLES FOR DHARM.
    CALL DHARM(A,MM,INV,S,0,IFERR)
C C C C C
00002760
00002770
00002780
00002790
00002800
00002810
00002820
00002830
00002840
00002850
00002860
00002870
00002880
00002890
00002900
00002910
00002920
00002930
00002940
00002950
00002960
00002970
00002980
00002990
00003000
00003010
00003020
00003030
00003040
00003050
00003060
00003070
00003080
00003090
00003100
00003110
00003120
00003130
00003140
00003150
00003160
00003170
00003180
00003190
00003200
00003210
00003220
00003230

```

C
C
C

LAMINAR FLOW STREAM FUNCTION AND VELOCITY

```
DO 40 J=2,NM1
PHILAM(J)=.5*Y(J)*(Y(J)**2-3.)
U(J)=-1.5*(Y(J)**2-1.)
CCNT INUE
PHILAM(1)=1.
PHILAM(N)=-1.
U(1)=0.
U(N)=0.
```

40

C

RETURN
END

SUBROUTINE START /
COMMON / FIELDS /
COMMON / VECTOR /

1 COMMON / ARRAYS /
COMMON / PARAMS /

1 2 3
COMMON / FACTOR /

1 2 3
COMMON / SYMBOL /
DOUBLE PRECISION

1 2 3
DIMENSION PHI(64,201)
DOUBLE PRECISION

1 2 3
DIMENSION
DOUBLE PRECISION
PI,THETA,C,B,XL
DOUBLE PRECISION EPS,THETA2

C
C
C
C

BOUNDARY VALUES OF STREAM FUNCTION

PI=3.1415926535898

000033240
000033250
000033260
000033270
000033280
000033290
000033300
000033310
000033320
000033330
000033340
000033350
000033360
000033370

PHI,GAMA,FG,GAMOLD
T,A,S,XALPHA,FF,ETA,GA,X,Y
U,PHILAM,INV,IAO,IAP,MM(3)
IPC,IMO,NP1,NP2,NM1,NM2,NM3,NM4,NH,MPI,MP2,MP3,MM1,
M2M,MH,MHP,NPROB,ICOUNT,ITEL,INT,KSTEP,ISTART,
ISCIPI,MSCIPI,ITAPE,NITER,NITOI,NITMAX,IFIG,MCOMP,
KINT
DX,DX2,DXSQR,DXSQR4,DXSQR8,DY,DY2,DYSQR,R,RSQR,
RSQRP,REYNLD,REY,FRACEL,XLAMDA,TIME,DT,DTT,PI,H,
EKMEAN,EKTURB,UVBAR,ATERM,BTERM,ALPHA,BETA,XM,XN,
XNM1,UMNFLO,UFLO,TOL,FA,FB,FC,F1,F2,F3,F4,F5,F6
DOT,BLANK,XXX
DX,DX2,DXSQR,DXSQR4,DXSQR8,DY,DY2,DYSQR,R,RSQR,
RSQRP,REYNLD,REY,FRACEL,XLAMDA,TIME,DT,DTT,PI,H,
EKMEAN,EKTURB,UVBAR,ATERM,BTERM,ALPHA,BETA,XM,XN,
XNM1,UMNFLO,UFLO,TOL,FA,FB,FC,F1,F2,F3,F4,F5,F6
XNM1,UMNFLO,UFLO,TOL,FA,FB,FC,F1,F2,F3,F4,F5,F6
GAMA(64,201),GAMA(64,201),FG(64,201),GAMOLD(64,201),
UMEAN(201),TEMP(201),TURBKE(201),U(201),
PHILAM(201),T(201),A(128),S(32),XALPHA(64),
PHMEAN(201),GAMA(201),
ETA(201),GA(201),
IPO(64),IMO(64),INV(32),IAO(64),IAP(64)
PI,THETA,C,B,XL

000033380
000033390
000033400
000033410
000033420
000033430
000033440
000033450
000033460
000033470
000033480
000033490
000033500
000033510
000033520
000033530
000033540
000033550
000033560
000033570
000033580
000033590
000033600
000033610
000033620

000033640
000033650
000033660
000033670
000033680
000033690


```

DO 10 I=1,M
PHI(I,1)=0.
PHI(I,N)=0.
CC
10 CONTINUE
CC
ESTABLISH INITIAL VALUES OF STREAM FUNCTION
USE ARRAYS UMEAN AND TEMP FOR TEMPORARY STORAGE
CC
      A1,B,D,D,E,F ARE DUMMY VARIABLES
      DO 60 J=1,NH
      READ(5,11) PHMEAN(J),GAMEAN(J),A1,B,C,D,E,F
      FORMAT(8F10.0)
      CC
      CONTINUE
      NHM=NH-1
      DO 65 J=1,NHM
      JC=N-J+1
      PHMEAN(JC)=PHMEAN(J)
      GAMEAN(JC)=GAMEAN(J)
      CC
      CONTINUE
      CC
      FORMAT(10X,3(F12.6,3X))
      EPS=.1DO/DSQRT(2.0DO)
      EPS=EPS*1.8DO
      EPS=1.0DO
      EPS=.2DO
      EPS=.01DO
      DO 71 J=1,N
      C=PHMEAN(J)
      B=GAMEAN(J)
      DO 70 I=1,M
      THETA=X(I)
      PHI(I,J)=EPS*(C*DCOS(THETA)+B*DSIN(THETA))
      CC
      CONTINUE
      WRITE(6,12) Y(J),C,B
      CC
      CONTINUE
      CC
      COMPUTE INITIAL VALUES OF VORTICITY
      CC
      DO 15 I=1,M
      IP=IPO(I)
      IM=IMG(I)
      GAMA(I,N)=(8.0DO*PHI(I,NM1)-PHI(I,NM2))*ATERM
      GAMA(I,1)=(8.0DO*PHI(I,2)-PHI(I,3))*ATERM
      GAMA(I,N)=(1.5*PHI(I,NM2)-4.*PHI(I,NM3)/9.)/DYSQR
      GAMA(I,1)=(1.5*PHI(I,3)-4.*PHI(I,4)/9.)/DYSQR
      GAMOLD(I,1)=GAMA(I,1)
      GAMOLD(I,N)=GAMA(I,N)
      DO 15 J=2,NM1
      GAMA(I,J)=(RSQR*(PHI(I,J+1)+PHI(I,J-1))+PHI(IP,J)+PHI(IM,J))

```

```

1 GAMOLD(I,J)=GAMA(I,J)-2.DC*RSQR*PHI(I,J))/DXSQR
15 CONTINUE
CALL MEANS
CALL TIMER
WRITE(6,99)(I,I=1,10)
WRITE(6,100)J=1,15
DO 131 J=1,15
WRITE(6,101)J,Y(J), (GAMA(I,J), I=1,10)
CONTINUE
131 FORMAT(1H0,3X,'INITIAL DISTURBANCE GAMA',
99 FORMAT(1H,5X,'I=',11X,10(13,8X)),
100 FORMAT(1X,'J=',13,1X,'Y=',F6.3,2X,10(
101 RETURN
END

```

SUBROUTINE	MEANS	COMMON	/	FIELDS	/	COMMON	/	VECTOR
1	PHI, GAMA, FG, GAMOLD	CCOMMON	/	T, A, S, XALPHA, PHMEAN, G, X, Y	/	00012450		
1	U, PHILAM, FF, ETA, GA, X, Y	CCOMMON	/	IPO, IMO, INV, IAO, IAP, MM(3)	/	00012460		
2	N, M, NP1, NP2, NM1, NM2, NM3, NM4, NH, MP1, MP2, MP3, MM1,	COMMON	/	M2M, MH, MHP, NPROB, ICOUNT, ITTEL, INT, KSTEP, ISTART,	/	00012470		
3	ISCIPI, MSCIP, ITAPE, NITER, NITOT, NITMAX, IFIG, MCOMP,	COMMON	/	KINT	/	00012480		
1	DX, DX2, DXSQR, DXSQR4, DXSQR8, DY, DY2, DYSQR, R, RSQR,	CCOMMON	/	RSQR, REYNLD, REY, FRACCEL, XLAMDA, TIME, DT, DTT, PI, H,	/	00012490		
2	EKMEAN, EKTURB, UVBAR, ATERM, BTERM, ALPHA, BETA, XM, XN	COMMON	/	XNM1, UMNFLQ, UFLQ, TOL, FFA, FB, FC, FI, F2, F3, F4, F5, F6	/	00012500		
3	DOT, BLANK, XXX	COMMON	/	DO, BLANK, XXX	/	00012510		
1	DX, DX2, DXSQR, DXSQR4, DXSQR8, DY, DY2, DYSQR, R, RSQR,	DOUBLE	/	RSQR, REYNLD, REY, FRACCEL, XLAMDA, TIME, DT, DTT, PI, H,	/	00012520		
2	EKMEAN, EKTURB, UVBAR, ATERM, BTERM, ALPHA, BETA, XM, XN	DOUBLE	/	XNM1, UMNFLQ, UFLQ, TOL, FFA, FB, FC, FI, F2, F3, F4, F5, F6	/	00012530		
3	XNM1, UMNFLQ, UFLQ, TOL, FFA, FB, FC, FI, F2, F3, F4, F5, F6	DOUBLE	/	XNM1, UMNFLQ, UFLQ, TOL, FFA, FB, FC, FI, F2, F3, F4, F5, F6	/	00012540		
1	PHI(64, 201), GAMA(64, 201), FCG(64, 201), GAMOLD(64, 201)	DIMENSION		U(64, 201), TEMP(201), TURBKE(201), U(201),		00012550		
2	U(64, 201), TEMP(201), TURBKE(201), U(201),	DOUBLE		PHILAM(201), T(201), A(128), S(32), XALPHA(64),		00012560		
3	PHILAM(201), T(201), A(128), S(32), XALPHA(64),	DOUBLE		PHMEAN(201), GAMEAN(201), X(64), Y(201), FF(32),		00012570		
1	ETA(201), GA(201)	DIMENSION		IPO(64), IMO(64), INV(32), IAO(64), IAP(64)		00012580		
2	IPO(64), IMO(64), INV(32), IAO(64), IAP(64)	DOUBLE				00012590		
3		DIMENSION				00012600		
1		DOUBLE				00012610		
2		DOUBLE				00012620		
3		DOUBLE				00012630		
1		DOUBLE				00012640		
2		DOUBLE				00012650		
3		DOUBLE				00012660		
1		DOUBLE				00012670		
2		DOUBLE				00012680		
3		DOUBLE				00012690		

```

*****
THIS ROUTINE COMPUTES THE MEAN VALUES OF PHI AND GAMA
ARRAY A IS USED FOR TEMPORARY STORAGE.
DO 10 J=1,N

```

00012760
00012770
00012780
00012790
00012800
00012810
00012820
00012830
00012840
00012850
00012860
00012870
00012880

```

DO 20 I=1,M
A(I)=PHI(I,J)
CONTINUE
CALL ASUM(A,M,SUM)
PHMEAN(J)=SUM/XM
DO 30 I=1,M
A(I)=GAMA(I,J)
CONTINUE
CALL ASUM(A,M,SUM)
GAMEAN(J)=SUM/XM+3.DO*Y(J)
10 CONTINUE
END

```

00004180
00004190
00004200
00004210
00004220
00004230
00004240
00004250
00004260
00004270
00004280
00004290
00004300
00004310
00004320
00004330
00004340
00004350
00004360
00004370
00004380
00004390
00004400
00004410
00004420
00004430
00004440
00004450
00004460
00004470
00004480
00004490
00004500

```

SUBROUTINE TITLE /
COMMON / FIELDS /
COMMON / VECTOR /
1 CGCOMMON / ARRAYS /
COMMON / PARAMS /
1 2 3
COMMON / FACTOR /
1 2 3
COMMON / SYMBOL /
DOUBLE PRECISION
1 2 3
DIMENSION PHI(64,201),GAMA(64,201),TEMP(201),TURBKE(201),
DOUBLE PRECISION
1 2 3
DIMENSION UMEAN(201),T(201),A(128),S(32),XALPHA(64),
PHMEAN(201),GAMA(201),ETA(201),
IPO(64),IMO(64),INV(32),IAO(64),IAP(64)
* * * * *
WRITE(6,11)
WRITE(6,22)
WRITE(6,12)NPROB
IF(NPROB.LT.0) WRITE(6,23)
WRITE(6,13)M,N
WRITE(6,14)REYNLD

```

C C C


```

WRITE(6,15)DX
WRITE(6,16)DY
WRITE(6,18)TOL
WRITE(6,19)XLAMDA
WRITE(6,21)FRACEL
HH=PI/H
WRITE(6,24)H,HH
FORMAT(1H,10X,1T)
FCRMMAT(1H,10X,1P)
FCRMMAT(1H,10X,1M)
FCRMMAT(1H,10X,1R)
FCRMMAT(1H,10X,1D)
FCRMMAT(1H,10X,1T)
FCRMMAT(1H,10X,1F)
FCRMMAT(1H,10X,1C)
FCRMMAT(1H,10X,1C)
RETURN
END

```

```

SUBROUTINE PRINT
COMMON / FIELDS /
COMMON / VECTOR /
1
COMMON / ARRAYS /
COMMON / PARAMS /
1
COMMON / FACTOR /
1
COMMON / SYMBOL /
COMMON / DCUBLE PRECISION
1
DIMENSION PHI(
DOUBLE PRECISION
1
DIMENSION
1
```

[illegible][illegible]


```

THIS ROUTINE COMPUTES THE AVERAGE KINETIC ENERGIES OF BOTH THE
MEAN AND THE TURBULENT COMPONENTS OF THE FLOW
00013670
00013680
00013690
00013700
00013710
00013720
00013730
00013740
00013750
00013760
00013770
00013780
00013790
00013800
00013810
00013820
00013830
00013840
00013850
00013860
00013870
00013880
00013890
00013900
00013910
00013920
00013930
00013940
00013950
00013960
00013970
00013980
00013990
00014000

CALL EDDYS(10)
CALL STRESS
MEAN FLOW. T IS USED FOR TEMPORARY STORAGE
00012890
00012900
00012910
00012920
00012930
00012940
00012950
00012960
00012970
00012980
00012990
0000013000

DO 10 J=2,NM1
T(J)=UMEAN(J)**2
CONTINUE
T(1)=0.
CALL ASUM(T,NM1,SUM)
EKMEAN=SUM/(2.00*XNM1)

TURBULENT FLOW. TURBULENT COMPONENTS OF PHI ARE STORED IN FG BY
EDDYS. ARRAY A IS USED FOR TEMPORARY STORAGE.
00013670
00013680
00013690
00013700
00013710
00013720
00013730
00013740
00013750
00013760
00013770
00013780
00013790
00013800
00013810
00013820
00013830
00013840
00013850
00013860
00013870
00013880
00013890
00013900
00013910
00013920
00013930
00013940
00013950
00013960
00013970
00013980
00013990
00014000

XM2=2.00*XM
TURBKE(N)=0.
TURBKE(1)=0.
DO 30 J=2,NM1
DO 20 I=1,M
IP=IPO(I)
IM=IMO(I)
A(I)=((FG(I,J+1)-FG(I,J-1))/DY2)**2+((FG(IP,J)-FG(IM,J))/DX2)**2
CCNT INUE
CALL ASUM(A,M,SUM)
TURBKE(J)=SUM/XM2
CCNT INUE
CALL ASUM(TURBKE,NM1,SUM)
EKTURB=SUM/XNM1
RETURN
END
00012890
00012900
00012910
00012920
00012930
00012940
00012950
00012960
00012970
00012980
00012990
0000013000

SUBROUTINE EDDYS(INDEX)
COMMON / FIELDS / PHI,GAMA,FG,GAMOLD
COMMON / VECTOR / T,A,S,XALPHA,PHMEAN,GAMEAN,UMEAN,TEMP,TURBKE,
1 U,PHILAM,FF,ETA,GAP,X,Y
COMMON / ARRAYS / IPO,IMO,INV,IAO,IAI,MM(3)
COMMON / PARAMS / NM,NP1,NP2,NM1,NM2,NM3,NM4,NH,MPI,MP2,MP3,MM1,
1 M2M,MH,MHP,NPROB,ICOUNT,ITEL,INT,KSTEP,ISTART,
2 ISCIPI,MSCIP,ITAPE,NITTER,NITOT,NITMAX,IFIG,MCOMP,
3 KINT
COMMON / FACTOR / DX,DX2,DXSQ,DXSQ4,DXSQ8,DY,DY2,DYSQR,R,RSQR,
1 RSQRP,REYNLD,REY,FRACEL,XLAMDA,TIME,DT,DTI,PI,H,
2 EKMEAN,EKTURB,UUVBAR,ATERM,BTERM,ALPHA,BETA,AXM,XN
3 XN00013000

```

```

3 COMMON / SYMBOL / ,XNM1,UMNFLO,UFLO,TOL,FA,FB,FC,F1,F2,F3,F4,F5,F6
DCUBLE PRECISION
1 DX,DX2,DXSQR,DXSQR4,DXSQR8,DY,DY2,DYSQR,R,RSQR,
2 RSQRP,REYNLD,REY,FRACEL,XLAMDA,TIME,DT,DTT,PI,H,
3 EKMEAN,EKTURB,UVBAR,ATERM,BTERM,ALPHA,BETA,XM,XN
DIMENSION PHI(64,201),GAMA(64,201),GAMOLD(64,201)
DOUBLE PRECISION
1 UMEAN(201),TEMP(201),TURBKE(201),U(201),
2 PHILAM(201),T(201),A(128),S(32),XALPHA(64),
3 PHMEAN(201),GAMEAN(201),X(64),Y(201),FF(32),
ETA(201),GA(201)
DIMENSION
1 IPO(64),IMO(64),INV(32),IAQ(64),IAP(64)
* * * * *
ASSUMES SUBROUTINE MEANS HAS GENERATED CURRENT VALUES OF PHMEAN
AND GAMEAN

IF INDEX > 0 ROUTINE PUTS TURBULENT COMPONENTS OF STREAM
FUNCTION IN ARRAY FG

IF INDEX < 0 ROUTINE PUTS TURBULENT COMPONENTS OF VORTICITY
IN ARRAY FG

IF (INDEX .LT. 0) GO TO 15
1 DC 10 J=1,N
CO 10 I=1,M
FG(I,J)=PHI(I,J)-PHMEAN(J)
10 CCNT INUE
GC TO 25
15 DO 20 J=1,N
DC 20 I=1,M
FG(I,J)=GAMA(I,J)-GAMEAN(J)
20 CONTINUE
25 RETURN
END

```

CCCCCCCCCCCCCCCC

```

SUBROUTINE STRESS
COMMON / FIELDS /
COMMON / VECTOR /
1 PHI,GAMA,FG,GAMOLD
2 T,A,S,XALPHA,PHMEAN,GAMEAN,UMEAN,TEMP,TURBKE,
3 U,PHILAM,FF,ETA,GA,X,Y
COMMON / ARRAYS /
COMMON / PARAMS /
1 IPC,IMO,INV,IAQ,IAP,MM(3)
2 N,M,NP1,NP2,NM1,NM2,NM3,NM4,NH,MP1,MP2,MP3,MM1,
3 M2M,MH,MHP,NPROB,ICOUNT,ITEL,INT,KSTEP,ISTART,
ISCIP,MSCIP,ITAPE,NITER,NITOT,NITMAX,IFIG,MCOMP,
00014010
00014020
00014030
00014040
00014050
00014060
00014070
00014080

```

```

3 CCOMMON / FACTOR / KINT
1 DX,DX2,DXSQR,DXSQR4,DXSQR8,DY,DY2,DYSQR,R,RSQR,
2 RSQRP,REYNLD,REY,FRACEL,XLAMDA,TIME,DT,DTT,PI,H,
3 EKMEAN,EKTURB,UVBAR,ATERM,BTERM,ALPHA,BETA,XM,XN
CCOMMON / SYMBOL /
DCUBLE PRECISION
1 DX,DX2,DXSQR,DXSQR4,DXSQR8,DY,DY2,DYSQR,R,RSQR,
2 RSQRP,REYNLD,REY,FRACEL,XLAMDA,TIME,DT,DTT,PI,H,
3 EKMEAN,EKTURB,UVBAR,ATERM,BTERM,ALPHA,BETA,XM,XN
DIMENSION PHI(64,201),GAMA(64,201),FG(64,201),GAMOLD(64,201)
DCUBLE PRECISION
1 UMEAN(201),TEMP(201),TURBKE(201),U(201),
2 PHILAM(201),T(201),A(128),S(32),XALPHA(64),
3 PHMEAN(201),GAM(201)
DIMENSION IPO(64),IMO(64),INV(32),IAO(64),IAP(64)
* * * * *
ASSUMES THAT FLUCTUATING CGMP. OF PHI IS STORED IN FG
COMPUTES REYNOLDS STRESSES AND MEAN VELOCITIES.
TEMP(1)=0.
TEMP(N)=0.
DO 20 J=2,NM1
DO 10 I=1,M
IP=IPO(I)
IM=IMO(I)
A(I)=(1.DO*FG(I,J-1)-FG(I,J+1))*(1.DO*FG(IP,J)-FG(IM,J))
10 CONTINUE
CALL ASUM(A,M,SUM)
TEMP(J)=SUM/BTERM
20 CCNTINUE
CALL ASUM(TEMP,NM1,SUM)
UVBAR=SUM/XNM1
MEAN VELOCITY
DO 30 J=2,NM1
UMEAN(J)=(PHMEAN(J-1)-PHMEAN(J+1))/DY2+U(J)
30 CONTINUE
UMEAN(1)=0.
UMEAN(N)=0.
CALL ASUM(UMEAN,NM1,SUM)
UMNFLO=SUM/XNM1
UFLO=(2.DO+PHMEAN(2)-PHMEAN(NM1)+PHILAM(2)-PHILAM(NM1))/4.DO
RETURN
END

```

CCCCC

CC

00014090
00014100
00014110
00014120
00014130
00014140
00014150
00014160
00014170
00014180
00014190
00014200
00014210
00014220
00014230
00014240
00014250
00014260
00014270
00014280
00014290
00014300
00014310
00014320
00014330
00014340
00014350
00014360
00014370
00014380
00014390
00014400
00014410
00014420
00014430
00014440
00014450
00014460
00014470
00014480
00014490
00014500
00014510
00014520
00014530
00014540
00014560
00014570


```

SUBROUTINE PLOT /
COMMON / FIELDS /
COMMON / VECTOR /
1 COMMON / ARRAYS /
COMMON / PARAMS /
1
2
3
COMMON / FACTOR /
1
2
3
COMMON / SYMBOL /
COMMON / PICTUR /
DOUBLE PRECISION
1
2
3
DIMENSION PHI(64,201),GAMA(64,201),INV(32),IAO(64),IAP(64)
DOUBLE PRECISION
1
2
3
DIMENSION
THIS ROUTINE PRINTS ONLINE PLOTS OF MEAN VELOCITY,VORTICITY,
TURBULENT KINETIC ENERGY AND REYNOLDS STRESS AS FUNCTIONS OF Y.
* * * * *
IFIG=1
III=-1
PUT UMEAN IN APLOT , TEMP IN BPLLOT
DC 10 J=1,N
APLOT(J)=UMEAN(J)
BPLLOT(J)=TEMP(J)
10 CCNTINUE
TITLE
WRITE(6,11)
11 FCRMAT(1H0,4X,'UMEAN',25X,'UMEAN',34X,'UVBAR',28X,'UVBAR')

```

```

CCC14720
C0014730
C0014740
C0014750
C0014760
C0014770
C0014780
C0014790
C0014800
C0014810
C0014820
C0014830
C0014840
C0014850
C0014860
C0014870
C0014880
C0014890
C0014900
C0014910
C0014920
C0014930
C0014940
C0014950
C0014960
C0014970
C0014980
C0014990
C0015000
C0015010
C0015020
C0015030
C0015040
C0015050
C0015060
C0015070
C0015080
C0015090
C0015100
C0015110
C0015120
C0015130
C0015140
C0015150
C0015160
C0015170

```

```

CCCCCCCC
CC
CC

```

```

C C C FIND LARGEST ELEMENTS IN APLOT AND BPLOT
15 ABIG=0.
   BBIG=0.
   DO 20 J=1,N
     ABIG=AMAX1(ABIG,ABS(APLOT(J)))
     BBIG=AMAX1(BBIG,ABS(BPLOT(J)))
20 CONTINUE

C C C SET UP TOP HORIZONTAL AXIS
DO 30 I=1,49
  ALINE(I)=DOT
  BLINE(I)=DOT
30 CONTINUE
12 WRITE(6,12)ALINE,BLINE
   FORMAT(14X,49A1,20X,49A1)

C C C BLANK ALINE AND BLINE AND PUT PLOTTING SYMBOL IN COMPUTED ELEMENT
DO 40 I=1,49
  ALINE(I)=BLANK
  BLINE(I)=BLANK
40 CONTINUE
   ALINE(1)=DOT
   BLINE(25)=DOT
   J=N
DO 50 JC=1,N,2
  JC=1,N,2
  JB=APLOT(J)/ABIG*48.+1.
  JB=BPLOT(J)/BBIG*24.+25.
  ALINE(JA)=XXX
  BLINE(JB)=XXX
  WRITE(6,13)APLOT(J),ALINE,J,BPLOT(J),BLINE
13 FORMAT(1X,E10.4,2X,49A1,2X,I3,3X,E10.4,2X,49A1)
   ALINE(JA)=BLANK
   BLINE(JB)=BLANK
   ALINE(1)=DOT
   BLINE(25)=DOT
   J=J-2
50 CONTINUE

C C C SET UP BOTTOM HORIZONTAL AXIS
DO 60 I=1,49
  ALINE(I)=DOT
  BLINE(I)=DOT
60 CONTINUE

```

```

00015180
00015190
00015200
00015210
00015220
00015230
00015240
00015250
00015260
00015270
00015280
00015290
00015300
00015310
00015320
00015330
00015340
00015350
00015360
00015370
00015380
00015390
00015400
00015410
00015420
00015430
00015440
00015450
00015460
00015470
00015480
00015490
00015500
00015510
00015520
00015530
00015540
00015550
00015560
00015570
00015580
00015590
00015600
00015610
00015620
00015630
00015640
00015650

```



```

C
C
C
14      WRITE(6,14)ALINE,BLINE
      FCRMAT(14X,49A1,20X,49A1//)
      IF(III.GT. 0)GO TO 100
C
C
      PUT TURBKE IN APLOT , GAMEAN IN BPLOT
C
65      DO 70 J=1,N
      APLOT(J)=TURBKE(J)
      BPLOT(J)=GAMEAN(J)
70      CONTINUE
      III=1
C
C
C
      TITLE
C
      WRITE(6,16)
      FORMAT(1H0,4X,'TURBKE',25X,'TURBKE',32X,'GAMEAN',26X,'GAMEAN')
      GO TO 15
100     RETURN
      END

```

```

SUBROUTINE ADVANC
COMMON / FIELDS /
COMMON / VECTOR /
1      COMMON / ARRAYS /
COMMON / PARAMS /
1      N,M,MH,MHP,NPROB,ICOUNT,ITEL,INT,KSTEP,ISTART,
2      ISCIPI,MSCIP,ITAPE,NITER,NITOT,NITMAX,IFIG,MCCOMP,
3      KINT
1      DX,DX2,DXSQR,DXSQR4,DXSQR8,DY,DY2,DYSQR,R,RSQR,
2      RSQRP,REYNLD,REY,FRACEL,XLAMDA,TIME,DT,DTT,PI,H,
3      EKMEAN,EKTURB,UVBAR,ATERM,BTERM,ALPHA,BETA,XM,XN
COMMON / SYMBOL /
COMMON / PRECISION /
1      DX,DX2,DXSQR,DXSQR4,DXSQR8,DY,DY2,DYSQR,R,RSQR,
2      RSQRP,REYNLD,REY,FRACEL,XLAMDA,TIME,DT,DTT,PI,H,
3      EKMEAN,EKTURB,UVBAR,ATERM,BTERM,ALPHA,BETA,XM,XN
1      XNM1,UMNFLO,UFLD,TOL,FA,FB,FC,F1,F2,F3,F4,F5,F6
2      XNM1,UMNFLO,XX
3      DIMENSION PHI(64,201),GAMA(64,201),FG(64,201),GAMOLD(64,201)
DOUBLE PRECISION
1      UMEAN(201),TEMP(201),TURBKE(201),U(201),
2      PHILAM(201),T(201),A(128),S(32),XALPHA(64),
3      PHMEAN(201),GAMEAN(201),X(64),Y(201),FF(32),
      ETA(201),GA(201)
1      IPO(64),IMO(64),INV(32),IAO(64),IAP(64)
2      GJ1,GJ2,GJ3,GJ,Q
3      DIMENSION PRECISION
DOUBLE PRECISION
1      LAMDA,LAMDAB,LAMDAC,LAMDAD,LAMDAE,LAMDAF,LAMDAG
2      COMMON MRLOAD,NCYCLES,LINR
3

```

```

00015660
00015670
00015680
00015690
00015700
00015710
00015720
00015730
00015740
00015750
00015760
00015770
00015780
00015790
00015800
00015810
00015820
00015830
00015840

```

```

00006750
00006760
00006770
00006780
00006790
00006800
00006810
00006820
00006830
00006840
00006850
00006860
00006870
00006880
00006890
00006900
00006910
00006920
00006930
00006940
00006950
00006960
00006970
00006980
00006990
00007000

```

CCCCCCCC C

```

* * * * *
THIS ROUTINE GENERATES INTERIOR VALUES OF VORTICITY AT TIME=T+DT
BY SECOND ORDER CENTRAL TIME DIFFERENCE FINITE DIFFERENCE ANALOGS FOR THE CONVECTIVE
GJ1,GJ2,GJ3 ARE EACH FINITE DIFFERENCE ANALOGS FOR THE CONVECTIVE
TERMS. Q IS THE DISSIPATION TERM
ARRAY FG IS USED FOR TEMPORARY STORAGE OF THE NEW VALUES OF
ARRAY GAMOLD STORES OLD VALUES OF THE VORTICITY FOR THE CENTRAL
VORTICITY
TIME DIFFERENCING.

IF(ICOUNT.EQ.KSTEP)GO TO 30

1  LAMDA=2.DO*DT*RSQR/(REYNLD*DXSQR)
   LAMDAB=(1.-LAMDA)/(1.+LAMDA)
   LAMDAC=2.*DT/(DXSQR*(1.+LAMDA))
   LAMDAD=DT/(DX*(1.DO+LAMDA))
   LAMDAE=3.DO*LAMDAD
   DO 10 I=1,M
   IP=IPO(I)
   IM=IMO(I)
   IMM=IMO(IM)
   IPP=IPO(IP)
   DO 10 J=2,NM1
   JP=J+1
   JM=J-1
   IF(LINR.EQ.1)GO TO 8
   GJ1= (PHI(IM,J)-PHI(IP,J))* (GAMA(I,JP)-GAMA(I,JM))
   1  GJ2= GAMA(IP,JP)* (PHI(I,JP)-PHI(IP,J))
   1  +GAMA(IM,JM)* (PHI(I,JP)-PHI(IP,J))
   2  +GAMA(IP,JM)* (PHI(IM,J)-PHI(IP,J))
   3  +GAMA(IM,JP)* (PHI(IM,J)-PHI(IP,J))
   1  GJ3= GAMA(I,JP)* (PHI(IM,JP)-PHI(IP,JP))
   2  +GAMA(IM,JM)* (PHI(IM,JP)-PHI(IP,JP))
   3  +GAMA(I,JM)* (PHI(IP,JM)-PHI(IP,J))
   GJ=(GJ1+GJ2+GJ3)/12.DO
   GJ=R*GJ
   GO TO 81
8  GJ=Q.DO
81  CONTINUE
   Q=RSQR*(GAMA(I,JP)+GAMA(I,JM))+GAMA(IP,J)+GAMA(IM,J)
   Q=Q*REY
   FG(I,J)=LAMCAB*GAMOLD(I,J)+LAMDAC*(GJ+Q)
00007010
00007020
00007030
00007040
00007050
00007060
00007070
00007080
00007090
00007100
00007110
00007120
00007130
00007140
00007150
00007160
00007170
00007180
00007190
00007200
00007210
00007220
00007230
00007240
00007250
00007260
00007270
00007280
00007290
00007300
00007310
00007320
00007330
00007340
00007350
00007360
00007370
00007380
00007390
00007400
00007410
00007420
00007430
00007440

```

00007450
00007460
00007470

```

1  -LAMDA*U(J)*(GAMA(IP,J)-GAMA(IM,J))
2  -LAMDAE*(PHI(IP,J)-PHI(IM,J))
10 CCNTINUE
C  COMPUTE GAMA AT WALL FROM TRANSPORT EQN. FOR COMPARISON WITH
C  GAMA COMPUTED FROM THE POISON EQN.
DC 11 I=1,M
IM=IMO(I)
IP=IPO(I)
LAMDA=2. DO*CT/(REYNLD*DXSQR)
Q=RSQR*(GAMA(I,NM2)-2.*GAMA(I,NM1)+GAMA(I,N))+GAMA(IP,N)
1  -2.*GAMA(I,N)+GAMA(IM,N)
FG(I,N)=GAMOLD(I,N)+LAMDA*Q
11 CCNTINUE
DC 21 I=1,M
GAMOLD(I,N)=GAMA(I,N)
21 CCNTINUE
DC 20 I=1,M
DC 20 J=2,NM1
GAMOLD(I,J)=GAMA(I,J)
GAMA(I,J)=FG(I,J)
20 CCNTINUE
L=ICOUNT+1
IF(ICOUNT.EQ.KSTEP)GO TO 69
IF(L.NE.INT)GO TO 69
CCMPARE VALUES OF GAMA COMPUTED FROM TRANSPORT EQN WITH VALUES
CCCOMPUTED FROM POISSON EQN

```

00007480
00007490
00007500
00007510
00007520

```

WRITE(6,105)ICOUNT
WRITE(6,58)(I,I=1,10)
DO 17 J=NM4,N
WRITE(6,99)J,Y(J),( FG(I,J),I=1,5 )
17 CCNTINUE
WRITE(6,98)(I,I=11,20)
DO 19 J=NM4,N
WRITE(6,99)J,Y(J),( FG(I,J),I=6,10)
19 CCNTINUE
69 CCNTINUE
58 FORMAT(1X,5X,I=,11X,10(I3,8X))
99 FORMAT(1X,J=,13,1X,Y=,F6.3,2X,5(E14.7,1X))
105 FORMAT(1H0,GAMA NEAR WALL COMPUTED FROM TRANSPORT EQN CYCLE',I4)
CALL PRESUR
TIME=TIME+DT
NITER=0
GC TO 40

```

00007530
00007540
00007550
00007560
00007570
00007580
00007590
00007600

```

C 30 CALL STEP
KSTEP=KSTEP+KINT
40 RETURN

```


END

SUBROUTINE PRESUR

COMMON / FIELDS /

COMMON / VECTOR /

1 COMMON / ARRAYS /

COMMON / PARAMS /

1 2 3

COMMON / FACTOR /

1 2 3

DOUBLE PRECISION

1 2 3

COMMON MRLOAD, NCYCLES, LINR

DIMENSION PHI(64,201), GAMMA(64,201), FG(64,201), GAMOLD(64,201)

DOUBLE PRECISION

1 2 3

DIMENSION

1 2 3

THIS ROUTINE SOLVES A POISSON EQUATION FOR THE STREAM FUNCTION

BY MEANS OF THE DISCRETE FOURIER TRANSFORM.

OBTAIN THE FOURIER TRANSFORM OF GAMMA. STCRE IN ARRAY PHI.

CC 20 J=1,N

DO 10 I=1,M

IA=IAO(I)

IP=IAP(I)

A(IA)=GAMA(I,J)

A(IP)=0.

10 CCNTINUE

CALL DHARM(A,MM,INV,S,2,IFERR)

PHI(1,J)=A(1)

DO 20 I=2,M

PHI(I,J)=A(I+1)

20 CCNTINUE

00007610

00007620

00007630

00007640

00007650

00007660

00007670

00007680

00007690

00007700

00007710

00007720

00007730

00007740

00007750

00007760

00007770

00007780

00007790

00007800

00007810

00007820

00007830

00007840

00007850

00007860

00007870

00007880

00007890

00007900

00007910

00007920

00007930

00007940

00007950

00007960

00007970

00007980

00007990

00008000

00008010

00008020

00008030

00008040

00008050

```

C      OBTAIN THE MEAN VALUE OF GAMMA FROM THE ZERO MODE
DO 25 J=1,N
  GAMMEAN(J)=PHI(1,J)/XM+3.DO*Y(J)
CCNTINUE
C      OBTAIN THE SPECTRUM OF SQUARED VORTICITY
L=ICOUNT+1
IF(L.EQ. INT) CALL SPCTRM(-1)

C      SOLVE FOR THE FOURIER TRANSFORM OF PHI. STORE IN ARRAY PHI.
DO 40 I=1,M
  PHI(I,N)=0.
  PHI(I,1)=0.
  ALPHA=XALPHA(I)
DO 30 J=1,NM4
  T(J)=PHI(I,J+2)
CCNTINUE
CALL TRISOL
DO 41 J=3,NM2
  PHI(I,J)=T(J-2)
CCNTINUE
PHI(I,2)=PHI(I,3)*.25
PHI(I,1)=PHI(I,NM1)=PHI(I,NM2)*.25
PHI(I,2)=.5*PHI(I,3)-PHI(I,4)/9.
PHI(I,NM1)=.5*PHI(I,NM2)-PHI(I,NM3)/9.
CCNTINUE
C      OBTAIN THE MEAN VALUE OF PHI FROM THE ZERO MODE
DO 45 J=2,NM1
  PHMEAN(J)=PHI(1,J)/XM
CCNTINUE
PHMEAN(N)=0.DO
PHMEAN(1)=0.DO
C      OBTAIN THE ENERGY SPECTRUM.
IF(L.EQ. INT) CALL SPCTRM(1)

C      1000
CCNTINUE
IF(L.EQ. MRLOAD)CALL MODES(1,2,1)
IF(L.EQ. MRLOAD)CALL MODES(3,4,1)
IF(ICOUNT.EQ. NCYCCLS) CALL MODES(1,2,1)
IF(ICOUNT.EQ. NCYCCLS)CALL MODES(3,4,1)

C      1004
CCNTINUE
C      INVERT THE FOURIER TRANSFORM OF PHI
DO 70 J=2,NM1
  A(1)=PHI(1,J)

```

```

00008060
00008070
00008080
00008090
00008100
00008110
00008120
00008130
00008140
00008150
00008160
00008170
00008180
00008190

```

```

00008220
00008230

```

```

00008260
00008270
00008280
00008290
00008300
00008310
00008320
00008330
00008340
00008350
00008360
00008390

```

```

00008450
00008460
00008470
00008480
00008490
00008500
00008510

```


00008520
00008530
00008540
00008550
00008560
00008570
00008580
00008590
00008600
00008610
00008620
00008630
00008640
00008650
00008660
00008670
00008680
00008690
00008700
00008710
00008720
00008730
00008740
00008750
00008760

00008770
00008780

00008790

```

A(2)=0.
DO 50 I=3,MP1
  A(I)=PHI(I-1,J)
CONTINUE
A(MP2)=0.
IC=5
DO 60 I=MP3,M2M,2
  A(I)=PHI(I-IC,J)
  IP=I+1
  A(IP)=-PHI(IP-IC,J)
  IC=IC+4
CCCONTINUE
CALL DHARM(A,MM,INV,S,-2,IFERR)
DO 70 I=1,M
  IA=IAO(I)
  PHI(I,J)=A(IA)
CONTINUE
11 FORMAT(10X,*** FFT OF GAMA ***)
12 FORMAT(10X,*** SOLUTION FOR FFT OF PHI ***)
13 FORMAT(10X,*** SOLUTION FOR PHI ***)
14 FORMAT(10X,*** FFT OF EXACT SOLUTION FOR PHI ***)

CCCOMPUTE NEW VALUES OF VORTICITY AT WALLS

DO 80 I=1,M
  IP=IPO(I)
  IM=IMO(I)
  GAMA(I,2)=(PHI(IP,2)-2.*PHI(I,2)+PHI(IM,2))/DXSQR +(PHI(I,3)
1  -2.*PHI(I,2))/DYSQR
  GAMA(I,NM1)=(PHI(IP,NM1)-2.*PHI(I,NM1)+PHI(IM,NM1))/DXSQR
1  + (PHI(I,NM2)-2.*PHI(I,NM1))/DYSQR
  GAMA(I,N)=(8.*DO*PHI(I,2)-PHI(I,3))*ATERM
  GAMA(I,1)=(8.*DO*PHI(I,2)-PHI(I,3))*ATERM
  GAMA(I,N)=(1.5*PHI(I,NM2)-4.*PHI(I,NM3)/9.)/DYSQR
  GAMA(I,1)=(1.5*PHI(I,3)-4.*PHI(I,4)/9.)/DYSQR
CONTINUE
80 IF(ICOUNT.EQ.KSTEP)GO TO 87
  IF(L.NE.INT)GO TO 87
  WRITE(6,109)ICOUNT
  WRITE(6,98)(I,I=1,10)
  DO 18 J=NM4,N
    WRITE(6,99)J,Y(J),(GAMA(I,J),I=1,5)
  CONTINUE
18 WRITE(6,98)(I,I=11,20)
  DO 21 J=NM4,N
    WRITE(6,99)J,Y(J),(GAMA(I,J),I=6,10)
  CONTINUE
21 IF IG=1

```

C
C
C

```

98 FORMAT(1H,5X,'I=',11X,10(I3,8X))
99 FORMAT(1H,5X,'J=',11X,10(I3,8X),F6.3,2X,5(E14.7,1X))
109 FORMAT(1H,2X,'GAMA NEAR WALL COMPUTED FROM POISSON EQN CYCLE',I4)
87 RETURN
END

```

000C8810

```

SUBROUTINE SPCTRM(INDEX)
COMMON / FIELDS / PHI,GAMA,FG,GAMOLD
COMMON / VECTOR / T,A,S,XALPHA,PHMEAN,GAMEAN,UMEAN,TEMP,TURBKE,
1 U,PHILAM,FF,ETA,GA,X,Y
COMMON / ARRAYS / IPQ,IMO,INV,IAO,IAP,MM(3)
COMMON / PARAMS / N,M,NP1,NP2,NM1,NM2,NM3,NM4,NH,MP1,MP2,MP3,MM1,
1 M2M,MH,MHP,NPROB,ICOUNT,ITEL,INT,KSTEP,ISTART,
2 M2M,MH,MHP,NPROB,ICOUNT,ITEL,INT,KSTEP,ISTART,
3 ISCIIP,MSCIP,ITAPE,NITER,NITOT,NITMAX,IFIG,MCOMP,
KINT
COMMON / FACTOR / DX,DX2,DXSQR,DXSQR4,DXSQR8,DY,DY2,DYSQR,R,RSQR,
1 RSQRP,REYNLD,REY,FRACEL,XLAMDA,TIME,DT,DTT,PI,H,
2 EKMEAN,EKTURB,UVBAR,ATERM,BTERM,ALPHA,BETA,XM,XN,
3 XNM1,UMNFLO,UFLD,TOL,FA,FB,FC,F1,F2,F3,F4,F5,F6
COMMON / SYMBOL / DOT,BLANK,XXX
DOUBLE PRECISION
1 DX,DX2,DXSQR,DXSQR4,DXSQR8,DY,DY2,DYSQR,R,RSQR,
2 RSQRP,REYNLD,REY,FRACEL,XLAMDA,TIME,DT,DTT,PI,H,
3 EKMEAN,EKTURB,UVBAR,ATERM,BTERM,ALPHA,BETA,XM,XN,
XNM1,UMNFLO,UFLD,TOL,FA,FB,FC,F1,F2,F3,F4,F5,F6
DIMENSION PHI(64,201),GAMA(64,201),FG(64,201),GAMOLD(64,201)
DOUBLE PRECISION
1 UMEAN(201),T(201),TURBKE(201),U(201),
2 PHILAM(201),TEMP(201),S(32),XALPHA(64),
3 PHMEAN(201),GAMEAN(201),X(64),Y(201),FF(32),
ETA(201),GA(201)
DIMENSION IPO(64),IMO(64),INV(32),IAO(64),IAP(64)

```

THIS ROUTINE COMPUTES THE KINETIC ENERGY OF THE DISTURBANCE
MOTION AS A FUNCTION OF Y AND WAVE NUMBER IN THE X DIRECTION.
WAVE OR MODE NUMBER ONE CORRESPONDS TO THE MEAN VALUE OF THE
DISTURBANCE. THE SPECTRUM OF THE TURBULENT ENERGY IS CONTAINED
IN MODE NUMBERS TWO THROUGH NH.
ARRAY FG IS USED FOR STORAGE OF THE SPECTRAL VALUES

```

IF(ICOUNT.EQ.KSTEP) RETURN
IFIG=1
IF(INDEX.LT.0) GO TO 40
5 L=MH+1
DO 10 J=2,NM1
JM=J-1

```

CCCCCCCCCCCC

00009970
00009980
00009990
00010000
00010010
00010020
00010030
00010040
00010050
00010060
00010070
00010080
00010090
00010100
00010110
00010120
00010130
00010140
00010150
00010160
00010170
00010180
00010190
00010200
00010210
00010220
00010230
00010240
00010250
00010260
00010270
00010280
00010290
00010300
00010310
00010320
00010330
00010340
00010350
00010360
00010370

```

JP=J+1
FG(I,J)=FC*(PHI(1,JM)-PHI(1,JP))**2
FG(L,J)=FC*(PHI(M,JM)-PHI(M,JP))**2
DO 10 I=2,MH
LL=IAO(I)
LP=LL+1
LM=LL-1

1  FG(I,J)=FA*(FB*((PHI(LM,JM)**2+PHI(LL,JM)**2+PHI(LM,JP)**2
2  +PHI(LL,JP)**2)-2.DO*(PHI(LM,JP)*PHI(LM,JM)+
3  PHI(LL,JP)*PHI(LL,JM)))
  +FF(I)*(PHI(LM,J)**2+PHI(LL,J)**2))
10 CCNTINUE
C
C  MEAN VALUES
C
T(1)=0.DO
DO 20 I=1,MHP
DO 15 J=2,NM1
T(J)=FG(I,J)
15 CCNTINUE
CALL ASUM(T,NM1,SUM)
ETA(I)=SUM/XNM1
GA(I)=FG(I,NH)
20 CCNTINUE
C
C  TITLE
C
L=ICOUNT+1
WRITE(6,22) L
FORMAT(10X,'ENERGY SPECTRUM FOR CYCLE NUMBER ',I5)
22 WRITE(6,21)
FORMAT(14X,'MEAN SPECTRUM',36X,'MODE',20X,'MIDSTREAM SPECTRUM')
21 CALL PLOTSP(ETA,GA,MHP)
DO 30 I=1,MHP
ETA(I)=FG(I,16)
GA(I)=FG(I,186)
30 CCNTINUE
WRITE(6,23) Y(16),Y(186)
23 FORMAT(10X,'SPECTRUM FOR Y=',F6.4,32X,'MODE',18X,'SPECTRUM FOR Y=
  F6.4)
1 CALL PLOTSP(ETA,GA,MHP)
C
C  IF(ICOUNT.GT.-1) GO TO 100
C  PRINT THE ENERGY IN SEVERAL MODES AS FUNCTIONS OF Y.
C  ETA(1)=0.DO
C  ETA(N)=0.DO
C  GA(1)=0.DO

```

```

00010380
00010390
00010400
00010410
00010420
00010430
00010440
00010450
00010460
00010470
00010480
00010490
00010500
00010510
00010520
00010530
00010540
00010550
00010560
00010570
00010580
00010590
00010600
00010610
00010620
00010630
00010640
00010650
00010660
00010670
00010680
00010690
00010700
00010710
00010720
00010730
00010740
00010750
00010760
00010770
00010780
00010790
00010800
00010810
00010820
00010830
00010840

```



```

GA(N)=C.DO
I1=2
I2=3
DO 39 KL=1,2
DO 35 J=2,NM1
ETA(J)=FG(I1,J)
GA(J)=FG(I2,J)
CONTINUE
35 WRITE(6,36) I1,I2
36 FORMAT(14X,'ENERGY IN MODE ',I2,'20X','ENERGY IN MODE ',I2)
CALL PLOTSP(ETA,GA,N)
I1=4
I2=5
39 CONTINUE
GO TO 100

C
C
C
SIMILAR OPERATIONS FOR THE SPECTRUM OF SQUARED VORTICITY

40 F6=1.DO/XM**2
DO 50 J=1,N
F6(I,J)=F6*PHI(I,J)**2
FG(MHP,J)=F6*PHI(M,J)**2
DO 50 I=2,MH
LL=IAO(I)
FG(I,J)=F6*(PHI(LL-1,J)**2+PHI(LL,J)**2)
50 CONTINUE

C
DC 60 I=1,MHP
DO 55 J=1,N
T(J)=FG(I,J)
55 CONTINUE
CALL ASUM(T,N,SUM)
ETA(I)=SUM/XNM1
GA(I)=FG(I,NH)
60 CONTINUE

C
C
C
TITLE

L=ICOUNT+1
WRITE(6,61) L,VORTICITY SPECTRUM FOR CYCLE NUMBER ',I5)
61 FCRMAT(10X,'
WRITE(6,21)
CALL PLOTSP(ETA,GA,MHP)
DO 70 I=1,MHP
ETA(I)=FG(I,16)
GA(I)=FG(I,186)
70 CONTINUE
WRITE(6,23) Y(16),Y(186)

```

```

00010850
00010860
00010870
00010880
00010890
00010900
00010910
00010920
00010930
00010940
00010950
00010960
00010970
00010980
00010990
00011000
00011010
00011020
00011030
00011040
00011050
00011060
00011070
00011080
00011090
00011100
00011110
00011120
00011130
00011140
00011150
00011160
00011170
00011180
00011190
00011200
00011210
00011220
00011230
00011240
00011250
00011260
00011270
00011280
00011290
00011300
00011310
00011320

```



```

10  ETA(1)=T(1)/GA(1)
    GA(2)=-ALPHA-XFF/GA(1)
    ETA(2)=(T(2)-ETA(1))/GA(2)
    DO 10 J=3,NM5
    GA(J)=-ALPHA-1.00/GA(J-1)
    ETA(J)=(T(J)-ETA(J-1))/GA(J)
    CCNTINUE
    GA(NM4)=GA(1)-XFF/GA(NM5)
    ETA(NM4)=(T(NM4)-XFF*ETA(NM5))/GA(NM4)
    T(NM4)=DYSQR*ETA(NM4)
    J=N-5
    DO 20 JC=2,NM4
    T(J)=DYSQR*ETA(J)-T(J+1)/GA(J)
    J=J-1
    CCNTINUE
20  RETURN
    END

```

```

SUBROUTINE MODES(IMOD1,IMOD2,ISTYLE)
COMMON / FIELDS / PHI,GAMA,FG,GAMOLD
COMMON / VECTOR / T,A,S,XALPHA,PHMEAN,GAMEAN,UMEAN,TEMP,TURBKE,
1  COMMON / ARRAYS / IPC,IMO,INV,IAO,IAP,MM(3)
COMMON / PARAMS / NM1,NP1,NP2,NM1,NM2,NM3,NM4,NH,MPI,MP2,MP3,MM1,
2  M2M,MH,MHP,NPROB,ICOUNT,ITEL,INT,KSTEP,ISTART,
3  ISCIPI,MSCIP,ITAPE,NITER,NITOT,NITMAX,IFIG,MCOMP,
    KINT
COMMON / FACTOR / DX,DX2,DYSQR,DXSQR4,DXSQR8,DY,DY2,DYSQR,R,RSQR,
1  RSQRP,REYNLD,REY,FRACEL,XLAMDA,TIME,DT,DTT,PI,H,
2  EKMEAN,EKTURB,UVBAR,ATERM,BTERM,ALPHA,BETA,XM,XN
3  XNMI,UMNFLO,UFLO,TOL,FA,FB,FC,F1,F2,F3,F4,F5,F6
COMMON / SYMBOL / DOT,BLANK,XXX
COMMON / PRECISION / DX,DX2,DYSQR,DXSQR4,DXSQR8,DY,DY2,DYSQR,R,RSQR,
1  RSQRP,REYNLD,REY,FRACEL,XLAMDA,TIME,DT,DTT,PI,H,
2  EKMEAN,EKTURB,UVBAR,ATERM,BTERM,ALPHA,BETA,XM,XN
3  XNMI,UMNFLO,UFLO,TOL,FA,FB,FC,F1,F2,F3,F4,F5,F6
    DIMENSION PHI(64,201),GAMA(64,201),FG(64,201),GAMOLD(64,201)
    DOUBLE PRECISION UMEAN(201),TEMP(201),TURBKE(201),U(201),
1  PHILAM(201),T(201),A(128),S(32),XALPHA(64),
2  PHMEAN(201),T(201),GAMEAN(201),X(64),Y(201),FF(32),
3  ETA(201),GA(201)
    DIMENSION IPO(64),IMO(64),INV(32),IAO(64),IAP(64)
    * * * * *
    THIS ROUTINE COMPUTES AND PRINTS NORMALIZED MODAL FUNCTIONS
    OF THE DISTURBANCE STREAM FUNCTION.
    C C C C C

```

```

C0009290
C0009300
C0009310
C0009320
C0009330
C0009340
C0009350
C0009360
C0009370
C0009380
C0009390
C0009400
C0009410
C0009420
C0009430
C0009440
C0009450
C0009460
C0009470
C0009480
C0009490
C0009500
C0009510
C0009520
C0009530
C0009540
C0009550
C0009560
C0009570

```

C

```

10 IM1=IAP(IMOD1)
11 IM1P=IM1+1
12 IM2=IAP(IMOD2)
13 IF(ISTYLE.EQ. 2) GO TO 20
14 A1=PHI(IM1,NH)**2+PHI(IM1P,NH)**2
15 A2=PHI(IM1,NH)/A1
16 A3=-PHI(IM1P,NH)/A1
17 A4=PHI(IM2,NH)
18 WRITE(6,11) IMOD1,IMOD2
19 DO 10 J=1,N
20 ETA(1)=A2*PHI(IM1,J)-A1*PHI(IM1P,J)
21 ETA(2)=A1*PHI(IM1,J)+A2*PHI(IM1P,J)
22 ETA(3)=PHI(IM2,J)-A3
23 ETA(4)=PHI(IM2P,J)-A4
24 WRITE(6,12) J,ETA(1),ETA(2),Y(J),ETA(3),ETA(4),J
25 CCNTINUE
26 FORMAT(1H0,5X,'J',4X,'REAL MODE ',I3,' IMAG',11X,'Y',9X,
27 1 REAL MODE ',I3,' IMAG',6X,'J',)
28 1 FORMAT(4X,2(3X,F10.6),6X,F7.4,6X,2(F10.6,3X),I3)
29 GC TO 40
30 WRITE(6,21) IMOD1,IMOD2
31 DO 30 J=1,N
32 ETA(1)=PHI(IM1,J)**2+PHI(IM1P,J)**2
33 ETA(1)=DSQRT(ETA(1))/XM
34 ETA(2)=ATAN2(PHI(IM1,J),PHI(IM1P,J))
35 ETA(3)=PHI(IM2,J)**2+PHI(IM2P,J)**2
36 ETA(3)=DSQRT(ETA(3))/XM
37 ETA(4)=ATAN2(PHI(IM2,J),PHI(IM2P,J))
38 WRITE(6,12) J,ETA(1),ETA(2),Y(J),ETA(3),ETA(4),J
39 CCNTINUE
40 FORMAT(1H0,5X,'J',4X,'MAG MODE ',I3,' PHAS',11X,'Y',9X,
41 1 MAG MODE ',I3,' PHAS',6X,'J',)
42 1 IFIG=1
43 RETURN
44 END

```

SUBROUTINE STEP / PHI,GAMA,FG,GAMOLD
COMMON / FIELDS / T,A,S,XALPHA,PHMEAN,GAMEAN,TEMP,TURBKE,
COMMON / VECTOR / U,PHILAM,FF,ETA,GAX,Y
1 COMMON / ARRAYS / IPC,IMO,INV,IAQ,IAP,MM(3)
COMMON / PARAMS / N,M,NP1,NP2,NM1,NM2,NM3,NM4,NH,MP1,MP2,MP3,MM1,
2 M2M,MH,MHP,NPROB,ICOUNT,ITEL,INT,KSTEP,ISTART,
ISCIP,MSCIP,ITAPE,NITER,NITOT,NITMAX,IFIG,MCOMP,C00004790

00009580
00009590
00009600
00009610
00009620
00009630
00009640
00009650
00009660

00009700
00009710
00009720
00009730

00009760
00009770
00009780
00009790
00009800
00009810
00009820
00009830
00009840
00009850
00009860
00009870
00009880
00009890
00009900
00009910
00009920
00009930
00009940
00009950
00009960

00004720
00004730
00004740
00004750
00004760
00004770
00004780
00004790


```

3 CCOMMON / FACTOR /
1 DX,DX2,DXSQR,DXSQR4,DXSQR8,DY,DY2,DYSQR,R,RSQR,
1 RSQR,REYNLD,REY,FRACEL,XLAMDA,TIME,DT,DTT,PI,H,
3 EKMEAN,EKTURB,UVBAR,ATERM,BTERM,ALPHA,BETA,XM,XN
CCOMMON / SYMBOL /
DOUBLE PRECISION
1 DOT,BLANK,XXX
1 DX,DX2,DXSQR,DXSQR4,DXSQR8,DY,DY2,DYSQR,R,RSQR,
2 RSQR,REYNLD,REY,FRACEL,XLAMDA,TIME,DT,DTT,PI,H,
3 EKMEAN,EKTURB,UVBAR,ATERM,BTERM,ALPHA,BETA,XM,XN
1 XNMI,UMNFLO,UFLD,TOL,FA,FB,FC,F1,F2,F3,F4,F5,F6
2 XNMI,UMNFLO,UFLD,TOL,FA,FB,FC,F1,F2,F3,F4,F5,F6
3 XNMI,UMNFLO,UFLD,TOL,FA,FB,FC,F1,F2,F3,F4,F5,F6
1 DIMENSION PHI(64,201),GAMA(64,201),GAMOLD(64,201)
2 UMEAN(201),TEMP(201),TURBKE(201),U(201),
3 PHILAM(201),T(201),A(128),S(32),XALPHA(64),
1 PHMEAN(201),GAMEAN(201),X(64),Y(201),FF(32),
2 ETA(201),GA(201)
3 IPO(64),IMO(64),INV(32),IAO(64),IAP(64)
1 DCUBLE PRECISION GJ,GJ1,GJ2,GJ3,Q
2 DCUBLE PRECISION CRIT,TST,PUNT,GAMAIJ
3 COMMON MRLOAD,NCYCLS,LINR
* * * * *
REAL*8 LAMDA,LAMDAB,LAMDAC,LAMDAD,LAMDAE
THIS ROUTINE COMPUTES NEW VALUES OF VORTICITY AT TIME+DT BY
MODIFIED EULER IMPLICIT TIME DIFFERENCING.
ARRAY FG IS USED TO STORE TERMS EVALUATED AT TIME T.
IF(KINT.EQ.1) GO TO 6
IF(ICOUNT.EQ.0) GO TO 6
DO 5 I=1,M
DO 5 J=1,N
GAMA(I,J)=.5*(GAMA(I,J)+GAMOLD(I,J))
GAMOLD(I,J)=GAMA(I,J)
CONTINUE
5 CALL PRESUR
TIME=TIME-DT/2.00
CALL TIMER
LAMDA=RSQR*DT/((REYNLD*DXSQR)
LAMDAE=(1.00-LAMDA)/(1.00+LAMDA)
LAMDAC=DT/(2.00*(1.00+LAMDA)*DXSQR)
LAMDAE=DT/(4.00*(1.00+LAMDA)*DX)
DO 10 I=1,M
IP=IPO(I)
IM=IMO(I)
DO 10 J=2,NM1
JP=J+1

```

CCC CCCC

```

JM=J-1
IF(L INR.EQ.1)GO TO 8
GJ1= (PHI(IM,J)-PHI(IP,J))*GAMA(I,JP)-GAMA(I,JM))
      + (PHI(I,JP)-PHI(I,JM))*GAMA(IP,J)-GAMA(IM,J))
1 GJ2= GAMA(IP,JP)*(PHI(I,JP)-PHI(IP,J))
      +GAMA(IM,JM)*(PHI(I,JM)-PHI(IM,J))
2 GJ3= GAMA(IP,JP)*(PHI(IP,J)-PHI(I,JP))
      +GAMA(IM,JM)*(PHI(IM,J)-PHI(IP,J))
3 GJ3= GAMA(IM,J)*(PHI(IM,JP)-PHI(IP,JP))
      +GAMA(I,JP)*(PHI(IP,JP)-PHI(IM,JP))
1 GJ3= GAMA(IM,J)*(PHI(IM,JP)-PHI(IP,JP))
      +GAMA(I,JP)*(PHI(IP,JP)-PHI(IM,JP))
2 GJ3= GAMA(IM,J)*(PHI(IM,JP)-PHI(IP,JP))
      +GAMA(I,JP)*(PHI(IP,JP)-PHI(IM,JP))
3 GJ3= GAMA(IM,J)*(PHI(IM,JP)-PHI(IP,JP))
      +GAMA(I,JP)*(PHI(IP,JP)-PHI(IM,JP))
GJ=(GJ1+GJ2+GJ3)/12.D0
GJ=R#GJ
GO TO 81
8 GJ=0.D0
81 CCNTINUE
Q=RSQR*(GAMA(I,JP)+GAMA(I,JM))+GAMA(IP,J)+GAMA(IM,J)
Q=Q#REY
FG(I,J)=LAMDAB*GAMA(I,J)+LAMDAC*(GJ+Q)
      -LAMDAD*U(J)*GAMA(IP,J)-GAMA(IM,J))
      -LAMDAE*(PHI(IP,J)-PHI(IM,J))
1
2 CCNTINUE
10 CCNTINUE
NITSUM=0

FIRST SWEEP. START Y PASS AT LOWER WALL

NITER=0
PUNT=0.
DO 20 I=1,M
IP=IPO(I)
IM=IMO(I)
DO 20 J=3,NM2
JP=J+1
JM=J-1
IF(L INR.EQ.1)GO TO 18
GJ1= (PHI(IM,J)-PHI(IP,J))*GAMA(I,JP)-GAMA(I,JM))
      + (PHI(I,JP)-PHI(I,JM))*GAMA(IP,J)-GAMA(IM,J))
1 GJ2= GAMA(IP,JP)*(PHI(I,JP)-PHI(IP,J))
      +GAMA(IM,JM)*(PHI(I,JM)-PHI(IM,J))
2 GJ3= GAMA(IP,JP)*(PHI(IP,J)-PHI(I,JP))
      +GAMA(IM,JM)*(PHI(IM,J)-PHI(IP,JP))
3 GJ3= GAMA(IM,J)*(PHI(IM,JP)-PHI(IP,JP))
      +GAMA(I,JP)*(PHI(IP,JP)-PHI(IM,JP))
1 GJ3= GAMA(IM,J)*(PHI(IM,JP)-PHI(IP,JP))
      +GAMA(I,JP)*(PHI(IP,JP)-PHI(IM,JP))
2 GJ3= GAMA(IM,J)*(PHI(IM,JP)-PHI(IP,JP))
      +GAMA(I,JP)*(PHI(IP,JP)-PHI(IM,JP))
3 GJ3= GAMA(IM,J)*(PHI(IM,JP)-PHI(IP,JP))
      +GAMA(I,JP)*(PHI(IP,JP)-PHI(IM,JP))
GJ=(GJ1+GJ2+GJ3)/12.D0
GJ=R#GJ

```

C C C

```

00005270
00005280
00005290
00005300
00005310
00005320
00005330
00005340
00005350
00005360
00005370
00005380
00005390

00005400
00005410
00005420
00005430
00005440
00005450
00005460
00005470
00005480
00005490
00005500
00005510
00005520
00005530
00005540

00005560
00005570

00005580
00005590
00005600
00005610
00005620
00005630
00005640
00005650
00005660
00005670
00005680
00005690

```

```

18 GO TO 118
118 GJ=0.DO
CONTINUE
Q=RSQR*(GAMA(I,JP)+GAMA(I,JM))+GAMA(IP,J)+GAMA(IM,J)
Q=Q*REY
GAMA(I,J)=LAMDAC*(GJ+Q)-LAMDAC*U(J)*(GAMA(IP,J)-GAMA(IM,J))
- LAMDAE*(PHI(IP,J)-PHI(IM,J))+FG(I,J)
1 CONTINUE
20 CALL PRESUR

SECOND SWEEP. START Y PASS AT UPPER WALL

DO 30 I=1,M
IP=IPO(I)
IM=IMO(I)
J=NM2
DO 30 JC=3,NM2
JP=J+1
JM=J-1
IF(LINR.EQ.1)GO TO 28
GJ1=+(PHI(I,JP)-PHI(I,JM))*(GAMA(IP,J)-GAMA(IM,J))
1 GJ2=+GAMA(IP,JP)*(PHI(I,JP)-PHI(IP,J))
1 +GAMA(IM,JM)*(PHI(I,JP)-PHI(IM,J))
2 +GAMA(IP,JM)*(PHI(IP,J)-PHI(I,JM))
3 +GAMA(IM,JP)*(PHI(IM,J)-PHI(I,JP))
1 GJ3=+GAMA(I,JP)*(PHI(IM,JP)-PHI(IP,JP))
2 +GAMA(IM,J)*(PHI(IM,JM)-PHI(IM,JP))
3 +GAMA(I,JM)*(PHI(IP,JM)-PHI(IM,JM))
GJ=(GJ1+GJ2+GJ3)/12.DO
GJ=R*GJ
GC TO 128
GJ=0.DO
CONTINUE
Q=RSQR*(GAMA(I,JP)+GAMA(I,JM))+GAMA(IP,J)+GAMA(IM,J)
Q=Q*REY
TST=GAMA(I,J)
GAMA(I,J)=LAMDAC*(GJ+Q)-LAMDAC*U(J)*(GAMA(IP,J)-GAMA(IM,J))
- LAMDAE*(PHI(IP,J)-PHI(IM,J))+FG(I,J)
1 TEST FOR CCNVERGENCE
CRIT=DABS(1.-GAMA(I,J)/GAMA(IJ)
PUNT=PUNT+CRIT
29 GAMA(I,J)=GAMA(IJ)
J=J-1
30 CONTINUE

```

00005700
00005710
00005720
00005730
00005740
00005750
00005760
00005770
00005780
00005790
00005800
00005810

00005840
00005850

00005860
00005870
00005880
00005890
00005900
00005910
00005920
00005930
00005940
00005950
00005960
00005970

00005980
00005990
00006000
00006010
00006020
00006030
00006040
00006050
00006060
00006070
00006080
00006090
00006100


```

UMAX=0.
VMAX=0.
DO 10 I=1,M,4
  IP=IPO(I)
  IM=IMO(I)
  DO 10 J=1,NH,2
    FLIP=(PHI(I,J)-PHI(I,J+2))/DY2+U(J+1)
    FLIPR=(PHI(IP,J)-PHI(IM,J))/DX2
    UMAX=AMAX1(UMAX,ABS(FLIP))
    VMAX=AMAX1(VMAX,ABS(FLIPR))
  CONTINUE
  DTT=FRACEL*DX/UMAX
  DT=FRACEL*DY/VMAX
  DT=DMIN1(DT,DTT)
  ITEL=1
  IF(DT.EQ.DTT) ITEL=-1
  DT=FRACEL*DX*DY/(UMAX*DY+VMAX*DX)
  DTT=XLAMDA*DX*DY*REYNLD/4.00
  DT=DMIN1(DT,DTT)
  IF(DT.EQ.DTT) ITEL=0
  RETURN
END

```

10

```

SUBROUTINE PLOTSP(AX,BX,NN)
COMMON / SYMBOL / DOT,BLANK,XXX
COMMON / PICTUR / ALINE(49),BLINE(49),APLOT(201),BPLLOT(201)
THIS ROUTINE PRINTS ONLINE PLOTS OF THE POSITIVE NN-DIMENSIONAL
VECTORS AX AND BX.

```

```

** ** ** ** **
DCUBLE PRECISION AX(1),BX(1)
PUT AX & BX IN APLOT & BPLLOT
DO 10 I=1,NN
  APLOT(I)=AX(I)

```

```

  BPLLOT(I)=BX(I)
10 CCNTINUE

```

```

FIND LARGEST ELEMENT IN APLOT & BPLLOT

```

```

ABIG=0.
BBIG=0.
DO 20 I=1,NN
  ABIG=AMAX1(ABIG,ABS(APLOT(I)))
  BBIG=AMAX1(BBIG,ABS(BPLLOT(I)))
20 CONTINUE

```

20

00006560
00006570
00006580
00006590
00006600
00006610
00006620
00006630
00006640
00006650
00006660
00006670
00006680
00006690
00006700
00006710
00006720
00006721
00006722
00006723
00006730
00006740

00011360
00011370
00011380
00011400
00011410
00011420
00011430
00011440
00011390
00011450
00011470
00011480
00011460
00011490
00011500
00011510
00011520
00011530
00011540
00011550
00011560
00011570
00011580
00011590

C
C
C
C
C
C
C
C

```

C
C
C
      SET UP TCP HORIZONTAL AXIS
      DO 30 I=1,49
      BLINE(I)=DOT
      CCNTINUE
30    WRITE(6,31) ALINE,BLINE
      ALINE(I)=DOT
31    FORMAT(14X,49A1,20X,49A1)
      BLANK ALINE & BLINE. PUT PLOTTING SYMBOL IN CGMPUTED ELEMENT
C
C
C
      DO 40 I=2,49
      ALINE(I)=BLANK
      BLINE(I)=BLANK
      CCNTINUE
40    ALINE(I)=DOT
      BLINE(I)=DOT
C
C
C
      DO 50 I=1,NN
      JA=APLOT(I)/ABIG*48.+1.
      JB=BPLOT(I)/BBIG*48.+1.
      ALINE(JA)=XXX
      BLINE(JB)=XXX
      WRITE(6,51) APLOT(I),ALINE,I,BPLOT(I),BLINE
51    FORMAT(1X,E10.4,2X,49A1,2X,I3,3X,E10.4,2X,49A1)
      ALINE(JA)=BLANK
      BLINE(JB)=BLANK
      ALINE(I)=DOT
      BLINE(I)=DOT
50    CONTINUE
C
C
C
      SET UP BOTTCM HORIZONTAL AXIS
      DO 60 I=1,49
      ALINE(I)=DOT
      BLINE(I)=DOT
      CCNTINUE
60    WRITE(6,61) ALINE,BLINE
61    FORMAT(14X,49A1,20X,49A1//)
      RETURN
      END
C
C
C

```

```

00011600
00011610
00011620
00011630
00011640
00011650
00011660
00011670
00011680
00011690
00011700
00011710
00011720
00011730
00011740
00011750
00011760
00011770
00011780
00011790
00011800
00011810
00011820
00011830
00011840
00011850
00011860
00011870
00011880
00011890
00011900
00011910
00011920
00011930
00011940
00011950
00011960
00011970
00011980
00011990
00012000
00012010

```


00014580
00014590
00014600
00014610
00014620
00014630
00014640
00014650
00014660
00014670
00014680
00014690
00014700
00014710

SUBROUTINE ASUM(A,NN,SUM)
DOUBLE PRECISION A(1)
DCUBLE PRECISION SUMM
THIS ROUTINE COMPUTES THE SUM OF THE FIRST NN ELEMENTS OF A,
AND STORES THE RESULT IN SUM

SUMM=0.0
DO 10 I=1,NN
SUMM=SUMM+A(I)
CCNT INUE
SUM=SUMM
RETURN
END

10

00017630
00017640
00017650
00017660
00017670
00017680
00017690
00017700
00017710
00017720
00017730
00017740
00017750
00017760
00017770

SUBROUTINE LOAD
COMMON / FIELDS / PHI,GAMA,FG,GAMOLD
COMMON / VECTOR / T,A,S,XALPHA,PHMEAN,GAMEAN,UMEAN,TEMP,TURBKE,
1 COMMON / ARRAYS / IPO,IMO,INV,IAO,IAP,MM(3)
COMMON / PARAMS / FACTO
COMMON / FACTOR /
COMMON / SYMBOL / DOT,BLANK,XXX
DCUBLE PRECISION FACTO(42)
DIMENSION PHI(64,201),GAMA(64,201),FG(64,201),GAMOLD(64,201)
DOUBLE PRECISION UMEAN(201),TEMP(201),TURBKE(201),U(201),
PHILAM(201),T(201),A(128),S(32),XALPHA(64),
PHMEAN(201),GAMEAN(201),X(64),Y(201),FF(32),
ETA(201),GA(201)
IPO(64),IMO(64),INV(32),IAO(64),IAP(64)
1
2
3

00017780
00017790

DIMENSION PHIO(2,101)
DIMENSION PHICGM/PHIO
COMMON MRLOAD
ITAPE=NUMBER(25)
REWIND ITAPE
READ(ITAPE) PHIO
READ(ITAPE) MRLOAD
READ(ITAPE) PHI,GAMA,FG,GAMOLD
READ(ITAPE) T,A,S,XALPHA,PHMEAN,GAMEAN,UMEAN,TEMP
READ(ITAPE) TURBKE,U,PHILAM,FF,ETA,GA,X,Y
READ(ITAPE) IPC,IMO,INV,IAO,IAP,MM
READ(ITAPE) NUMBER
READ(ITAPE) FACTO
READ(ITAPE) DOT,BLANK,XXX
REWIND ITAPE
CALL DHARM(A,MM,INV,S,0,IFER)
RETURN

00017800
00017810
00017820
00017830
00017840
00017850
00017860
00017870
00017880
00017890

C
C
C

END

```
SUBROUTINE RELOAD
COMMON / FIELDS /
COMMON / VECTOR /
1 COMMON / ARRAYS /
COMMON / PARAMS /
COMMON / FACTOR /
COMMON / SYMBOL /
DCUBLE PRECISION PHI(64)
DIMENSION PHI(64)
DCUBLE PRECISION
1 PHI,GAMA,FG,GAMOLD
2 T,A,S,XALPHA,PHMEAN,GAMEAN,UMEAN,TEMP,TURBKE,
3 U,PHILAM,FF,ETA,GA,X,Y
IPO,IMO,INV,IAO,IAP,MM(3)
NUMBER(31)
FACTO
DOT,BLANK,XXX
FACTO(42)
GAMA(64,201),FG(64,201),GAMOLD(64,201)
UMEAN(201),TEMP(201),TURBKE(201),U(201),
PHILAM(201),T(201),A(128),S(32),XALPHA(64),
PHMEAN(201),GAMEAN(201),X(64),Y(201),FF(32),
ETA(201),GA(201)
IPO(64),IMO(64),INV(32),IAO(64),IAP(64)
DIMENSION PHICCM/PHIO
COMMON MRLOAD
DIMENSION PHIO(2,101)
ITAPE=NUMBER(25)
REWIND ITAPE
WRITE(ITAPE)PHIO
WRITE(ITAPE)MRLOAD
WRITE(ITAPE) PHI,GAMA,FG,GAMOLD
WRITE(ITAPE) T,A,S,XALPHA,PHMEAN,GAMEAN,UMEAN,TEMP
WRITE(ITAPE) TURBKE,U,PHILAM,FF,ETA,GA,X,Y
WRITE(ITAPE) IPO,IMO,INV,IAO,IAP,MM
WRITE(ITAPE) NUMBER
WRITE(ITAPE) FACTO
WRITE(ITAPE) DOT,BLANK,XXX
REWIND ITAPE
RETURN
END
```

00017900

00017910
00017920
00017930
00017940
00017950
00017960
00017970
00017980
00017990
00018000
00018010
00018020
00018030
00018040
00018050

00018060
00018070

00018080
00018090
00018100
00018110
00018120
00018130
00018140
00018150
00018160
00018170

```
SUBROUTINE PRMTRS
COMMON / FIELDS /
COMMON / VECTOR /
1 COMMON / ARRAYS /
COMMON / PARAMS /
2 M2M,MH,MHP,NPROB,ICOUNT,ITEL,INT,KSTEP,ISTART,
3 ISCIP,MSCIP,ITAPE,NITER,NITOT,NITMAX,IFIG,MCOMP,
KINT
COMMON / FACTOR /
1 DX,DX2,DXSQR,DXSQR4,DXSQR8,DY,DY2,DYSQR,R,RSQR,
RSQRP,REYNLD,REY,FRACEL,XLAMDA,TIME,DT,DTT,PI,H,
```

```
PHI,GAMA,FG,GAMOLD
T,A,S,XALPHA,PHMEAN,GAMEAN,UMEAN,TEMP,TURBKE,
U,PHILAM,FF,ETA,GA,X,Y
IPO,IMO,INV,IAO,IAP,MM(3)
N,M,NP1,NP2,NM1,NM2,NM3,NM4,NH,MP1,MP2,MP3,MM1,
M2M,MH,MHP,NPROB,ICOUNT,ITEL,INT,KSTEP,ISTART,
ISCIP,MSCIP,ITAPE,NITER,NITOT,NITMAX,IFIG,MCOMP,
KINT
DX,DX2,DXSQR,DXSQR4,DXSQR8,DY,DY2,DYSQR,R,RSQR,
RSQRP,REYNLD,REY,FRACEL,XLAMDA,TIME,DT,DTT,PI,H,
```

```

2      EKMEAN,EKTURB,UVBAR,ATERM,BTERM,ALPHA,BETA,XM,XN
3      ,XNM1,UMNFLO,UFLO,TOL,FA,FB,FC,F1,F2,F3,F4,F5,F6
1      DX,DX2,DXSQR,DXSQR4,DXSQR8,DY,DY2,DYSQR,R,RSQR,
2      RSCR,P,REYNLD,REY,FRACEL,XLAMOA,TIME,DT,DTT,PI,H,
3      EKMEAN,EKTURB,UVBAR,ATERM,BTERM,ALPHA,BETA,XM,XN
1      ,XNM1,UMNFLO,UFLO,TOL,FA,FB,FC,F1,F2,F3,F4,F5,F6
2      DX,DX2,DXSQR,DXSQR4,DXSQR8,DY,DY2,DYSQR,R,RSQR,
3      RSCR,P,REYNLD,REY,FRACEL,XLAMOA,TIME,DT,DTT,PI,H,
1      EKMEAN,EKTURB,UVBAR,ATERM,BTERM,ALPHA,BETA,XM,XN
2      ,XNM1,UMNFLO,UFLO,TOL,FA,FB,FC,F1,F2,F3,F4,F5,F6
3      PHM(64,201),GAMA(64,201),FG(64,201),GAMOLD(64,201)
1      DIMENSION PHM(64,201)
2      DOUBLE PRECISION PHM(64,201),TEMP(201),TURBKE(201),U(201),
3      PHILAM(201),T(201),A(128),S(32),XALPHA(64),
1      PHMEAN(201),GAMEAN(201),X(64),Y(201),FF(32),
2      ETA(201),GA(201)
3      IPO(64),IMO(64),INV(32),IAO(54),IAP(64)
1      DIMENSION PHASE(11,6)
2
3      COMPTES PHI PHASE AT VARIOUS Y LOCATIONS
1      IF(ICOUNT.EQ.KSTEP)GO TO 11
2      JJ=1
3      WRITE(6,10) (Y(J),J=NH,181,20)
1      DO 20 J=NH,181,20
2      DO 19 I=2,11
3      LL=IAO(I)
1      LM=LL-1
2      ARG=PHI(LL,J)
3      ARG=PHI(LM,J)
1      PHASE(I,JJ)=ATAN2(ARGI,ARGR)
2      IF(J.NE.181)GO TO 19
3      ARG=PHI(LL,196)
1      ARG=PHI(LM,196)
2      PHASE(I,6)=ATAN2(ARGI,ARGR)
3      CONTINUE
19      JJ=JJ+1
20      CONTINUE
21      MMX=1
22      DO 30 I=2,11
23      WRITE(6,40) ICOUNT, TIME,(PHASE(I,J),J=1,6),MMX
24      MMX=MMX+1
25      CONTINUE
26      FORMAT(1H0,3X,'CYCLE',7X,'TIME',3X,'PHASE AT Y=',F6.3,4(5X,F6.3)
27      1,10X,',',55',7X,'MODE:'),
28      FORMAT(1H7,3X,F10.6,3X,F8.3,10X,5(F8.3,5X),13)
29      IF IG=1
30      RETURN
31      END

```

DISTRIBUTION LIST

	No. Copies
1. Defense Documentation Center Cameron Station Alexandria, Virginia 22314	20
2. Library, Code 0212 Naval Postgraduate School Monterey, California 93940	2
3. Chairman, Department of Aeronautics Naval Postgraduate School Monterey, California 93940	1
4. Professor T. H. Gawain, Code 57Gn Department of Aeronautics Naval Postgraduate School Monterey, California 93940	5
5. Assistant Professor W. H. Clark, Code 57Cv Department of Aeronautics Naval Postgraduate School Monterey, California 93940	5
6. Lieutenant Commander George D. O'Brien, USN 4817 Bayard Boulevard Washington, D. C. 20016	3
7. Mr. Ronald Bailey Theoretical Branch NASA Ames Research Center Moffett Field, California 94035	1
8. Information Research Associates 2140 Shattuck Avenue Berkeley, California 94720	2
9. Los Alamos Scientific Laboratory Los Alamos, New Mexico 87544 Attn: Dr. F. Harlow	1
10. Commander Naval Air Systems Command Attn: Dr. E. S. Lamar - 1 Dr. H. J. Mueller - 1 Navy Department Washington, D. C. 20360	2

11. Commanding Officer 2
Naval Ship Research and Development Center
Carderoc, Maryland
Attn: Dr. F. Frenkiel - 1
Dr. J. Schott - 1
12. Office of Naval Research 2
Navy Department
Washington, D. C. 20360
Attn: Morton Cooper; Code 438 - 1
Ralph Cooper - 1
13. Dr. W. C. Reynolds 1
Dept. of Mechanical Engineering
Stanford University
Stanford, California 94034
14. Professor C. E. Menneken, Code 023 1
Dean of Research Administration
Naval Postgraduate School
Monterey, California 93940
15. Dr. Jacob Fromm 1
International Business Machines, Corp.
Research Laboratories
San Jose, California 95114

UNCLASSIFIED

Security Classification

DOCUMENT CONTROL DATA - R & D

(Security classification of title, body of abstract and indexing annotation must be entered when the overall report is classified)

1. ORIGINATING ACTIVITY (Corporate author) Naval Postgraduate School Monterey, California 93940		2a. REPORT SECURITY CLASSIFICATION Unclassified	
		2b. GROUP	
3. REPORT TITLE A Numerical Investigation of the Non-Linear Mechanics of Wave Disturbances in Plane Poiseuille Flows			
4. DESCRIPTIVE NOTES (Type of report and, inclusive dates) Technical Report			
5. AUTHOR(S) (First name, middle initial, last name) T. H. Gawain and W. H. Clark			
6. REPORT DATE 2 September 1971	7a. TOTAL NO. OF PAGES 121	7b. NO. OF REFS 16	
8a. CONTRACT OR GRANT NO.	9a. ORIGINATOR'S REPORT NUMBER(S) NPS-57Gn71091A		
b. PROJECT NO.			
c.	9b. OTHER REPORT NO(S) (Any other numbers that may be assigned this report)		
d.			
10. DISTRIBUTION STATEMENT This document has been approved for public release and sale; its distribution is unlimited.			
11. SUPPLEMENTARY NOTES		12. SPONSORING MILITARY ACTIVITY Naval Postgraduate School Monterey, California 93940	
13. ABSTRACT <p>The response of a plane Poiseuille flow to disturbances of various initial wavenumbers and amplitudes is investigated by numerically integrating the equation of motion. It is shown that for very low amplitude disturbances the numerical integration scheme yields results that are consistent with those predictable from linear theory. It is also shown that because of non-linear interactions a growing unstable disturbance excites higher wavenumber modes which have the same frequency, or phase velocity, as the primary mode. For very low amplitude disturbances these spontaneously generated higher wavenumber modes have a strong resemblance to certain modes computed from the linear Orr-Sommerfeld equation.</p> <p>In general it is found that the disturbance is dominated for a long time by the primary mode and that there is little alteration of the original parabolic mean velocity profile. There is evidence of the existence of an energy equilibrium state which is common to all finite-amplitude disturbances despite their initial wavenumbers. This equilibrium energy level is roughly 3-5% of the energy in the mean flow which is an order of magnitude higher than the equilibrium value predicted by existing non-linear theories.</p>			

DD FORM 1473

1 NOV 66

(PAGE 1)

S/N 0101-807-6811

120

UNCLASSIFIED

Security Classification

A-31408

Security Classification

14.

KEY WORDS

LINK A

LINK B

LINK C

ROLE

WT

ROLE

WT

ROLE

WT

Plane Poiseuille Flow